Thermodynamics and dissociation constants of acetohydroxamic acid (AHA), pyrocatechol (PYR), acetic acid (AA) and glycolic acid (GA) at variable ion strength and temperature in NaCl solution and the corresponding activity correction to improve speciation scheme for U and V in cement leachates

Congying Chen

Thesis submitted for the Degree of Master of Philosophy

Department of Earth Science and Engineering

Imperial College London

I hereby declare that the research presented in this thesis is my own work and that all mention to work carried out by others is appropriately referenced

Abstract

The uptake of uranium and vanadium in the leakage of geological disposal facilities (GDF) via ligands sourced from vegetation, bacterial and fungi are widely discussed. It probably results in the remobilisation of these two pollutants and lead to the radioactive and heavy-metal contamination in the environment. The quantification of their complexes is the important section to provide environment risk management with scientific evidences. In this study, acetohydroxamic acid (HAHA), pyrocatechol (PYR), glycolic acid (GA) and acetic acid (AA) as typical representatives of common ligands under natural conditions were investigated via potentiometric titration (PT). It aims to determine their dissociation constants (pKa) and thermodynamic parameters (Gibbs energy ΔG, enthalpy ΔH and entropy ΔS values) for improving U(VI)-L and V(IV)-L complexing models in sodium chloride (NaCl) solution. To increase the understanding of the effect of ion strength and temperature on ligands as well as their coordination with UO_2^{2+} and VO^{2+}, their pKa values at ion strength of 0.1M, 0.5M, 1.0M, 2.0M and 3.0M and at temperature of 298.15K, 315.15K and 335.15K were measured and showed the differences compared with the results in previous studies. Based on Van't Hoff equation, their thermodynamic parameters are also calculated. As a result, the effect of ion strength on the pKa values among these ligands showed a decrease from ion strength from 0.1 to 1.0 M, while an increase was found as ion strength increased to 3.0 M. The pKa values of HAHA and PYR displayed a high sensitivity to the temperature in this work, while the ones of GA and AA were inert to the variation of the temperature. In the calibration of intrinsic values, specific Ion Interaction Theory (SIT) showed the high consistency of pKa values obtained from 1.0 M to 3.0 M, while the Davies equation (DE) was suitable for ion strength 0.1 M to 0.5M. Meanwhile, it was found that the intrinsic pKa values of HAHA and PYR respective to the calculation of SIT and DE existed large differences referred to the literature values. In Hyss models, the new pKa values showed differences combing with the established models. Additionally, according to the speciation curves of M-L complexes with the intrinsic pKa values, the curves derived from the SIT and DE was basically showed lower contents of targeted M-L complexes than the experimental ones. Based on the highest formative percentages in their complexing species, the affinity to the metal ions followed the order: HAHA>PYR>GA>AA in terms of their largest formation percentages. The study showed an appropriate method to determine the ligand protonation under old cement leachate (OCL) and provide geological models with the data regarding the coordination of the targeted ligands with metal ions like uranyl and vanadyl ions as well.

Acknowledgments

First and foremost, I would like to thank my supervisors, Professor Dominik Weiss for keeping me grounded during my MPhil and teaching me a great deal about science. I would like to thank all members of the Environmental Geochemistry group for providing me with great feedback and advice in numerous group meetings. In particular, thanks to Dr George Northover for teaching me how to do lab work, and for teaching me about potentiometric titration. Thanks to Prof. Enrique Garcia for teaching me how to analyse pKa values and hydrolytic constants in HYPERQUAD models. The work presented during my MPhil employed a wide variety of experimental techniques which I would not have been able to use successfully on my own. Last but not least, thanks to my family, Wenxin , Yuelan and Huichun for supporting me during my MPhil. I couldn't have reached this stage without their unending support

Table of Contents

1   Introduction

1.1   Motivation

Why we use geological facilities Leakage from waste disposal facilities associated with mining and industrial activities lead to increasing release of radionuclides into the natural environment (McKinley, Alexander et al. 2007). The early period of radioactive waste disposal was rather basic since a large percentage (41%) of total waste was simply diluted and discharged into sewers (Miller, Fahnoe et al. 1954). In 1955, the concept of geological disposal was introduced following the contract made by USAEC (United States Atomic Energy Commission) and NRC (National Research Council) to advise reasonable disposal methods involving surface and underground sites (NRC 1999).

Development of GDF In modern waste managements, near-surface and deep underground disposal are employed to deal with LLW and ILW (low and intermediate-level waste), SL (short-lived wastes), and HLW (high-level wastes), SF (spent fuel) respectively. The Rokkasho 1 and 2 waste disposal sites in Japan are examples of repositories for storing LLW. The sites are only a few tens of metres deep as LLW with short half-live wastes is not requiring the long-term isolation (McKinley, Alexander et al. 2007). However, the disposal of nuclear waste with high radioactive with long half-lives commonly employs the deep geological repository or geological disposal facilities (GDF), normally up to several hundreds of metres or kilometres in depth (Hicks, Baldwin et al. 2008). In all cases, GDF basically relied on a multi-barrier concept regarding not only sophisticated technique, but also stable geographic situations. The EBS (engineered barrier system) developed in Switzerland consists of glass matrix, steel canister, bentonite backfill and geological barriers.

Types of GDF Besides the deep disposal, solidification/stabilization (S/S) techniques are alternatively employed to dispose of low-level radioactive waste via mixing of cementitious materials with heavy metals to weaken the mobility of contaminant metal ions (Shi and Spence 2004). The method is widely used to retard toxic and radionuclides because of low cost, high waste loading possible, and high-resistant biodegradation (Shi and Spence 2004). It was well known that the interaction between cementitious materials and groundwater produces hyper-alkaline condition (pH>13) firstly and continuously falling to 12.5 (Alexander, Arcilla et al. 2008). As the function of groundwater flow, pH values found in cement leachates will be decreased to 10.5. According to different pH ranges, cement leachates are defined as YCL (young cement leachates) with pH from 13.5 to 12.5, ICL (intermediate cement leachates) with pH from 12.5 to 10.5 and OCL (old cement leachate) with lower pH ranges (Morris 2016). Therefore, although the destruction of facilities with unpredictable geological activities like earthquake likely releases the waste into the ambient within a long-term storage, the application of cement materials as the second barrier plays an important role in immobilising waste since the produced high-alkalinity condition with groundwater can precipitate it.
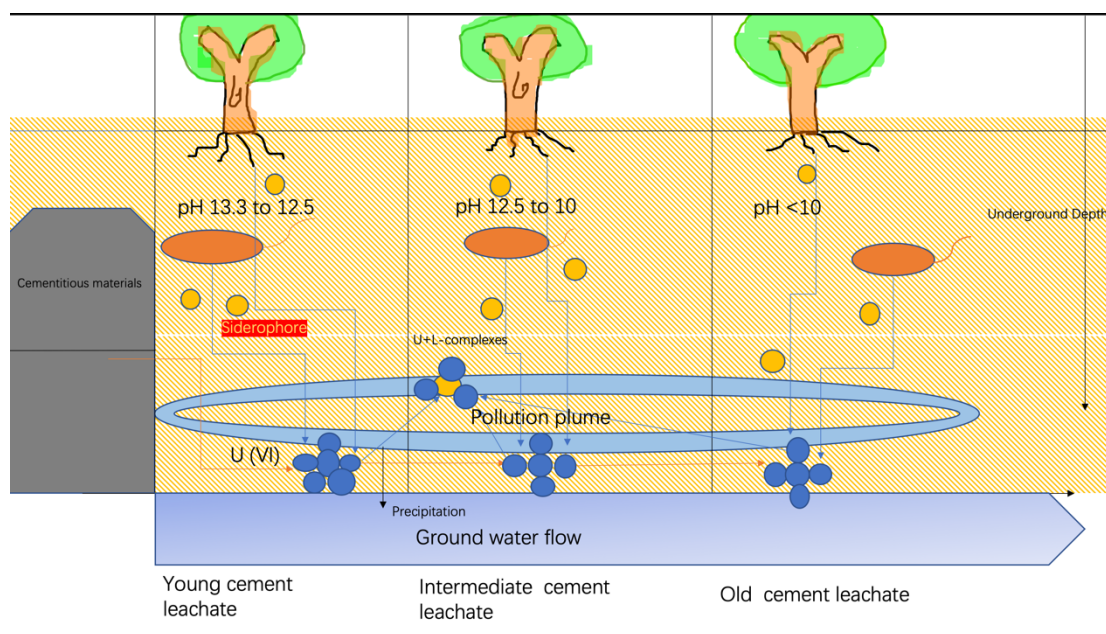
Figure 1 Schematic of the complexing progress occurred in the after of leakage from GDF, pH ranges changed by the function of groundwater are divided in to 3 types of leachate: young cement leachate (YCL), immediate cement leachate (ICL) and old cement leachate (OCL).

Uranium and organic matter Uranium, a predominant energy source, is used by power plants and military activities (Edwards and Oliver 2000). However, its isotopes also become contaminant source with highly radioactive and long half-live properties. The half-live period of U^{238} and U^{235} is about 4.5 billion and 700 million years respectively. In alkaline solution without organic matter, hexavalent uranium (U^{VI}) in presence of a dioxide format can be precipitated, and the beginning of its precipitation occurs in pH values at 4 (Cahill and Burkhart 1990). Therefore, cement leachates can immobilize it as the formation of the precipitation under hyper alkaline conditions. However, the presence of organic matters likely enhances its mobility in alkaline solution. In the study of (Kirby, Sonnenberg et al. 2020), a precipitation experiment of uranyl ions (UO_2^{2+}) carried out by adding different concentrations of Desferrioxamine B (DFOB) under the condition of pH=11.5. It elucidated that ratios of U^{VI} passed through filters (0.3 to 1μm pore meter) were 11-12%, 41-53%, 95-96% and 100% in presence of 4.2, 42, 130 and 420 μM DFOB solution respectively. Meantime, it also demonstrated that hydroxamate, a functional group, played an important role in complexing with U^{VI} as two species of $[UO_2(OH)_3(L_{mono})]^{2-}$ and $[UO_2(OH)_2(L)]^-$. In the study of (Mullen, Gong et al. 2007), it argued effective functional groups found in DFOB were hydroxamate groups, similar to acetohydroxamic acid (AHA), a ligand that is proposed for actinide complexation in advanced separation as well. In the reactive progress from pH of 3 to 10.5, there were three types of products as formats of UO_2DFOH_2, UO_2DFOH and $UO_2OHDFOH$ corresponding to their stability constants (logβ) of 22.93±0.04, 17.12±0.35 and 22.76±0.34 respectively.

1.2 Research and Knowledge Gap

Naturally occurring organic ligands make huge contribution to the mobility of contaminant metals because of their high affinity to metal ions. Higher solubility of heavy metals in soil solution at alkaline pH was attributed to enhanced formation of organic matter metal complexes after ionization of weak

acid groups. Extensive evidence exists that in this pH range most dissolved heavy metals are present as metal soluble organic ligand complexes (Sherene 2010). In studies of organic ligands, the determination of their dissociation constants and stability constants of their complexes made huge contribution to the thermodynamics of contaminated metal ions. In the determination of hydroxamic acids and their complexes with vanadium (IV), the dissociation constants of acetohydroxamic acid, benzohydroxamic acid were 9.25 and 8.65 at 298.15K in 0.2 M KCl solution respectively (Buglyó and Pótári 2005). The complexation of vanadium (IV) with these two ligands produced 3 types of species related to forms of VL, VL_2 and VLOH. Stability constants of VL as predominant species were 8.69 and 8.43 found in acetohydroxamic acid and benzohydroxamic acid (Buglyó and Pótári 2005). However, The measurements in previous studies has not been comprehensive to denote the effect of ion strength and temperature on pKa values of acetohydroxamic acid, acetic acid, glycolic acid, and pyrocatechol and their following complexing reactions with targeted metals. Thus, the qualifying work based on stability constants and regarding pKa values still lacks the support of precise parameters. Meantime, there are remarkably complicated conditions containing pH values, ion strength and temperatures found in the underground and surface environment of disposal facilities. Therefore, it is important that the investigation of organic ligands has impact on the complexation of radionuclides as well as metal from facility materials in natural environment. pKa values of acetohydroxamic acid, acetic acid, glycolic acid, and pyrocatechol play an important role in quantifying work of available ligands to the metals in facilities since the calculation of stability constants of their complexes results from the values of the ligands. To be more systematic and accurate in quantifying works, the effect of temperatures and ion strength on the dissociation constants of targeted ligands and the simulating models are necessary to be developed for the metal-ligand complexing formation.

1.3   Aim and Objectives

This research aims to advance understanding of functional groups found in siderophores with possible affinity to uranyl ions in aqueous chemistry. A special focus is placed on the measurements of their thermodynamic parameters and dissociation constants at variable conditions of ion strength and temperatures. To address this, a multidisciplinary approach consisting of statistics methods and experimental techniques will be applied. This is the outline of my thesis followed:

- Chapter 2 a review of literatures for functional groups and metal-ligand complexation chemistry
- Chapter 3 an outline of methodology applied in my research
- Chapter 4 Thermodynamics and dissociation constants of acetohydroxamic acid (AHA), pyrocatechol (CAT), acetic acid (ACE) and glycolic acid (GLY) at variable ion strength and temperature in NaCl solution and improved speciation scheme for U and V in leachates
- Chapter 5 summarize key findings from the research
- Chapter 6 highlight future research requirements

2 Literature Review

The aim of this chapter is to provide background information relevant to work presented in this research. These include:

- The introduction to hydrolysis of uranium(VI), vanadium (IV) and vanadium (V) in aqueous chemistry
- The summary of complexation of uranium(VI), vanadium (IV) and vanadium (V) with ligands with targeted functional groups
- An introduction to ligands with targeted functional groups: acetohydroxamic acid (hydroxamate), pyrocatechol (catecholate), acetic acid (α-carboxylate) and glycolic acid (β-carboxylate)
- An introduction to activity correction for dissociation constants of ligands: Debye-Huckle equations, Davis equation, specific ion theory
- An introduction to the application of Van't Hoff equation to determine thermodynamic parameters
- An introduction to HYPERQUAD for analysing potentiometric titration data

2.1 Association constants previously determined

2.1.1 Acid dissociation constants for acetohydroxamic acid (aha), pyrocatechol (cat), acetic acid (ace) and glycolic acid (gly)

Dissociation constants is demonstrated for reflecting a relationship between pH and pKa. The calculating equation called as Henderson-Hasselbalch equation was developed by Henderson and Hasselbalch and (1) that is a now standard method to measure pKa values for ligands as pH conditioning in aqueous environment (Reijenga, Van Hoof et al. 2013).

$$pH = pKa + \log ([A^{n-}]/[H_nA]) \qquad (1)$$

where $[A^{n-}]$ and $[H_nA]$ means equilibrium concentrations of dissociated acid and non-dissociated acid after deprotonation. To be more specific, there is a sigmoid cure (Figure 2) demonstrated the degree of dissociation in solution. Parameter α represents this degree α ranging from 0 to 1. where α at inflection point 0.5, pH equals to pKa. The equation for α was provided by:

$$\alpha = [A^{n-}]/([H_nA] + [A^{n-}]) \qquad (2)$$

Combing equation (1) and (2):

$$\log(\alpha/1-\alpha) = pH - pKa \qquad (3)$$

However, for concentrated solutions or pKa's near the extremes of the pH scale, it has been shown that there are significant differences between the predicted and actual concentration of the hydrogen ion (Po and Senozan 2001).

The dissociation constant in stepwise deprotonated ligand also can be related to Henderson-Hasselbalch equation. However, experimental data only reflect real-time concentrations of hydrogen ions and potential in sample solutions. Therefore, the appropriate equation can be written as:

$$pKa_i = -\log ([H][H_{n-i}L])/[H_{n-i} + L]$$

where i means the order of deprotonated step, [H], $[H_{n-i}L]$ and $[H_{n-i} + L]$ means equilibrium concentrations of dissociated hydrogen ions, non-dissociated ligands and the summary of dissociated hydrogen ions and ligands.

Natural ligands with the functional groups including hydroxamate, carboxylate, α-carboxylate and catecholate are able to complex contaminant metal ions released from nuclear waste containers (Runde 2000). They are widely found in siderophores produced via biological activities of fungi, bacteria and vegetation (Ahmed and Holmström 2014). Previous studies showed organic ligands commonly found in near surface or deep underground environment has high affinity with metal ions including most of radionuclides can form metal-ligand complexes with high mobility to break through the second barrier and result in high-risk pollution (Kuippers, Morris et al. 2021).
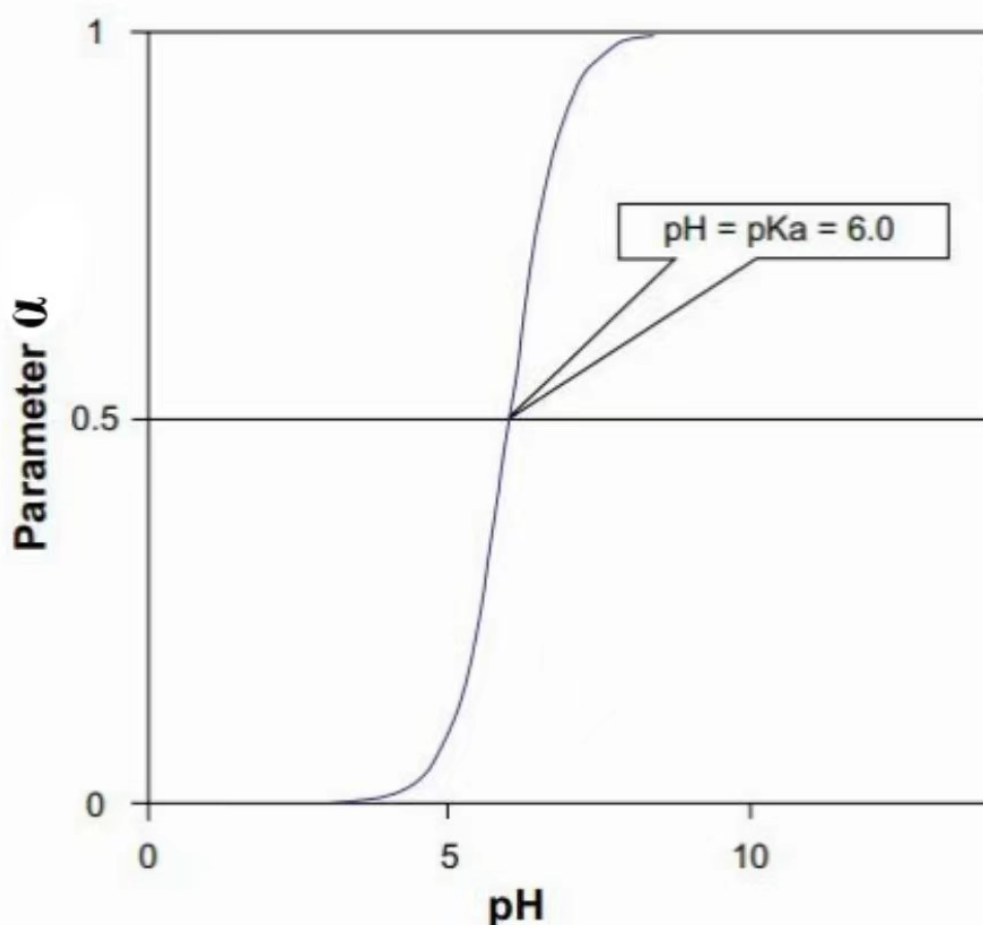
Figure 2 A classic example of a sigmoidal curve created by plotting a measured quantity versus pH. The inflection point corresponds to pKa (Reijenga, Van Hoof et al. 2013).

2.1.1.1   Acetohydroxamic acid

Acetohydroxamic acid is one of typical ligands with hydroxamate. Dissociation constants for weak acids with hydroxamate groups normally are ranging from 8-9, also can act as weak bases in presence of NC=O moiety (Munoz-Caro, Nino et al. 2000; (Fazary 2005). It is well know most of metal-ligand complexes involving the participation of hydroxamic acids are coordinated occurs by the deprotonation of hydroxyl groups and the subsequent coordination of deprotonated OH and the carbonyl oxygen (Yale 1943, Munoz-Caro, Nino et al. 2000). On the basis of the formation of stable, and five-membered [O,O]

11

hydroxamate chelates, numerous microorganisms developed hydroxamate type metal sequestering siderophores for the uptake, storage and transport metal ions with the biological relevance (Aksoy 2010).
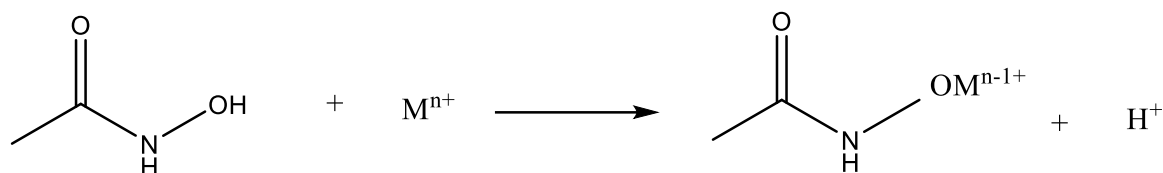
acetohydroxamic acid

Figure 3 The progress of complexing reactions between acetohydroxamic acid and metal ions. The binding position can be found at the hydroxyl group.

The determination of pKa values of hydroxamate acids conducted via the acid-base titration was critically reviewed (Fazary 2005). The increase of OH^- concentrations results in the enhancement of deprotonation among weak acids in base titration. The measurement of dissociation constants for acetohydroxamic acid found in previous studies was carried out under fixed conditions, while different species of electrolyte led to the difference of pKa values in this weak acid. Dissociation constants of AHA were measured in 0.1M $NaNO_3$ and 0.1M KNO_3 were 9.28 and 9.33 under T=298.15K respectively (Fazary 2005, Aksoy 2010). The effect of temperatures on this acid was discussed in many materials. In the study of Aksoy (2010), the pKa values in 0.1M $NaNO_3$ solution mixed with Dioxane were 9.28, 9.09, 8.94 and 8.79 at 298.15K, 310.15K,318.15K and 328.15K respectively. pKa values of acetohydroxamic acids in variable ion strength as well as electrolyte solution are shown in Table 1.

Table 1 The acid dissociation constants (expressed as -logKa) of acetohydroxamic acid at 0.1M in different electrolyte solution

I (M)	Medium	pKa	Ref.
0.1	KNO_3	9.33±0.01	(Aksoy 2010)
0.1	KNO_3	9.29±0.06	
0.1	$NaNO_3$	9.28	(Fazary 2005)
0.2	KCl	9.25	(Buglyó and Pótári 2005)
0.1	KCl	9.36	(Evers, Hancock et al. 1989)

2.1.1.2 Glycolic acid

Glycolic acid (GA), the simplest hydroxycarboxylic acid, is colourless, translucent and odourless solid substance at room temperature (Partanen, Juusola et al. 2001). The production of this acid is originated from biological activities in nature. It can be found from the vegetation e.g. in sugar beet and unripe grapes, and from metabolic pathways found in some of microorganisms e.g. *Escherichia coli*, *Corynebacterium glutamicum* and yeast (Partanen, Juusola et al. 2001, Salusjärvi, Havukainen et al. 2019).

The use of GA is widely found in many industries. It was well known that GA is the main components of dyeing and tanning agents for textile industries, in food industry, GA involving in the production of a flavour and preservative as well as a skin care agent in pharmaceutic industry (Salusjärvi, Havukainen et al. 2019).
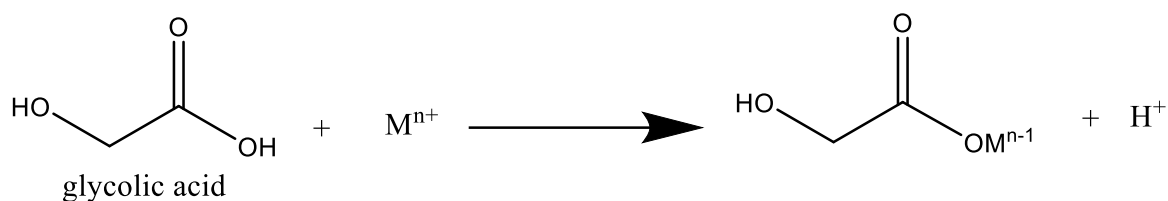
Figure 4 The progress of complexing reactions between glycolic acid and metal ions. The binding position can be found at the carboxyl group.

Glycolic acid is recognised as important ligand in complexation with many metal ions. Since it has two different functional groups hydroxyl (-OH) and carboxyl (-COOH), its complexes show versatile coordination with metal ions (do Nascimento, Teixeira et al. 2017). To understand the affinity of the ligand with metal ions, its thermodynamic dissociation constants (pKa) was necessary to calculate stability constants regarding to M-L complexing species. In the determination of dissociation constants of GA, previous studies have shown a wide range of numbers according to different experimental conditions. The pKa values found in α-hydroxycarboxylate acid are 3.59±0.01 and more than 17 at carboxyl and hydroxyl respectively (Szabo and Grenthe 2000). Although the determination of stability constants for M-L species involving GA has been revealed, pKa values of the ligand were hardly mentioned because of particular measuring techniques. There are some of pKa values for glycolic acid found at different electrolyte and ion strength solution in Table 2.

Table 2 The dissociation constant of glycolic acid at 0.1M and 1.0M ion strength in different electrolyte solution

I (M)	Medium	pKa	Ref.
1.0	$NaClO_4$	3.61±0.01	(Kirishima, Onishi et al. 2007)
0.0	NaCl	3.83	(Stokes and Robinson 1959)

2.1.1.3 Acetic acid

Acetic acid (AA) as typical representative of carboxylic acid is widely distributed in natural and artificial environment. It is a corrosive acid with a sharp odour, burning taste, pernicious and blistering properties (Wagner and Staff 2000). Since the production of acetic acid results from fermentation of many vegetation, bacterial and fungi biological progress, the distribution of the weak acid can be found in natural condition widely including ocean, oilfield brines and rain, plant and animal liquid (Wagner and Staff 2000). The application of this acid is commonly found in food industry. For instance, the production of vinegar, a typical condiment, is mainly attributed to the function of this acid.
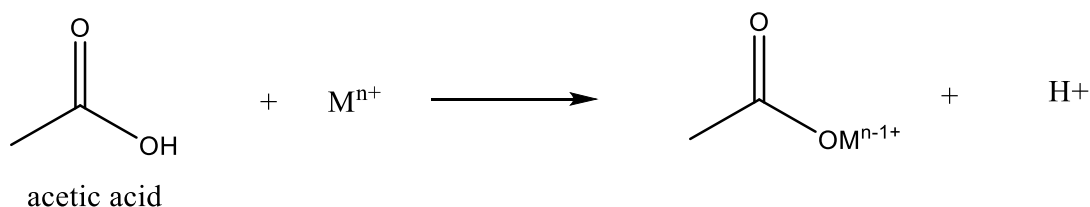
Figure 5 the schematic complexing reactions between acetic acid and metal ions, the deprotonation position is the carboxyl to bind metal ions.

The determination of dissociation constants for acetic acid was studied previously under various experimental conditions. In the study of complexation between acetic acid and uranium (VI), the dissociation constant investigated via the potentiometric method in 1.05M $NaClO_4$ solution was

13

4.59±0.01 at T=298.15K, 4.63±0.01 at T=318.15K and 4.72±0.02 at T=343.15K respectively (Jiang, Rao et al. 2002). The investigation of ion strength on pKa values of the acid demonstrated that its pKa values were 4.68, 4.64, 4.61 and 4.76 at ion strength equals to 0.01, 0.03, 0.1 and 1.0 M in tetraethylammonium iodide solution respectively (Daniele, Rigano et al. 1983).

Table 3 The dissociation constant of acetic acid at 0.1M in different electrolyte solution

Ion strength / M	medium	pKa value	Ref.
1.05	NaClO$_4$	4.59±0.01[a]	(Jiang, Rao et al. 2002)
0.01	tetraethylammonium iodide	4.68[b]	(Daniele, Rigano et al. 1983)
0.03	tetraethylammonium iodide	4.64[b]	
0.1	tetraethylammonium iodide	4.61[b]	
1.0	tetraethylammonium iodide	4.76[b]	

*a pKa value was measured at T=298.15K

*b pKa value was measured at T=310.15K

2.1.1.4 Pyrocatechol

Pyrocatechol or 1,2-dihydroxybenzene (DHBs) is one of typical weak acid with catecholate as the reactive functional groups to complex metal ions. Its chemical structure is demonstrated as a 6 carbon ring (benzene) with two phenol groups in ortho position. Previous studies have shown it antioxidant or prooxidant activities in several biological systems depending on the reaction conditions (Romero, Salgado et al. 2018). The mechanism of antioxidant properties is attributed to 2 types: radical scavenging properties disrupting a radical chain propagation and iron chelating disrupting the initiation step of radical chain reaction (Perron and Brumaghim 2009).
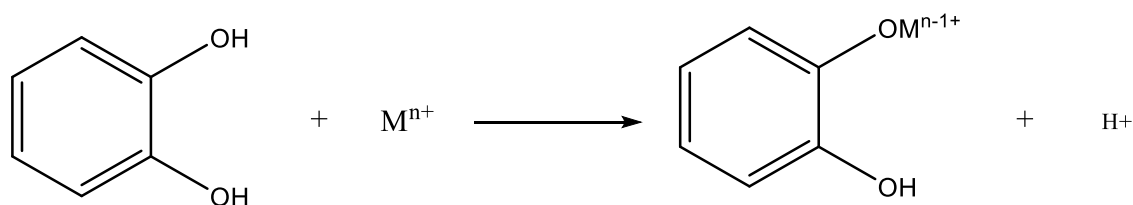
pyrocatechol

Figure 6 the schematic complexing reactions between pyrocatechol (1,2-Dihydroxybenzene) and metal ions. The coordinating progress occurs at the 1st phenol group and formed [MHL]$^+$ species.

The determination of pKa values is related to the deprotonation of two phenol groups at variable conditions including suitable pH values and temperatures. Potentiometric and spectrophotometric measurements advised that the ligand led to 2 particular deprotonated formats of [HL$^+$] and [L^{2+}] corresponding to the H$^+$ replacement at No.1 phenol group and No. 2 respectively (Nurchi, Pivetta et al. 2009). The calculation of dissociation constants found in catechol has been indicated based on particular experimental conditions. In the 0.1 M and 1.0 M KCl solution at 298.15K, the first deprotonated progress was at pH values of 9.17 and 9.14 respectively, and the second progress was at pH values of 14.3 and 13.8 respectively (Nurchi, Pivetta et al. 2009). However, the dissociation constant was found at 9.24 and 13 in the solution of NaClO$_4$ at 295.15K in the study of (Charkoudian and Franz 2006).

2.1.2 Hydrolysis of vanadium (IV), vanadium (V) and uranium(VI) in aqueous chemistry

Hydrolysis progress of metal ions plays an important role in affecting the reactivity of the ligands since it produces a variety of hydrolysing species corresponding to different environmental conditions such as pH values, ion strength and dioxides carbon contents. The investigation of hydrolysing progress has been carried out at 293.15K in the fixed ion strength system normally. However, owing to unpredictable and variable conditions found in surface and underground environment, the quantifying works for tracing hydrolysing species is obligatory to be supported via experimental dataset based on the environmental conditions.

2.1.2.1 Hydrolysis of vanadium (V) and vanadium (IV)

In the investigation of interactions between vanadium and natural ligands, the distribution of vanadium-ligand (V-L) complexes in the environment greatly depends on the hydrolysing progress involved its valence formats. The aquatic chemistry of vanadium is dominated by vanadium(V) and vanadium(IV) since their species VO^{2+}, $VO(OH)^+$, $H_2VO_4^-$ and HVO_4^{2-} normally can be found in natural water (Wehrli and Stumm 1989). VO^{2+}, a hard Lewis acid, coordinated with oxygen donor atoms, easily lead to extremely strong complexes with soluble organic chelates, while vanadate also has tendency to form surface complexes with ligands because of the function of hydrous oxides (Wehrli and Stumm 1989). Although vanadate like phosphate ($H_2PO_4^{2-}$) has three different dissociation constants, it normally exists in the form of momoanion rather than dianion found in phosphate nearly neutral pH value. Compared with high stability of phosphate, H_3VO_4 is difficultly observed and easily converted to VO^{2+} at pH 1.

$H_3VO_4 + H_2O \leftrightarrow H_2VO_4^- + H^+$ pKa 3.5

$H_2VO_4^- + H_2O \leftrightarrow HVO_4^{2-} + H^+$ pKa 7.8

$HVO_4^{2-} + OH^- \leftrightarrow VO_4^{3-} + H_2O$ pKa 12.7
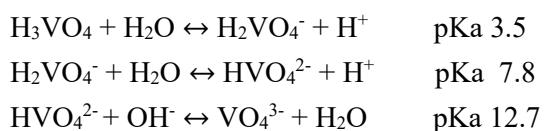
In the study of VO^{2+} hydrolysis, Wehrli and Stumm (1989) pointed out the oxidation of VO^{2+} was conducted by hydrolysis and adsorption to hydrous oxide surface, thus the hydrolysisng species from low pH conditions converted to ones at high pH values likely lead to the variety of the complex formation. The hydrolysis of VO^{2+} can be expressed by:

$pVO^{2+} + qH_2O \leftrightarrow (VO)_p(OH)_q^{2p-q} + qH^+$
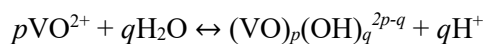
where p and q are positive integra numbers (Komura, Hayashi et al. 1977). The stability constants of VO^{2+} hydrolysis species can be written as:

$\beta_{pq} = [(VO)_p(OH)_q^{2p-q}][H^+]^q/[VO^{2+}]^p$

The speciation of vanadate (V) and vanadyl (IV) hydrolysis employed methods to detect and calculate complexing reactions normally including NMR, ESR and potentiometric titration, related to their hydrolysing constant was calculated under different ion strengths and electrolytes shown in Table 1. In the study of (Yamaki, Paniago et al. 1999), VO_2^+ is the prevailing form of vanadium (V) at low pH(from 1 to 3), and then while it tends to be hydrolysed under weakly acid conditions. In the coordinating

progress between VO_2^+ and acetohydroxamic, the VO_2^+ firstly formed vanadate ions ($H_2VO_4^{-}$) the complexing formula was followed by (Yamaki, Paniago et al. 1997):

$pH^+ + qH_2VO2^- + rHL = [(H^+)_P(H_2VO_4^-)q(HL)_r]^{p-q}$
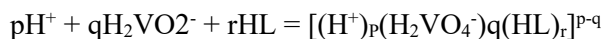
It however advised that VO_2^+ can form polymeric species including decavanadate, cyclic tetravanadate and diprotonated vanadate. Therefore, the complexation between vanadium (V) and ligands actually focuses on the competition between oligomerisation and the reaction of vanadate (Yamaki, Paniago et al. 1997).
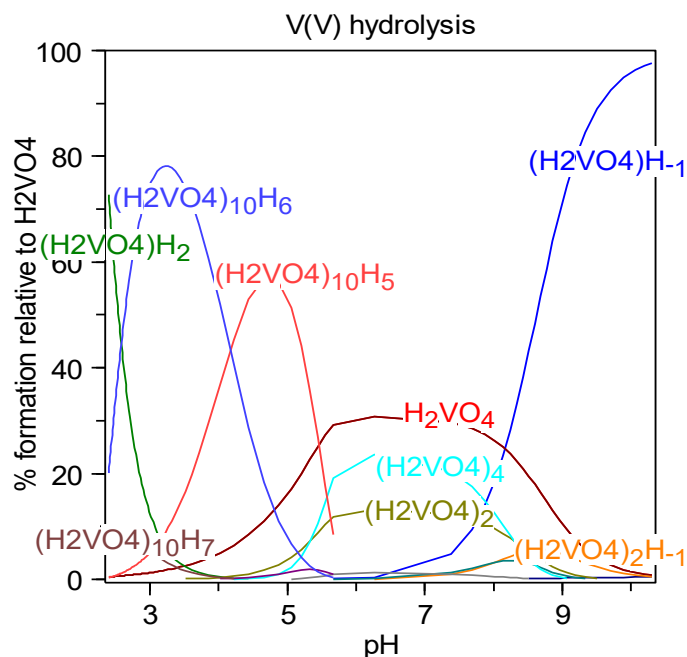
Figure 7 The protonation progress of vanadate (V) at 293.15K and 0.15M NaCl solution without CO_2. 1.67 mM $H_4VO_4^0$ was titrated via 2.5 mL of 0.1 M NaOH for increasing pH from 2.4 to 9.74 (Yamaki, Paniago et al. 1999).
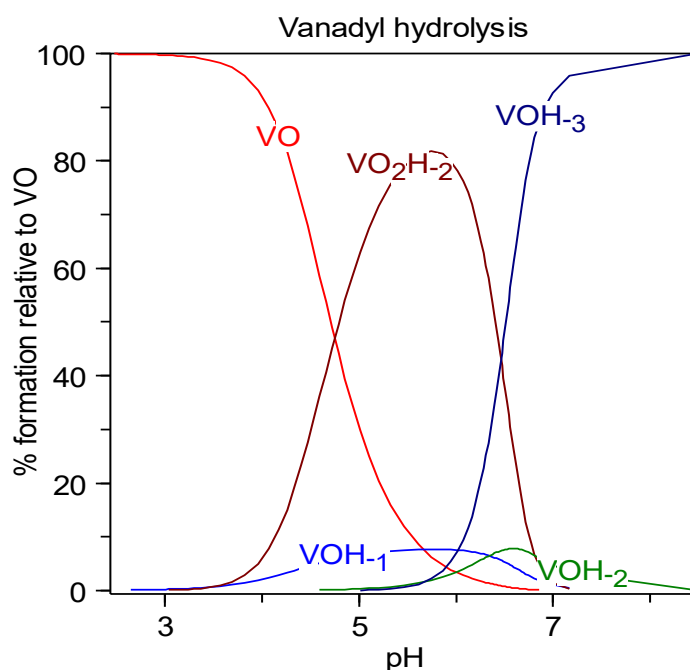
Figure 8 The hydrolysis progress of vanadate (IV) at 293.15K and 0.1 M $NaClO_4$ solution without CO2. VO^{2+} was titrated via 0.1 M NaOH for increasing pH from 2.5 to 10 (Wehrli and Stumm 1989).

Table 4 The hydrolysis constants of uranyl ions, vanadyl ions and the formation constants of vanadate in NaClO4 and NaCl solution, T= 25˚C

Formula	logβ	Ion Strength (M)	medium	Reference
UO_2^{2+}				(De Stefano, Gianguzza et al. 2002)
$UO_2^{2+} + OH^- \rightarrow UO_2OH^+$	-5.2	0	$NaClO_4$	
$UO_2^{2+} + 2OH^- \rightarrow UO_2(OH)_2$	-5.62	0	$NaClO_4$	
$3UO_2^{2+} + 4OH^- \rightarrow (UO_2)_3(OH)_4^{2+}$	-11.9	0	$NaClO_4$	
$3UO_2^{2+} + 5OH^- \rightarrow (UO_2)_3(OH)_4^+$	-15.55	0	$NaClO_4$	
$3UO_2^{2+} + 7OH^- \rightarrow (UO_2)_3(OH)_4^-$	-31	0	$NaClO_4$	
VO_2^+				(Yamaki, Paniago et al. 1999)
$2H_2O + VO_2^+ \rightarrow H_2VO_4^- + 2H^+$	-7.0	0.15	NaCl	
$H_2VO_4^- \rightarrow HVO_4^+ + H^+$	-15.17	0.15	NaCl	
$2H_2VO_4^- \rightarrow V_2O_7^{4-} + 2H^+$	-16.19	0.15	NaCl	
$2H_2VO_4^- \rightarrow HV_2O_7^{3-} + OH^-$	-5.85	0.15	NaCl	
$2H_2VO_4^- \rightarrow H_2V_2O_7^{2-} + H_2O$	2.65	0.15	NaCl	
$4H_2VO_4^- \rightarrow V_4O_{13}^{6-} + 3H_2O + 2H^+$	-9.98	0.15	NaCl	
$4H_2VO_4^- \rightarrow HV_4O_{13}^{5-} + 3H_2O + H^+$	0.63	0.15	NaCl	
$4H_2VO_4^- \rightarrow V_4O_{12}^{4-} + 4H_2O$	9.24	0.15	NaCl	
$5H_2VO_4^- \rightarrow V_5O_{15}^{5-} + 5H_2O$	11.17	0.15	NaCl	
$10H_2VO_4^- + 4H^+ \rightarrow V_{10}O_{28}^{6-} + 12H_2O$	50.28	0.15	NaCl	
$10H_2VO_4^- + 5H^+ \rightarrow HV_{10}O_{28}^{5-} + 12H_2O$	56.90	0.15	NaCl	
$10H_2VO_4^- + 6H^+ \rightarrow H_2V_{10}O_{28}^{4-} + 12H_2O$	61.07	0.15	NaCl	
$10H_2VO_4^- + 7H^+ \rightarrow H_3V_{10}O_{28}^{3-} + 12H_2O$	62.93	0.15	NaCl	
VO^{2+}				(Goncalves and Mota 1987)
$VO^{2+} + H_2O \rightarrow VOOH^+ + H^+$	-5.76	0.1	$NaClO_4$	
$2VO^{2+} + H_2O \rightarrow (VO)_2(OH)_2^{2+} + 2H^+$	-6.76	0.1	$NaClO_4$	
$VO^{2+} + 2H_2O \rightarrow VO(OH)_2^0 + 2H^+$	-12	0.7	Sea water	(Wehrli and Stumm 1989)
$VO^{2+} + 3H_2O \rightarrow VO(OH)_3^- + 3H^+$	-17.70	0.7	Sea water	

2.1.2.2 The hydrolysis of uranium (VI)

The investigation of hydrolytic progress of U(VI) was conducted by nuclear energy agency (NEA) for establish thermochemical database (Brown 2002). It was well known that the hydrolysis of uranium is able to lead to the formation of mono- or polynuclear species in its all oxidation states as well as complicated complexes with organic and inorganic ligands in the environment.

U(VI) hydrolysing species have essential impact on its colloidal formation and stability with pH varieties. The hydrolysis of uranyl was investigated at nitrate (0.1 M KNO_3) and sulphate (0.1 and 1.0 M Na_2SO_4) at early stage (Sylva and Davidson 1979, Comarmond and Brown 2000). The formula for U(VI) hydrolysing species as pH changes is followed by (Sylva and Davidson 1979):

$p\mathrm{UO}_2^{2+} + q\mathrm{H}_2\mathrm{O} \leftrightharpoons (\mathrm{UO}_2)_p(\mathrm{OH})_q^{(2p-q)+} + q\mathrm{H}^+$ (1)
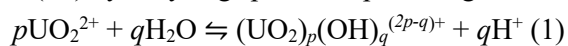
, and the calculation of their stability constants is followed by:

$\beta_{pq} = [(\mathrm{UO}_2)_p(\mathrm{OH})_q^{(2p-q)+}][\mathrm{H}^+]^q/[\mathrm{UO}_2^{2+}]^p$ (2)

.

where $[(UO_2)_p(OH)_q^{(2p-q)+}]$ represents the concentrations of U (VI) speciation at equilibrium condition, $[H^+]$ and $[UO_2^{2+}]$ are the equilibrium concentrations of H^+ and UO_2^{2+} in the hydrolysis reactions as a result of pH change.

However, there are differences among hydrolytic constants as result of various types of media. In the study of (Brown 2002), there were four media (NaCl, KCl, NaClO$_4$, NaNO$_3$ and KNO$_3$) used to investigate hydrolytic species of U(VI) via potentiometric titration. According to titration results, the species of UO_2OH^+, $(UO_2)_2(OH)_2^{2+}$, $(UO_2)_3(OH)_4^{2+}$, $(UO_2)_3(OH)_5^+$ were observed in all of media solution, while $(UO_2)_4(OH)_7^+$ was only detected in media of Na(K)NO$_3$ because of oxoanionic binding occurred in nitrate. Meanwhile, there were large deviation of the hydrolysis constants found in between perchlorate media and the others. In the case of $(UO_2)_2(OH)_2^{2+}$, it can be found that the hydrolysis constants at 298.15 K in 0.1 M NaCl or NaNO$_3$ solution were -5.74±0.04 and -5.75±0.05 respectively. However, the constant found in NaClO$_4$ was -5.91±0.04 under the same conditions (Brown 2002).
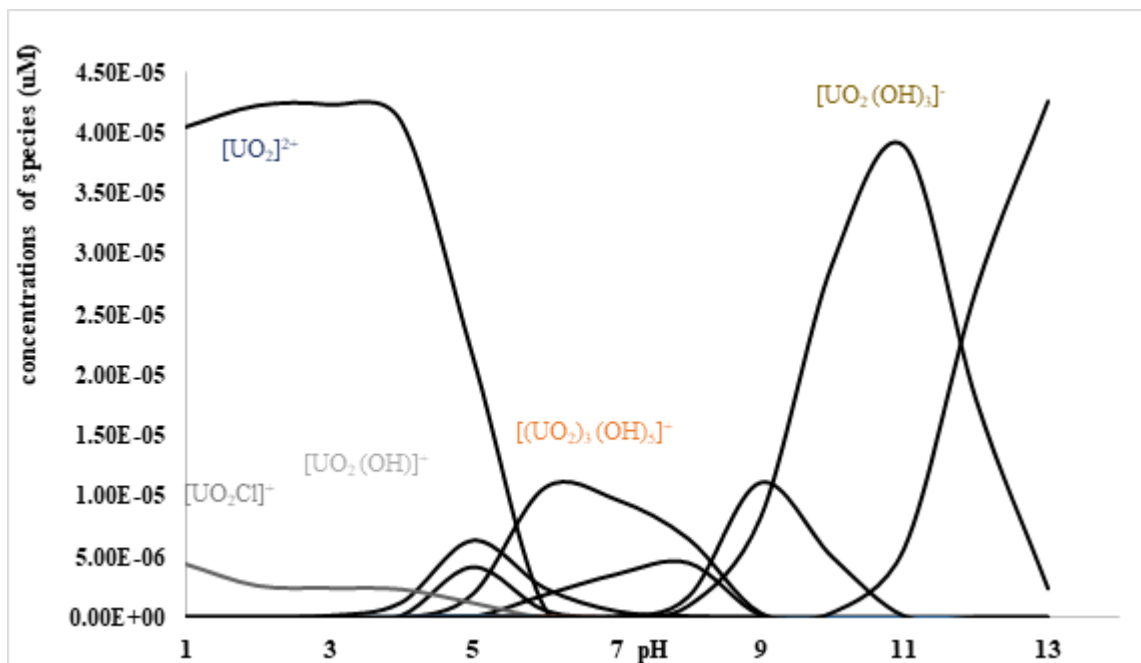
Figure 9 U(VI) speciation during its hydrolysis progress without the participating of CO2 under the condition of 0.2 atm O2, 42uM U(VI) and 0.1 NaCl solution.

2.1.1 Complexation of uranium(VI), vanadium (IV) and vanadium (V) with ligands with functional groups acetohydroxamic acid (hydroxamate), pyrocatechol (catecholate), acetic acid (α-carboxylate) and glycolic acid (β-carboxylate)

2.1.1.1 The influence of natural ligands

Previous studies showed organic ligands commonly found in near surface or deep underground environment has high affinity to metal ions including most of radionuclides can form metal-ligand complexes with high mobility to break through the second barrier and result in high-risk pollution (Kuippers, Morris et al. 2021). Determining the empirical relationship between ion strength and protonation constants of organic ligands complexing uranium and other toxic metals is central to the

accurate determination of the intrinsic protonation constants and its speciation in cement leachates (Thakur, Mathur et al. 2007).

In the case of the (tris)hydroxamate siderophore desferrioxamine B (DFOB), released from some of plants, bacterial and fungi, is widely distributed in a subsurface environment. It consists of six key functional groups: catecholate, hydroxamate, α-hydroxycarboxylate, α-aminocarboxylate, hydroxy-phenyloxazolonate, and α-hydroxyimidazolate. Since the chemical structure of DFOB is a linear hydroxamate one which contains three hydroxamate groups and an amine group, it has 4 different protonation constants (pKa) of 8.32, 8.97, 9.52 and 10.84 (Renshaw et al., 2002). The forms to react with U(VI) in these functional groups are the bidentate and monodentate structures by the ligands of O atoms and the monodentate one by the ligands of N atoms. Their stability based on the functional group interactions is followed by: α-hydroxycarboxylate (logβ=17.08); α-hydroxyimidazolate (logβ=16.55); catecholate (logβ=16.43); hydroxamate (logβ=9.00); hydroxy-phenyloxazolonate (logβ=8.43); α-hydroxycarboxylate bound via the carboxylate group (log β_{110} = 7.51) and α-aminocarboxylate (log β_{110} = 4.73) (Kirby et al., 2018). it can be found that the three species of functional groups, containing α-hydroxycarboxylate, α-hydroxyimidazolate and catecholate, dominate the complexing interactions with U(VI) since their stability is greater than that the other three of them. Therefore, ligands with high affinity to uranyl and vanadium ions play an important role in quantifying work to investigate environmental pollution.

Natural ligands with the functional groups including hydroxamate, carboxylate, α-carboxylate and catecholate are able to complex contaminant metal ions released from nuclear waste containers (Runde 2000). They are widely found in siderophores produced via biological activities of fungi, bacteria and vegetation (Ahmed and Holmström 2014).

The investigation of complexation of metal ions with organic ligands is the direct way to detect the effect of ligands on the mobility of contaminant metal ions in environment. In the study of Goncalves and Mota 1987, complexes between V(IV),U(VI) and phthalic acid indicates the effect of ion strength on the stability constants found in Table 5.

Table 5 Stability constants for vanadyl and uranyl systems with phthalic acid for the best model obtained with MINIQUAD (T = 25°C; I = 0.10, 0.40 and 0.70M in NaClO4)

	I (M)	Logβ_{111}[a]	Logβ_{110}	Logβ_{120}	Logβ_{222}	R
VO^{2+}	0.1	6.28 ± 0.08	3.97 ± 0.01	6.39 ± 0.06	1.75 ± 0.03	0.0002
	0.4	6.10 ± 0.07	3.68 ± 0.01	5.85 ± 0.06	0.27 ± 0.03	0.0002
	0.7	6.97 ± 0.09	3.61 ± 0.02	6.48 ± 0.07	0.74 ± 0.04	0.0002
UO$_2^{2+}$	0.1		4.742 ± 0.008	7.73 ± 0.03	2.37 ± 0.006	0.0022
	0.4		4.464 ± 0.006	7.38 ± 0.02	1.93 ± 0.05	0.0010
	0.7		4.43 ± 0.001	6.97 ± 0.04	1.58 ± 0.08	0.0032

a. Log$\beta_{n,m,l}$ represents metal-ligands complexes in the form of $M_nL_m(OH)_l$ in the table.

2.1.1.2   The interaction between hydroxamate (AHA) and uranium, vanadium

Hydroxamate is one of functional groups with high affinity to uranium and vanadium ions. Acetohydroxamic acid, one of organic acids normally is used to complex with metal ions since it is the simplest acid with only hydroxamate without other effects from extra functional groups. Previous studies have illustrated the measurement of stability constants during the progress of complexation of uranyl with acetohydroxamic acid. In the study of (Koide, Uchino et al. 1989), there were stability constants of 8.22 ± 0.03 and 15.30 ± 0.07 corresponding to two species $UO_2(AHA)^+$ and $UO_2(AHA)_2$ in 1.0 M KNO_3 solution at 25°C respectively. The measurement of U(VI)-AHA studies also were carried out in variable ion strength solution shown in Table 6. The complexation of vanadium (IV) and vanadium (V) with HAHA were investigated conducted by (Wehrli and Stumm 1989) shown in Table 7. it indicated the difference of stability constants between V(IV), V (V) and acetohydroxamic acid (HAHA) conducted by temperatures, it can be found their constants become larger as the increase of temperatures. Although many studies have pointed out precise stability constants of complexes under adaptive ion strength and temperature, the demand for establishing accurate quantification related to the field pollution is not specific because of variable electrolytes and temperatures. Therefore, it is necessary to use measured data and thermodynamic calculation like SIT, Davis equation and Debye Huckel equations to predict the effect of ion strength and temperature on contents of complexes in environment.

Table 6 stability constants of U(VI)-AHA species measured in $NaClO_4$ solution at 0.1M, 0.15M and 1.0M, at 25 °C (Chung, Choi et al. 2011)

Species	0.1M	0.15M	1.0M
$UO_2(AHA)^+$	8.22	7.62	7.22
$UO_2(AHA)_2$	15.30	14.25	14.89

Table 7 Stability constants of V(IV)-AHA and V(V)-AHA species found in temperatures of 35,40,45 and 50 °C, concentrations of V(IV) and V(V) = HAHA= 0.025mM titrated via 0.2 M NaOH (Wehrli and Stumm 1989).

Species	35°C	40°C	45°C	50°C
$VOAHA^+$	7.139	7.599	8.061	8.521
$VO(AHA)_2$	12.21	12.67	13.13	13.59
$V(AHA)_3^+$	17.04	17.50	17.96	18.42
$VAHA^{4+}$	7.021	8.011	9.202	11.10
$V(AHA)_2^{3+}$	10.11	11.05	12.31	13.21
$V(AHA)_3^{2+}$	11.30	12.21	13.12	14.33

2.1.1.3 The complexation of catecholate (PYR) and uranium, vanadium

Catecholate is one of functional groups to form extremely stable complexes with metal ions attributed to 2 deprotonated phenol groups with high binding ability. The study conducted by (Martell and Smith 1977) investigated complexing reactions between uranium (VI) and pyrocatechol according to their formation constants found in 4 complexing species (ML^0, MHL^+, MHL_2^- and $MH_2L_3^{2-}$) in Table 8. The species of V(IV)-catechol complexation are mainly [VOA] and [VOA$_2$]$^{2-}$ because of two major O$^-$ (Jezowska-Bojczuk, Kozłowski et al. 1990). In the spectrometry study, [VOA$_2$]$^{2-}$ and all the bis(catecholate) species are stable to hydrolysis as pH>12(Jezowska-Bojczuk, Kozłowski et al. 1990).

Table 8 Stability constant for complexation of U(VI) and catechol in solutions with an ionic strength of 0.7 M NaClO$_4$, and the complexation of oxovanadium with catechol in spectrometry (M^{2+} means UO$_2^{2+}$ and M* means VO^{2+}, L^{2-} means catechol)

Reaction	logK	Ref.
$LH^- = L^{2-} + H^+$	-12.99	(Martell and Smith 1977)
$LH_2 = LH^- + H^+$	-9.19	
$M^{2+} + L^{2-} = ML$	15.8	
$M^{2+} + HL^- = MHL^+$	6.2	
$ML + HL^- = MHL_2^-$	4.9	
$MHL_2^- + HL^- = MH_2L_3^{2-}$	3.7	
$M^*ws^{2+} + L^{2-} = M^*L$	16.75±0.02	(Jezowska-Bojczuk, Kozłowski et al. 1990)
$M^{*2+} + 2L^- = M^*L_2^{2-}$	31.58±0.03	
$M^* + HL^- = M^*HL^-$	10.21±0.15	
$2M^* + 2HL^- = (M^*HL)_2^{2-}$	22.92±0.24	

2.1.1.4 The complexation of uranium, vanadium and glycolic acid (GA)

Glycolic acid is a typical ligand for α-hydroxycarboxylic chelate. The complexation of metal ions and this acid normally was conducted by low pH condition (around pH=3). Although the binding method is similar to acetate (carboxylate replacement), the stability constant of its complexes is higher than other carboxylate ligands since glycolate contains an extra hydroxy group (α-OH) rather than CH$_3$ group and contains two oxygen atoms to improve electrodensities during its deprotonation. In the potentiometric investigation, [ML$^+$] dominated the large portion of products, with an equilibrium constant logK$_{[ML^+]}$ = -1.26±0.16 and logβ = 2.32±0.16 for this reaction according to a slope analysis (0.98±0.11) to validate reactions (Moll, Geipel et al. 2003). Due to the available pH limitation in potentiometric titration measurement, the complexation of U(VI) with the fully deprotonated glycolate [ML$_2$] cannot be detected as the fully deprotonated glycolic acid found at pH > 17. In the study of (Szabó and Grenthe 2000) and (Kirby, Sonnenberg et al. 2020) species produced from U(VI)-α-hydroxycarboxylate were proposed to represent [ML$^+$], [ML$_2$]^0 and [ML$_3$]$^-$ with their log β of 2.42±0.02, 3.92±0.03 and 4.20±0.05

respectively. The progress of uranium co-ordinate with α-hydroxycarboxylate form a bidentate complexes through U(VI) binds a carboxylate O and a deprotonated hydroxy group as pH>5 where pKa of the ligand will decrease from pH>17 to 3.64 (Kirby, Simperler et al. 2018).

According to the study of potentiometric titration, V(IV)-glycolate species were found in the form of $[ML]^+$, $[ML_2]^0$ and $[ML_3]^-$ with 2.56±0.01, 4.22±0.02 and 5.19±0.22 in $NaClO_4$ solution respectively (Di Bernardo, Tomat et al. 1988). The coordinated progress between V(IV) and glycolic acid is similar to the binding method occurred in U(IV)-glycolate complexing system where their binding sites also found at an oxygen from a carboxylate group and a deprotonated hydroxy group (Di Bernardo, Tomat et al. 1988). Meanwhile, an extra attention focus on glycine, one of α-hydroxycarboxylate ligands with three possible coordinated site-NH_3, -OH and -COOH, was only found 2 species $[ML]^-$ and $[ML_2]^0$ with logβ of 1.06±0.09 and 2.25±0.15 respectively.

Table 9 stability constants for the formation of U(VI) and V (IV) coordinated with glycolic acid at 25˚C and 1 mol dm^{-3} $NaClO_4$ solution.

Species	logβ	Ion strength (mol·dm^{-3})	medium	Ref.
$UO_2(GA)^+$	2.35±0.01	1.0	$NaClO_4$	(Di Bernardo, Tomat et al. 1988)
$UO_2(GA)_2^0$	3.97±0.04	1.0	$NaClO_4$	
$UO_2(GA)_3^-$	5.12±0.05	1.0	$NaClO_4$	
$VO(GA)^+$	2.56±0.01	1.0	$NaClO_4$	(Di Bernardo, Tomat et al. 1988)
$VO(GA)_2^0$	4.22±0.02	1.0	$NaClO_4$	
$VO(GA)_3^-$	5.19±0.02	1.0	$NaClO_4$	

2.1.1.5 The complexation of uranium, vanadium and acetic acid (AA)

Acetic is one of carboxylate with only one a coordination site provided by some oxygen from -COOH acid in comparison of glycolic acid or glycine. Although the ligand complexes U(VI) and V(IV) to form similar numbers of species and form bidentate fashion complexes in each acetate group, their stability is lower than ones containing α-hydroxycarboxylate coordination since its carboxylate is at the end of ligand and no monodentate binding structure supported via hydroxy group (Lucks, Rossberg et al. 2012). Their complexes containing U(VI) in the form of $[ML]^-$, $[ML_2]^0$ and $[ML_3]^-$ with 2.37±0.03, 4.37±0.14 and 6.86±0.04 at 25˚C in 1.0 mol dm^{-3} $NaClO_4$ solution (Jiang, Rao et al. 2002). As for V(IV), the stability of their complexes is lower than ones coordinated with U(IV) since the effective charge found in uranyl ions is higher than in vanadyl ions according to complexing formation governed by electrostatic forces (Di Bernardo, Tomat et al. 1988). Stability constants of Vanadyl-acetate complexes were provided by their thwo species of $[ML]^-$ and $[ML_2]^0$ which were 1.97±0.02 and 3.46±0.02 at 25˚C in 1.0 mol dm^{-3} $NaClO_4$ solution (Di Bernardo, Tomat et al. 1988). The summary of stability constants for acetate complexes with uranyl and vanadyl ions were provided in Table 10.

Table 10 stability constants for acetate complexes coordinated with uranyl and vanadyl at at 25°C in 1.0 mol dm^{-3} NaClO$_4$ solution

Species	logβ	Ion strength	Ref.
UO$_2$(AA)$^+$	2.37±0.03	1M	(Jiang, Rao et al. 2002)
UO$_2$(AA)$_2^0$	4.37±0.14	1M	
UO$_2$(AA)$_3^-$	6.86±0.04	1M	
VO(AA)$^+$	1.97±0.02	1M	(Di Bernardo, Tomat et al. 1988)
VO(AA)$_2^0$	3.46±0.02	1M	

2.2 Activity correction for dissociation constants of ligands: Derby-Huckle equations, Davis equation, Specific Ion Theory

Ion strength as an essential factor in the measurement of dissociation constant for organic acid and stability constants for the complexation of metal ions with organic acid (Daughney and Fein 1998, Cao, Lam et al. 2004, Nagai, Kuwabara et al. 2008). However, the validity of their constants measured from experimental conditions containing setting variable ion strength and electrolyte medium is not persuasive without systematic calculations. For example, intrinsic dissociation constant (acquired as I=0) is not available via fitting groups of dissociation constants obtained at different ion strength because of data from low ion strength or high ion strength lacking linear relationships. Meanwhile, utilization of literature data for aqueous ionic equilibria is hampered that the lack of ionic activity correction formula of demonstrated validity for solution of medium to high ionic strength (Sun, Harriss et al. 1980). The manipulation of activity correction practically denotes relationship between equilibrium constants as well as stability constants and ion strength, and is normally presented by calculating required activity coefficient. The demands for predictive electrolyte equation of state are tough and depend greatly on the application (Kontogeorgis, Maribo-Mogensen et al. 2018). Some empirical equations have been developed to acquire the coefficient with respect to correction to infinite dilution at variable ranges of ion strength applied in experiments and will be provided by following contents

2.2.1 Debye Huckel and extended DH (parametrisation)

In the determination of ionization constants (acid dissociation constants) and the pH values of acid and base in moderate concentrations, activity coefficient is expressed in terms of certain natural and derived constants (Manov, Bates et al. 1943). Derby Huckel equation (DH) one of popular methods to calculate activity coefficient is widely used in many studies (Manov, Bates et al. 1943, Sun, Harriss et al. 1980, Gagliardi, Castells et al. 2007). The equation is written as:

$$\log \gamma = -0.51z^2 \left(\frac{\sqrt{I}}{1+A\sqrt{I}} + BI \right) \qquad (4)$$

Where ɤ, z and I means activity coefficient, charge numbers of ion and ion strength in targeted solution respectively, while z^2 equals to $\sum (Z_{reactant}^2)$ - to $\sum (Z_{product}^2)$. Parameter A and B are constants depending on reactive temperature and Boltzmann constant relative to temperature in solution

respectively. The calculation for these two parameters has already developed to support accurate calculation of activity coefficient followed by (Manov, Bates et al. 1943):

$$A = (1.82455 \times 10^6)/(DT)^{1/2} \qquad (5)$$

$$B = (50.2904 \times 10^{-8})/(DT)^{1/2} \qquad (6)$$

Where D and T is dielectric constant and temperature respectively. Normally, where required activity coefficient ɤ is calculated at 25°C, thus A and B equals 0.509 and 0.328 respectively.

The prediction of equilibrium constants at low ion strength from at high ion strength can be relied on extended Debye Huckel equation (EDH) (Linder and Murray 1982). The application of EDH in comparison of DH shows larger range of ion strength (<0.1M) and is widely used to study activity correction (Linder and Murray 1982, Northover, Mao et al. 2021). Meanwhile, EDH involving ionic size as an important role in activity correction improves the accuracy of ɤ values in the system. The equation is similar to DH written as:

$$\log ɤ = -0.51z^2 \left(\frac{\sqrt{I}}{1+A\sqrt{I}} + B\alpha_i I\right) + CI \qquad (7)$$

where C and α_i is the only adjustable parameter and ionic size parameter estimated provided by (Kielland 1937), respectively.

The improvement of EDH is based on not only the precise parameter A and B, but also parameter C. therefore, there is a presumptive complexing reaction as an example to explain EDH theory (Linder and Murray 1982). According to a normal formula:

$$pM^{m+} + qL^{n-} \leftrightarrow M_pL_l^{(pm-qn)} \qquad (8)$$
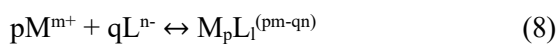
where m and l means charge numbers found in metal M ions and ligand L respectively. According to different equilibrium constants obtained at different ion strength, we assumed that K' and K'' are the constants measured from solution at ion strength of I' and I'' (Linder and Murray 1982), thus:

$$K'' = I'' K'/I' \qquad (9)$$

In equation (9), each I' is a quotient and expressed by:

$$I' = (ɤ_M)^p (ɤ_L)^q/ɤ_{M^p L}{}^q \qquad (10)$$

where $(ɤ_M)^p$, $(ɤ_M)^p$ and $ɤ_{M^p L}{}^q$ represents activity coefficient of species participated in the complexation above. These values is calculated possibly due to known C and α_i from EDH. When α_i is invalid, we can use the following equations (Kielland 1937):

For small organic ions: $\alpha_i = z_i + 4 \qquad (11)$

For small inorganic ions: $\alpha_i = 2z_i + 2$

In the next step, parameter C is same as the assumption in any equilibria complexation. Therefore, combing equation (9), (10) and EDH, it can be expressed as:

$$\log K'' = \log K' + A\int \left(\alpha_i, (I^{\frac{1}{2}})\right) + C(I''-I')(1-p-q) \qquad (12)$$

where,

$$\int \left(\alpha_i, (I^{\frac{1}{2}})\right) = (pz_M + qz_L)^2 \left(\frac{\sqrt{I''}}{1+A\sqrt{I''}} + B\alpha_{M_pL_q}I''\right) - \frac{\sqrt{I'}}{1+A\sqrt{I'}} + B\alpha_{M_pL_q}I') -$$

$$pz_M{}^2 \left(\frac{\sqrt{I''}}{1+A\sqrt{I''}} + B\alpha_M I''\right) - \frac{\sqrt{I'}}{1+A\sqrt{I'}} + B\alpha_M I') - qz_L{}^2 \left(\frac{\sqrt{I''}}{1+A\sqrt{I''}} + B\alpha_L I''\right) - \frac{\sqrt{I'}}{1+A\sqrt{I'}} + B\alpha_L I')$$

thus, the value of C is dependent on equation (11) to predict activity coefficient in EDH.

2.2.2 Davies equation

In fitting NaOH activity coefficient via four models (Figure 10), the experiment was practically calculate activity coefficient of OH⁻ via the variation of NaOH concentrations in the solution (from 0 to 1.0 mol·dm⁻³). Since the dissociation constant and activity of water and the molarity of alkaline were known, the activity coefficient of the alkaline can be measured and resulted in the pH difference referred to the theoretical values (Hausmann, Traynor et al. 2021). it can be found that Pitzer function shows the best fitting results among others and matches experimental data closely. However, DH and EDH accounted for significant deviations found at approximately 0.05 mol dm⁻³ and 0.1 mol dm⁻³ respectively. Compared with DH and EDH, there was only small deviation presented at around 0.5 mol dm⁻³ found in Davies equation (DE) model. The fitting results were also allowed by effective ion strength ranges up to 0.5 mol dm⁻³ for DE (Pankow 2018). Despite a persuasive ability to fit activity coefficient in Pitzer model, DE indicated an easier manipulation property with a simple equation provided by:

$$\log \gamma = -z_i^2 A I^{1/2} / [(1+3 \times 10^{-10}) B I^{1/2}] + C z_i^2 A I / 1000^{1/2} \text{ and } C = 0.2 \quad (13)$$

In many cases, DE also can be expressed as:

$$\log \gamma = -z_i^2 A [I^{1/2}/(1+I^{1/2}) - 0.3 \, I] \quad (14)$$
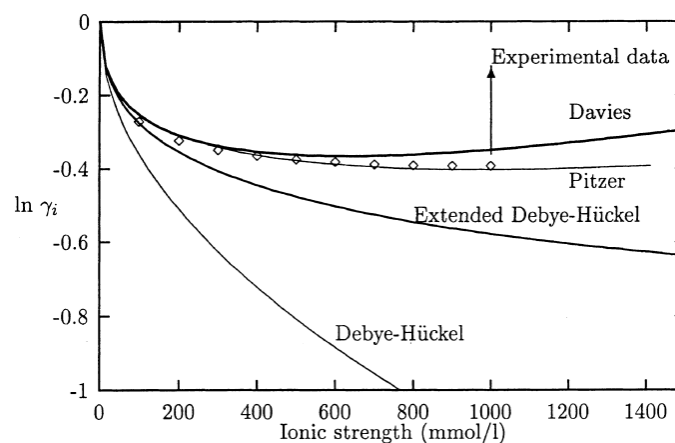
Figure 10 Comparison of NaOH activity coefficient for different models (Samson, Lemaire et al. 1999)

Nevertheless, the extra attention, interpreted the advantages of DE compared with DH and EDH, denoted the fact that DE tends to fit model to experimental values up to 0.5 mol·dm⁻³ reliably. DH is not suitable to fit data at extremely low ion strength (< 0.1 mol·dm⁻³) in Figure 10 (Li and Page 1998). Despite the obvious advantage of EDH, The value of α_i will lead to a large deviation in activity coefficient as the higher concentrations in solution (Samson, Lemaire et al. 1999). This behaviour is attributed to the less free water molecular as the increase of ionic concentrations (Bockris, Reddy et al. 1998). Moreover, due to the lack of knowledge of α_i, this value normally was regarded as a parameter with little physical meaning to fit models to experimental values, and it, therefore, was presented as negative values for catering to experimental data in some of cases (Shedlovsky 1943, Samson, Lemaire et al. 1999). In the study of (Sun, Harriss et al. 1980), since DH (eq. 4) model can be converted to DE as A = 1.0, B = -0.2 (Davies 1938), it summarized a modifeid DH model adaptive to ion strength rangeing from 0 to 0.5. the equation can be expressed as:

$$\Delta \log K = -0.51 z^2 [I^{1/2}/(1+A I^{1/2}) + B I] \quad (15)$$

In recent work, B is also used as -0.3 in DE. when A = 0.33α_i and B=0, the equation is referred to DH and α_i means the effective ion diameter in A. In some of the cases, A=1.5, B=0 were suggested as the parameters in eq. 15, while as ion strength was less than 0.1 mol·dm^{-3}, the values of A and B can be equal to 1.0 and 0 respectively (Sun, Harriss et al. 1980).

2.2.3 Pitzer equation

The application of Pitzer equation for calculating activity coefficients was invincible in terms of the considerations of substantial interaction parameters (Pitzer and Press 1991). Furthermore, it was reported that the use of Pitzer equation covered more available ranges of ion strength (Lopes, Farelo et al. 2001). In the study of (Liang, Lin et al. 2021), Pitzer equation as a form of virial equation derived from excess Gibbs free energy of electrolytic solutions and the Debye-Huckle equation with additional terms. Thus, the common equation involving three parameters was written by:

$$\ln_{\gamma\pm} = |Z_M Z_X| \int x + m(\frac{2v_M v_X}{v_M+v_X})B_{MX}^{\gamma} + m^2 \times \frac{2(v_M v_X)^{\frac{2}{3}}}{v_M+v_X} C_{MX}^{\gamma} \qquad (16)$$

and

$$\int x = -A[\frac{I^{\frac{1}{2}}}{1+bI^{\frac{1}{2}}} + \frac{21+bI^{\frac{1}{2}}}{b}] \qquad (17)$$

where $_{\gamma\pm}$ is the mean activity coefficient; v_M and v_X are the numbers of M and X ions in moles, and Z_M and Z_X means the charge numbers of M and X. m is the molarity. In Eq. 27, A and b are respective to the Debye-Huckle constant related to osmotic function and Boltzmann constant. B_{MX}^{γ} and C_{MX}^{γ} represent the second and the third virial parameters (Liang, Lin et al. 2021). The calculation of Pitzer equation was similar to a polynomial form especially in the case of the compensating interaction parameters (Thakur, Mathur et al. 2007).

2.2.4 Specific ion interaction theory (SIT)

Pitzer equations compared with DH,EDH and DE tend to be quite complete and available for modelling activity correction in wider range of ion strength in Figure 10. However, they are complicated and difficult to handle because of multiple parameters and restricted ionic conditions (Bretti, Foti et al. 2004). Meanwhile, the use of other three models is not applicable as ion strength in excess to 0.5 mol dm^3. The approach SIT is a prevalent replacement for activity correction modelling from 0.5 mol dm^3 to 3.0 mol dm^3 due to the simple operation only required one parameter (Bretti, Foti et al. 2004, Thakur, Mathur et al. 2007, Majlesi and Rezaienejad 2009).

SIT was derived from the Debye-Huckle equation (DH) but introduced a new concept related to interaction coefficients ϵ which is relied on ion properties and dependent of ion strength and temperature. The simplest expression of this model is following by:

$$\log\gamma = -z^2 D + \sum \epsilon m_i \qquad (18)$$

where D is the term of DH equals to $AI^{1/2}/(1+bI^{1/2})$, b, an empirical constant regarding the closest mean distance of ion from Debye-Huckle limit law, is normally phrased as 1.5 (Scatchard 2013). $\sum \epsilon m_i$ represents a parameter to reflect species ion of non-electrostatic interaction between ion strength and other species in the system (Majlesi and Rezaienejad 2009). To understand the relationship between activity coefficients and interaction coefficients, The theory assumes a single binary electrolyte $M_{v+}Y_{v-}$ (M^{z+}, Y^{z-}) in presence of targeted solution (Bretti, Foti et al. 2004). Thus:

$\Upsilon_{\pm} = (\Upsilon_{\pm}^{v+}, \Upsilon_{\pm}^{v-})$ (19)

and for equation (20), SIT can be extended to:

$\log \Upsilon_{\pm} = -(z^+ z^-)D + \varepsilon(M_{v+}Y_{v-})m_i[(2v^+v^-)/v] = = -(z^+ z^-)D + \varepsilon(M_{v+}Y_{v-})2m_iv$ (20)

where M, Y mean cations and anions in the system respectively, v^+, v^- mean number of cations and anions of per molecule electrolyte respectively and z^+, z^- represent number of charges in cations and anions respectively. while ε can be expressed as:

$\varepsilon = a + b(1+\log I)$ (21)

where a and b are true constant, combing Pitzer model:

$\varepsilon = \varepsilon\infty + (\varepsilon_0 - \varepsilon\infty)F(I)$ (22)

where $F(I) = [1-(1+2I^{1/2} – 2I)\exp(-2I^{1/2})]/4I$ (23)

with

$\lim_{I \to 0} F(I) = 1$

$\lim_{I \to \infty} F(I) = 0$

Therefore,

$\lim_{\varepsilon \to 0} \varepsilon = \varepsilon_0$

$\lim_{\varepsilon \to \infty} \varepsilon = \varepsilon\infty$

Another class of F(I) in eq. 24 can be expressed as:

$F(I) = \exp(-2I^{1/2})$

In the study of (Thakur, Mathur et al. 2007), $\sum \varepsilon m_i$ represents a slope in a linear relationship between $pKa_i + -z^2D$ and I. and the intercept is the intrinsic pKa value.

2.3   Application of Van't Hoff equation to determine thermodynamic parameters

The determination of pKa or stability constants for deprotonated and complexing reactions is influenced by not only ion strength but also temperature in solution. Previous studies measured dissociation constants and stability constants and calculated their thermodynamic parameters containing Gibbs' energy (ΔG), enthalpy (ΔH) and entropy(ΔS) related to temperature (Di Bernardo, Tomat et al. 1988, Ali, Fatima et al. 2005, Fazary 2005). The manipulation generally is to measure equilibrium constants at known T to plot lnK vs. 1/T , then the values of ΔG, ΔH and ΔS of acquired slope and intercept can be induced by known gas constant.

Table 11 Dissociation constants and thermodynamics parameters ΔG, ΔH and ΔS found in acetohydroxamic acid calibrated via Van't Hoff equation at 298.15K in water and dioxane solution.

I (mol·dm^{-3})	lnK	ΔG (kJ mol^{-1})	ΔH (kJ mol^{-1})	ΔS(J mol^{-1}K^{-1})	Ref.
0.00	9.28	12.77	10.73	6.84	Fazary 2005
0.083	9.49	13.07	10.73	7.85	
0.174	9.88	13.61	10.94	8.96	
0.33	10.28	14.11	12.83	4.30	

The expression of dissociation constants and stability constants for targeted organic acids and metal-ligand complexes depending on temperature is demonstrated via fitting Van't Hoff equation:

$$d\ln K/dT = \Delta H/RT^2 \qquad (24)$$

where $\ln K$ is the equilibrium constant for deprotonated and complexing reactions. ΔH is the enthalpy change in the reaction progress and R is gas constant (8.314 J mol^{-1}K^{-1}). It can be found that plotting $\ln K$ versus $1/T$ indicates a linear relationship with a slope of $\Delta H/R$ in eq.28. The value of ΔH in Gibbs' energy can be written by:

$$\Delta H = \Delta G + T\Delta S \qquad (25)$$

where ΔG and ΔS are Gibbs' energy change and entropy change in the system. At equilibrium condition, the relationship between $\ln K$ and ΔG can be plotted:

$$\Delta G = -RT\ln K \qquad (26)$$

Thus, the enthalpy and entropy can be calculated via obtained T and $\ln K$ expressed as:

$$\ln K = -\Delta H/RT^2 + \Delta S/R \qquad (27)$$

However, there is a shortage in some of cases since the value of ΔS is sensitive to T change. It will lead to a large deviation with fitting model and lack of validity to examine thermodynamic parameters.

2.4   HYPERQUAD for analysing potentiometric titration data

The application of HYPERQUAD is widely used to analyse thermodynamic studies like the determination of dissociation constants, and stability constants occurred in deprotonated and complexing progress. In many cases, potentiometric titration employed as main experimental sector detects electric signal referred to pH or concentration of H$^+$, then HYPERQUAD as main analysing sector calculates and determines equilibrium constants for targeted reactions later (Meloun, Ferenčíková et al. 2011, Fazary, Awwad et al. 2020).

In potentiometric titration measurement, concentrations of reactants and products will be represented via Nernst equation. For instance, in the deprotonated progress of a ligand (Fazary, Awwad et al. 2020), the reactive formula is normally expressed as:

$$H_aL = aH^+ + L^{a-} \qquad (28)$$
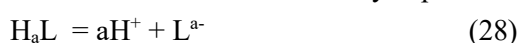
therefore, its equilibrium constant can be written as:

$$K_{HaL} = [H^+]^a[L^{a-}]/[H_aL] \qquad (29)$$

Where [H$_a$L], [H$^+$] and [L^{a-}] represented free concentrations of acids, hydrogen ions and ligands respectively. For dissociation reaction at constant ion strength, in many cases, The deprotonation of H$_a$L will arrive at equilibrium stepwisely. Thus, its equilibrium constant can be written as: $K_{a,j} = [H_{j-1}L]a_{H}^+/[H_jL]$, and the mass balance equations for L and H are following by:

$$L = [L^{a-}] + \sum_{j\to 1}^{j} K_j[L^{a-}] \qquad (30)$$

and:

$$H = [H^+] - K_w/[H^+] + \sum_{j\to 1}^{j} K_j[L^{a-}]$$

therefore, the potentiometric reading based on difference between working electrode and reference electrode can be written as:

$$E_{cell} = E^0 + (f.RT\ln10/F)\log a_{H}^+ + j_a a_{H}^+ - j_b K_w/a_{H}^+ - E_{ref} = E^0 + Slope\log[H^+] \qquad (31)$$

where E^0 is the standard potential of a glass electrode cell. K_w is the operational ion product of of water at a fixed temperature (T). and $a_H^+ = [H^+]y^+$, the liquid-junction potential E_j can be phrased as: $E_j = j_a a_H^+ - j_b K_w/a_H^+$. and slope = $(f \cdot RT\ln10)/F$ which is the slope of a glass electrode for a Nernstian response and f is the correction factor taken as an adjustable parameter.

According to the effect of the addition of titrant on concentrations of H^+ or measured potential of the targeted in constant ion strength solution. The relationship between volume of titrant from burette V_i and detected E_{emf} or a_H^+ with a vector of unknown parameters (b), is can be written as:

$V_i = \int(pH, b) = \int(pH;\ KHaL, p)$

where K_{HaL} and p mean stepwise dissociation constants and parameters applied in eq. 35 respectively. it can be recognised the vector of unknown parameters b consists of the total constants and parameters influencing values of eq. 35. Therefore, $p = (E_0, S, K_w, j_a, j_b, L_0, L_T, H_0, H_T)$, where L_0 and H_0 represent initial total concentrations of ligand and hydrogen ions in solution, and L_T and H_T means consuming quantities of concentrations of ligand and hydrogen ions derived burette.

In simulation of HYPEQUAD, the program is permitted by minimizing the error squares sum of potentials (U_b) (Urbaniak and Kokot 2009). The fitting equation refers to:

$U_b = \sum w_i(pH_{mea} - pH_{calc})^2$ (33)

where pH_{mea} and pH_{calc} mean pH values measured by the electrode and ones by the program calculation respectively. The pH_{calc} values is specifically calculated in the program iterating refinement of the deprotonation or complexing reactions (Gans, Sabatini et al. 1996). To be explicit, the equation employed via HEPERQUAD can be phrased as:

$U = e_T we$ or $= \sum_{i \to 1}^{n} w_i e_i^2$ (34)

where e is a vector of residues and represents a measurement in mV or pH, and w is a weight matrix. The SIGMA values is a criterion classifying the goodness of a fitting progress. It is a chi-squared statistic of the randomness where residues should follow the normal-distribution referring to:

$$SIGMA = \sqrt{\frac{\sum w_i e_i^2}{n-m}}$$

where the wights are calculated from the estimation of emf or $[a_{H+}]$. As the sigma is around 12 or less, the residues is allowed by the normal distribution (Gans, Sabatini et al. 1996). In the determination of pKa values, the fitting equation can be written as:

$U_b = \sum w_i(pKa_{mea} - pKa_{calc})^2$ (35)

and the calculation of pKa values is allowed by EDH referring to (Meloun, Ferenčíková et al. 2011):

$pKa = pKa^T - A(1-2z)I^{1/2}/(1+BaI^{1/2})$ (36)

and pKa^T values is an estimated one which is developed from empirical data (Meloun, Syrový et al. 2004, Meloun, Ferenčíková et al. 2011).

3   Methodology

3.1   Experimental design

To investigate the effect of ion strength and temperature on dissociation constants for HAHA, GA, AA and PYR, this work consisted of the measurement of potentiometric titration, thermodynamic calculation and activity correction. In the determination of pKa values among these 4 ligands, data analysis will be calibrated via HYPERQUAD analysis, then the method of EDH, DE and SIT were

employed to calculate the intrinsic pKa values for model fitting related to ion strength change, the thermodynamic calculation based on Van't Hoff equation was applied to identify their thermodynamic parameters during the ligand protonation.

3.2 Chemicals

Sample solution placed in vessel tested by potentiometric titration was divided into four different groups consisting of ligands, electrolyte and deionized water. The source of ligands came from acetohydroxamic acid (>98% $C_2H_5NO_2$, molar weight (MW) 75.06 g mol^{-1}, CAS No. 546-88-3) provided by Thermo Scientific, pyrocatechol (>99% $C_6H_6O_2$, MW 110.11 g mol^{-1}, CAS No. 120-80-9) provided by Sigma-Aldrich, glycolic acid (>99% $C_2H_4O_3$, MW 76.05 g mol^{-1}, CAS No. 79-14-1) provided by VWR and acetic acid (>99.7% H_3CCOOH, MW 60.05 g mol^{-1}, CAS No. 64-19-7) provided by VWR. The selection of electrolyte is sodium chloride (NaCl) (>98% NaCl, MW 58.44 g mol^{-1}, CAS No. 7647-14-5) provided by VWR. The deionized water was produced from 15 MΩ filter system. In Acid-base titration work, The choice of hydrochloric acid (HCl, 1 mol·dm^{-3}), MW 36.45, CAS No. 7647-01-0) and sodium hydroxide (NaOH, 1 mol dm^3, MW 58.44, CAS No. 7647-14-5) was used as acid and base solution respectively. The deaeration treatment was conducted by oxygen-free nitrogen gas (N_2) in 230 bar cylinder supported by BOC.

3.3 Analytic techniques

3.3.1 Potentiometric equipment and procedure

Potentiometric analysis was performed using a Metrohm 888 Titrando. 826 pH mobile (a pH meter) was used to improve the sensitivity calibration of the glass electrode in the Titrando, and data was automatically collected by the software Tiamo Ver. 2.4.

Figure 11 photography of potentiometric titration and pH meter

The pH meter was calibrated employing pH buffer solution (provided by VWR) with pH at 4, 7, 10 and 13. A pH calibration with 4 pH values was shown in Figure 11. Three duplications for each pH value (Std within ±0.016) were recorded and the statistics analysis via the linear regression function (pH values on y axis, potential values on x axis) using keyword LINEST in Microsoft Excel. According to

the regression line formula in Figure 12, the value of R equals to 1 which means the high goodness of reproducibility. The calibration of acid and base solution is the first step before all the measurements, since source of HCl and NaOH were bought from VWR with known concentrations, the calibration titrations was only carried out for 3 times and ensure the variance in the fourth decimal place. For all potentiometric titration measurements, the electrode couple was standardized (Glee test) in terms of pH = log[H$^+$] (concentration of free hydrogen ions) via the addition of strong acid like HNO$_3$ or HCl at a constant rate with the base solution (NaOH) to determine the potential E^0 (where concentrations of acid equals to the ones of base) (Cardiano, Falcone et al. 2011). In this study, Glee test was taken by that HCl as the acid titrant at rate of 0.2 mmol s^{-1} was added into 32 ml solution consisting of 2 ml of 1 mol dm^{-3} NaOH base solution and 30 ml deionized water. A water bath (provided by Galanze) was used to control temperature of solution at 25°C consistently. The purifying treatment for sample solution employed N$_2$ gas purging to avoid O$_2$ and CO$_2$ contamination.
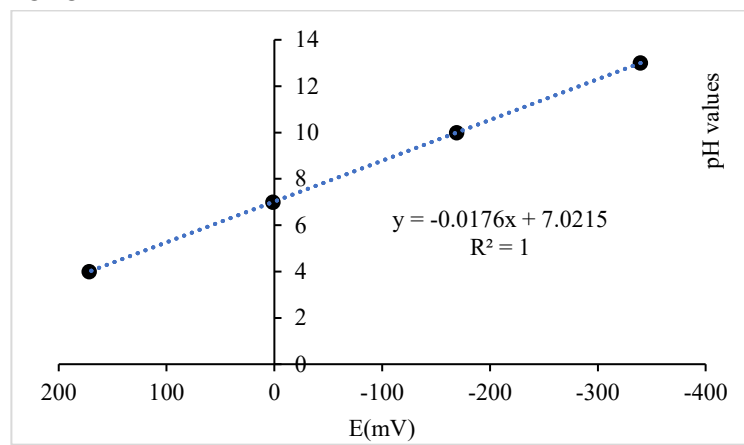

Figure 12 a pH calibration with four points at pH of 4, 7, 10 and 13, E(mV) is the potential values measured from a pH meter. In the linear regression function, it indicated that potential measured via the electrode exhibited a high reliability of pH values. As X equals to 0, which means the standard solution at neutral condition and pH equals to 7.02.

The determination of E^0 was described above in the way of Glee test by Gran method calibration. The method in the operation is to use a strong acid (0.1 M HCl) with given concentrations of H$^+$ to titrate with a strong base (0.1 M NaOH) with given concentrations of OH$^-$ in the galvanic cell (Rossotti and Rossotti 1965). Therefore, the potential variation can be expressed regarding the used volume of acid:

$$E = E^0 - RT\ln[H^+]_{\gamma H}/F - E_j \qquad (41)$$

Where E^0 is the potential of the reference half-cell and the standard potential of the probe half-cell, E$_j$ is the liquid junction potential. Thus, the concentrations of [H$^+$] can be written as:

$$[H^+] = (V_H - v^B)/(V + v) = VH(v_e - v)/v_e(V + v) = B(v_e - v)/V + v \qquad (42)$$

where V is the used volume of the strong acid, v is the given volume of base solution. B is concentrations of base solution, and v$_e$ is the volume of base solution at equivalence point. Therefore, the function to indicate [H$^+$] replaced with pH values:

$$\phi = (V + v)[H^+]_{\gamma H} = (V + v)10^{-pH} \qquad (43)$$

From equation (42) and (43):

$$\phi = (v_e - v)B_{\gamma H} \qquad (44)$$

from eq. 42, pH can be converted to the value of the potential E:

$$\psi = (V + v)10^{-EF/2.303RT} \qquad (45)$$

from eq. (41), (42) and (45):

$$\psi = 10^{-(E0 - Ej)F/2.303RT}(v_e - v)B_{\gamma H} \qquad (46)$$

After the equivalence point,

$$[H^+] = K_w/[OH^-] = K_w(V + v)/B(v-v_e) \qquad (47)$$

For use in alkaline range, function ϕ and ψ may be defined as:

$$\phi' = (V + v)[H^+]_{\gamma H} = (V + v)10^{pH} \qquad (48)$$

and $\psi' = 10^{-(E0 - Ej)F/2.303RT}(v_e - v)B_{\gamma H}/K_{w \gamma H} \qquad (49)$

therefore, as $K_{w, \gamma H}$ and E_j are constant at modified ion strength and temperature, the functions (ψ) and (ψ') show a linear relationship and both of two functions intersect at point of v_e which is the location to determine initial E in the Gran method. During the progress of measurements, five different ion strength (0.1, 0.5, 1.0, 2.0 and 3.0 M) and three different temperature (298.15K, 315.15K and 335.15K) were employed to investigate the impact of I and T on dissociation constants of targeted acid. Therefore, the determination of E^0 (the initial potential) with respect to the modified I and T was shown in Table 12.

Table 12 The determination of E_0 via Glee test in potentiometric titration. Ion strength (0.1, 0.5, 1.0, 2.0 and 3.0 M) adapted via NaCl solution and temperature (298.15,315.15 and 335.15K) controlled by water bath. The standardization was carried out from Feb of 2021 to Aug of 2021.

T	0.1 M	0.5 M	1.0 M	2.0 M	3.0 M
298.15K	394.1	401.1	402	413.85	423.65
	391.3	401.1	403.6	414.05	424.6
315.15K	413.9	418.8	422.2	435.83	445.2
	413.2	419.4	420.1	432.3	448.1
335.15K	/	/	437.5	444.05	458.9
	/	/	436.1	445.5	457.3

From eq 45, the determination of pKw influence results of K_w values. However, the species of electrolyte as well as the two factors (ion strength and temperature) is related to the collected data in Glee test in Table 13. In the determination of pKa values among targeted ligands, the required temperature was controlled by a water bath, and a thermal meter was used to calibrate T in sample solution. The prefixed ion strength in the study was modified concentrations of NaCl in the electrolyte solution. The lab balance (Sartorius) with 0.01g readability was employed to weigh NaCl converted from mole weight (mole) to mass (g), and the volume of DI water was replaced with the mass weighed by the balance as well, while the lab balance with 0.1 mg readability was used to weigh NaCl for producing 0.1 M and 0.5 M electrolyte solution.

Table 13 pKw values found at ion strength of 0.11, 0.51, 1.01, 2.01 and 3.01 M and at temperature of 0, 10, 20, 30, 40 and 50˚C in NaCl solution (Harned and Owen 1958)

I	0	10	20	30	40	50	R^2
0.1	14.73	14.32	13.95	13.61	13.31	13.03	0.9978
0.5	14.66	14.25	13.88	13.54	13.24	12.96	0.9964
1	14.68	14.27	13.9	13.56	13.25	12.97	0.9949
2	14.78	14.38	14.01	13.67	13.35	13.06	0.9958
3	14.93	14.53	14.15	13.81	13.49	13.19	0.9949

30 ml sample solution consisting of electrolyte solution and ligands was determined in potentiometric titration. The volumetric calibration for electrolyte solution was accomplished via a glass burette with

50 ml size. To minimize the ion strength variance, the burette was rinsed via the stock NaCl solution for twice at least, and then 30 ml of the stock solution was transferred into burette for the addition. The total moles of tested ligands was determined in basis of available pKa values (Jiang, Rao et al. 2002, Moll, Geipel et al. 2003, Fazary 2005, Charkoudian and Franz 2006) via prefixed model in Hyss simulation (Figure 12). According to modelling results, the suitable total mmoles applied in potentiometric measurements is approximately 0.025 for each ligands (0.0188g for HAHA, 0.0190 g for glycolic acid, 0.0275 g for pyrocatechol and 0.0150 g for acetic acid). The lab balance with 0.1mg readability was used to weigh corresponding mass for adding into electrolyte solution. According to chemical properties found in pyrocatechol, due to the degradation exposed to light, vessel for storing sample solution was required to isolate light source by foil cover. Meanwhile, 0.3 ml of 0.1 M HCl was required to be added into the vessel in prior to the measurements of acetic acid and glycolic acid since their initial pH in sample solution is nearby the start point of their dissociation progress leading to the lack of available data for the subsequent analysis.
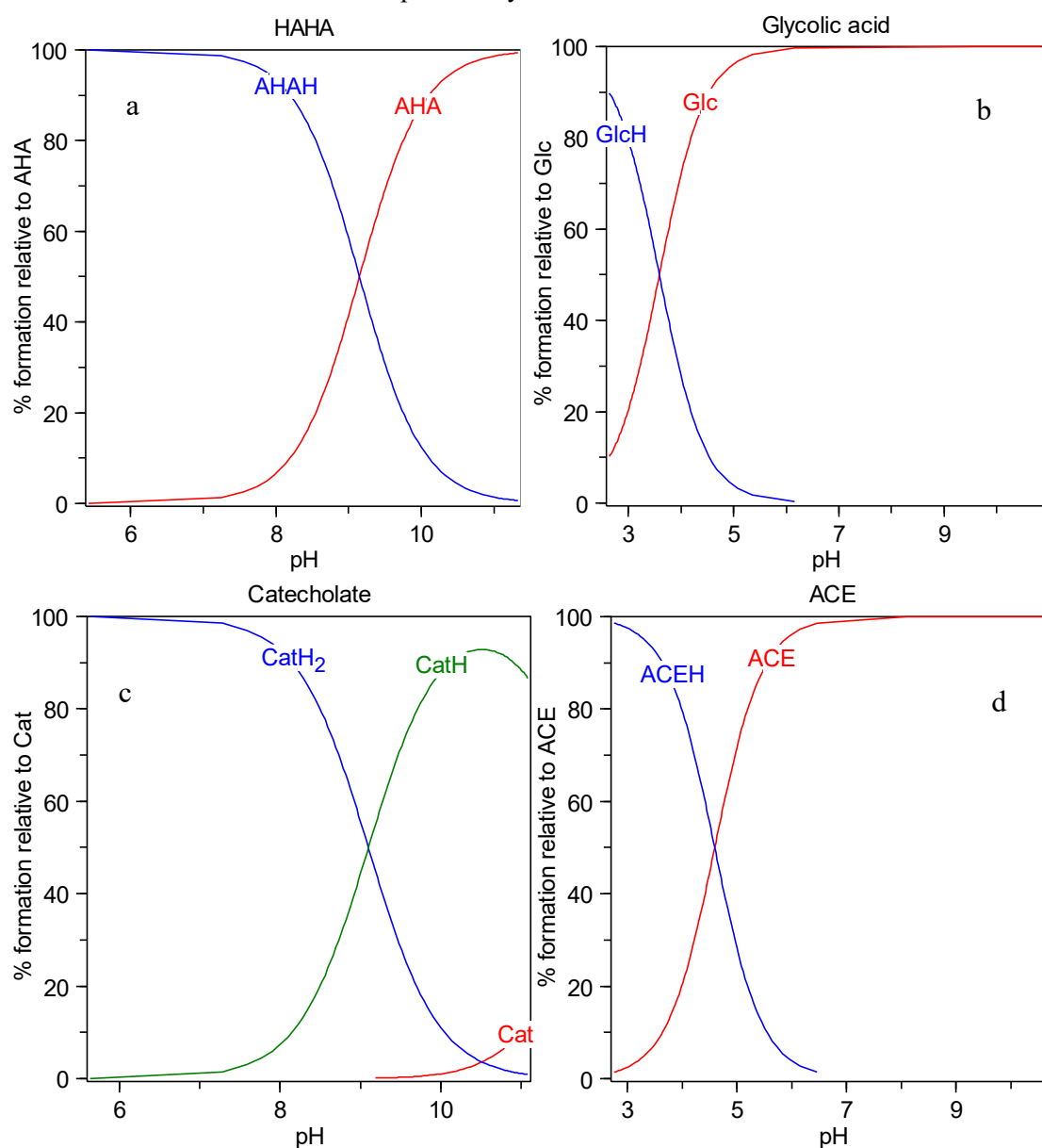

Figure 13 the speciation curve of ligands HAHA (a), glycolic acid (b), pyrocatechol (c) and acetic acid (d) in Hyss model. The pKa values for AHA, GA, ACE and CAT were 9.28 (Fazary 2005), 3.61(Kirishima, Onishi et al. 2007), 4.59 (Jiang, Rao

et al. 2002) and 9.19 (Van Den Berg and Huang 1984). All models based on the experimental conditions 30 mL sample solution titrated with 0.1 M NaOH with a 0.02ml increment. pH limitation is less than 10.5 in PT since the excessive hydroxides ions will lead to large errors in the measurement.

Parameter setting in titration was referred to signal draft of 0.2 mv/min, minimum for waiting time was 10 s and maximum for waiting time was 120 s. the increasement rate for base titrating was 0.02 ml. the total titrating volume of base solution depended on the endpoint of pH less than 10.5 according to simulating results. There were 3 duplications at least in each ligand titration and 2 duplications at least for glee test with respect to prefixed conditions of ion strength and temperature Thus, the total times for the ligand titration and glee test in this study were 180 and 60 respectively.

3.3.2   Data processing

The following computer program were used to collect experimental data and analyse it. The original potentiometric data was collected in Tiamo Ver. 2.4 including the consuming volume of base solution and the real-time potential values. The manipulation of HYPERQUAD to determine pKa values is basically comprised of Glee test and iteration calculations. According to the Nernst equation principal, the initial E_0 represents the solution potential at neutral condition where pH equals to 7.0. However, due to the function of temperature, ion strength and electrolyte species, the values of E_0 is not constant. Therefore, the use of Glee test is the progress for running acid-base titration without the addition of other reagents. Based on known ion strength and temperature in the specific medium solution, the E_0 values can be determined.

Combing determined E^0 values via Glee test, the iteration calculation aims to calculate pKa values via fitting pre-published model with the new potential points from potentiometric titration data (shown in Figure 14). Considering the deviation resulting from the addition of base, the total mmoles of ligands were not in excess of 0.5. the setting parameters for error and number of electron for this study were 0.3 mv and 1 respectively. According to obtained data and available constants, the software can refine pKa values via itself iterations, while sigma values (less than 12) and standard deviation can be defined shown in model. In Figure 14, there is an example of fitting progress of HAHA at 0.1, 0.5, 1.0, 2.0 and 3.0 M and in NaCl solution. It was reported that the analysis should keep 9 points at least within valid intervals (blue points) to produce the standard deviation in results (Gans, Sabatini et al. 1996). Red-colour points represent low-accuracy ones because of the disturbance of CO_2 at beginning and the approaching detecting limitation at the end. It is noticeable that the increasing numbers of blue points enable our results to minimise the deviation and improve the data quality.

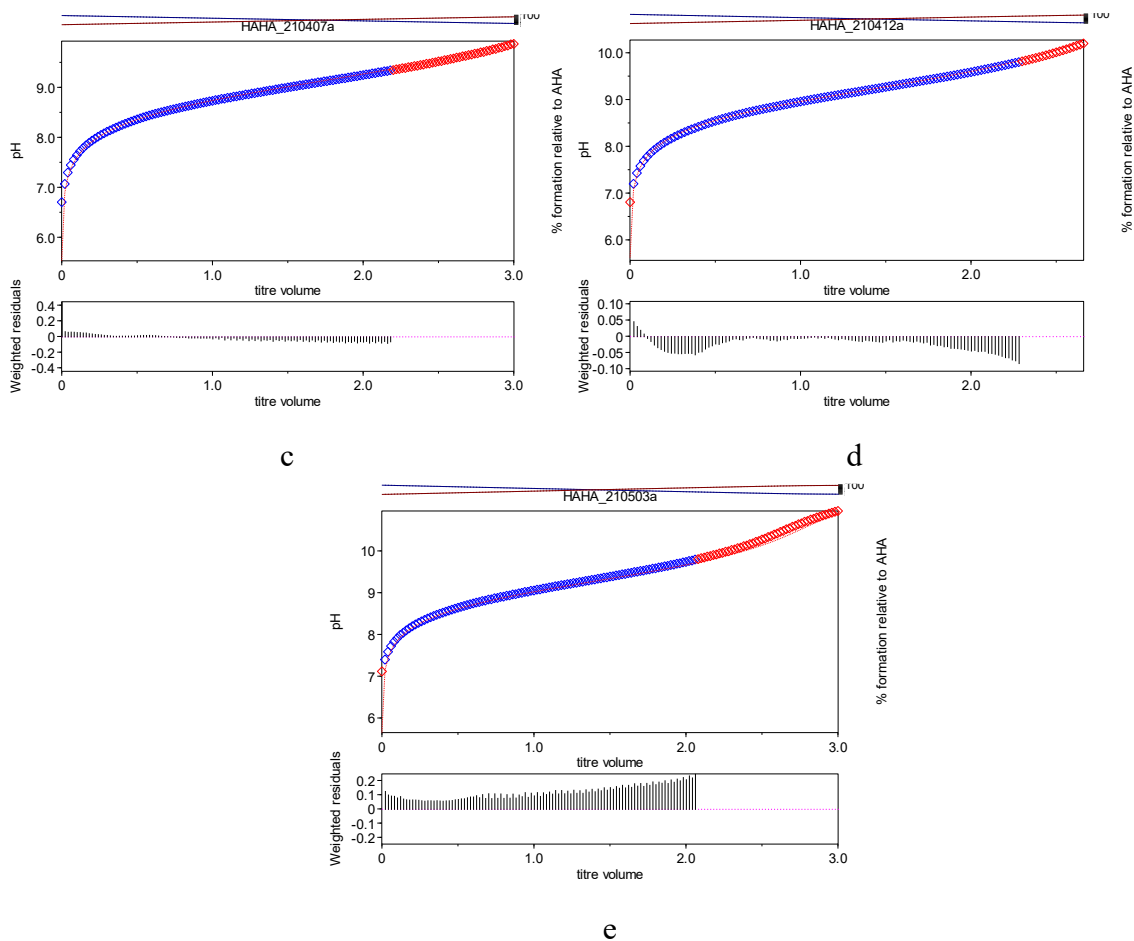a   b
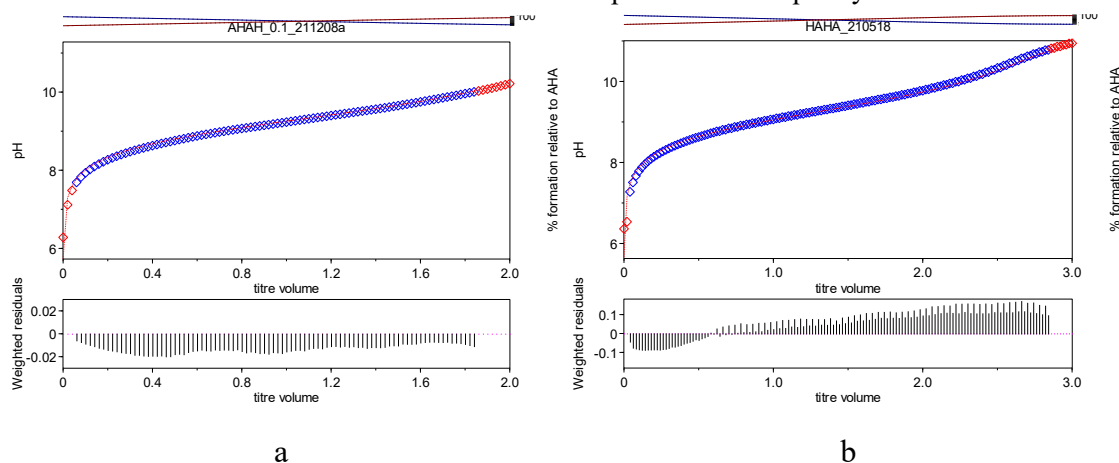
Figure 14 Analysing curves of acetohydroxamic acid (HAHA) in HYPERQUAD. Scheme (a), (b), (c), (d) and (e) represented titration curves of HAHA at 0.1, 0.5, 1.0, 2.0 and 3.0M, respectively. The temperature was at 298.15K. Blue points and red points means analysed and unanalysed points on curves since sigma values were required to be at <10 ranges and pH values should be lower than 10.5 for enhancing data preciseness.

The standard deviation (Stdev) of pKa values from HYPERQUAD was also discussed in the study of (Gans, Sabatini et al. 1996). In potentiometric titration, The calculation of Stdev firstly collects the specific potential points (E_j) under identical conditions (normally takes 9 points at least), these points mean not only the instrument conditions must be the same, but also the titration curves must not vary with the time (Gans, Sabatini et al. 1996). Thus the calculation of Stdev is followed:

$$\bar{E} = \frac{\sum_{j=1,n} E_j}{n} \tag{50}$$

$$S_E = \sqrt{\frac{\sum_{j=1,n} \bar{E} - E_j}{n-1}} \tag{51}$$

where $\bar{E}$ means the mean of potential values, n is the number of taken points from the curves, S_E is the standard deviation calculated via HYPERQUD. In this work, the ligand titration corresponding to single I and T conditions produced three independent S_E values since the 3-time titration was carried out separately. Thus, the new pKa values ($\overline{pKa} \pm \overline{S_E}$) showed in the study were followed:

$$\overline{pKa} = \frac{pKa' + S_E' + pKa' - S_E' + pKa'' + S_E'' + pKa'' - S_E'' + pKa''' + S_E''' + pKa''' - S_E'''}{6} = \frac{pKa' + pKa'' + pKa'''}{3} \tag{52}$$

$$\overline{S_E} = \sqrt{\frac{\sum_{j=1,3} \overline{pKa} - pKa_j}{3}} \tag{53}$$

where pKa', pKa'', and pKa''' mean three pka values sourced from the three different pKa values, and S_E', S_E'' and S_E''' mean their Stdev values calculated from HYPERQUAD. The new $\overline{S_E}$ indicated the deviation resulted from the experimental conditions for the 3-time titration.

The calculation of intrinsic pKa values and thermodynamics parameters was carried out in MS Excel. Plotting pKa values vs I and T based on calculated data from HYPERQUAD 2013 to reflect the linear trendline directly. As Ion strength at 0.1 M and 0.5 M, DE (Davis equation) was employed to calculate the intrinsic values by calculating activity coefficients during the deprotonating progress. SIT (specific ion interaction theory) also was used to calculate the intrinsic ones regarding high ion strength (1.0, 2.0 and 3.0 M) where a large deviation found in other methods (like EDH,DH and DE). The supplementary constant (A and ε) was calculated in modified formulas depending on the temperature and slope of function of pKa_i + $-z^2D$ against I.

Thermodynamics parameters were calculated in basis of Van't Hoff equation. The values of ΔH and ΔS are derived from the slope and intersect of plotting pKa values vs T respectively, and the determination of Gibbs energy was followed by eq. 26.

the data errors were calculated via equation STDEV in MS Excel.

The last stage is the developing uranyl-ligand titrating model, vanadyl-ligand and vanadate-ligand models in NaCl solutions. Based on acquired pKa values and available stability constants for metal-ligand complexes, Hyss was able to plot formation % of species vs pH variance.

4   Results and discussion

4.1   Determination of the dissociation constants via potentiometric titration

4.1.1   The analysis of pKa values acquired from potentiometric titration

The ion strength and temperature were adjusted to setting conditions to investigate their effects on dissociation constants among four ligands (acetohydroxamic acid, pyrocatechol, acetic acid and glycolic acid). According to their chemical structures shown in Figure 15, the equation for their dissociation constants found within the detecting limitation of potentiometric titration can be phrased:

$$HL^0 \leftrightarrow H^+ + L^- \text{ (for HAHA, AA and GA)}$$

$$H_2L \leftrightarrow H^+ + HL^- \text{ (for PYR), therefore,}$$
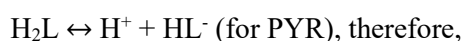
$$K_a = [H^+][L^-]/[HL], \text{ and}$$

$$K_a{}' = [H^+][HL^-]/[H_2L]$$

Where K_a and $K_a{}'$ represented dissociation constants as the first deprotonation arrived at equilibrium. All measurements were taken in NaCl solution as the adapting ion strength and temperature. In the progress of pKa calculation, 150 pointes were taken account for the valid points (up to pH 10.5) in potentiometric titration.

acetohydroxamic acid　2-hydroxyphenolate　　acetate　　　glycolic acid

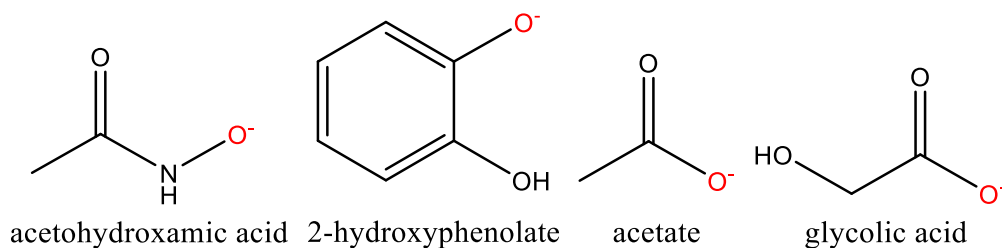Figure 15 The first deprotonation sites were observed in acetohydroxamic acid, pyrocatechol, acetic acid and glycolic acid. The secondary deprotonation would be occurred in the left hydroxyl presented in pyrocatechol and glycolic acid at pH more than 12 and cannot be detected via potentiometric titration because of the electrode limitation.

Based on pKa values from studies in Table 14, the dissociation constants differ significantly in terms of the background electrolyte types since there was an order (KCl>KNO$_3$> NaClO$_4$>NaCl) for pKa values in the study of (Daniele, Rigano et al. 1981). The recorded pKa values (Table 14) then were estimated for using in HYPERQUAD simulation. Although the pKa values can be determined in models, the determination of solution conditions including temperature and salinity (ion strength) also remarkably influences the accuracy of species formation. pKw values as one of important parameters can be used to reflect practical temp and ion strength in electrolyte solution. They are also related to formation curves in HYPERQUAD. The values can be estimated according to the trendline considering the variable ion strength and temperature shown in Figure 16. In this work, pKw values at 315.15K and 335.15K can be estimated in basis of exponential formulas.
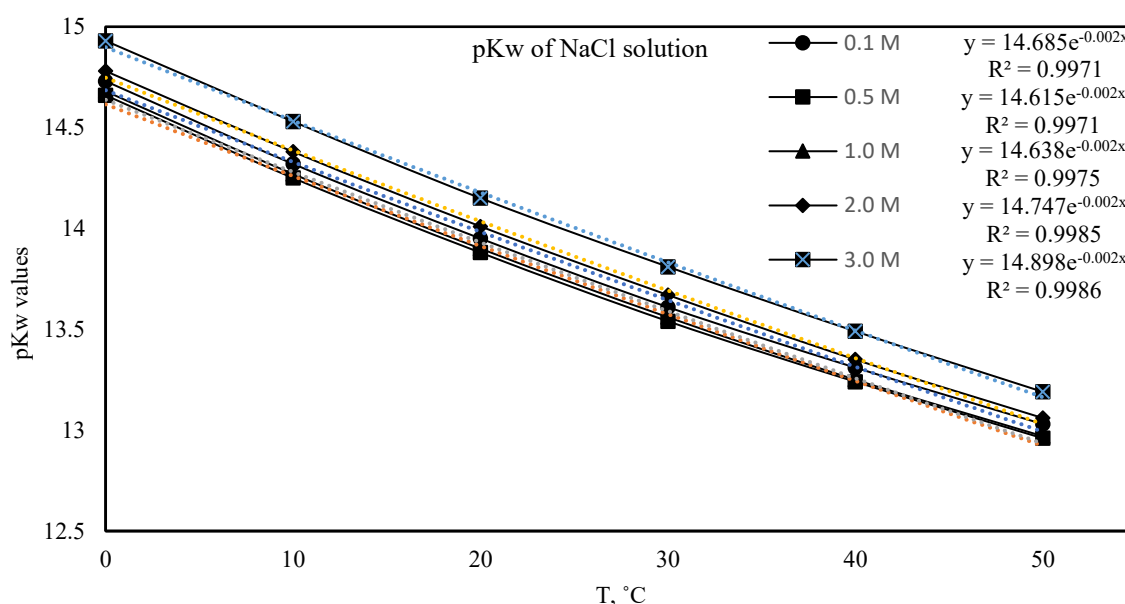
Figure 14 published relationship curves between pK$_w$ values and temperature in NaCl solution (Harned and Owen 1958). There were 5 trendlines with R^2 values >0.99 established in accordance with exponential formulas corresponding to 0.1, 0.5, 1.0, 2.0 and 3.0 M, which can be used to predict pKw values in wider ranges of temperature.

According to results acquired via HYPERQUAD 2013, equilibrium potentials from potentiometric titration were converted to pKa values related to the influence of ion strength and temperature shown in Table 14. The protonation of AA and GA were easier to be observed under acidic environment than the one of HAHA and PYR. The dissociation constants found in GA and AA were smaller than ones found in HAHA and PYR. The pKa values for HAHA and PYR were determined at pH of 9.32±0.02 and 9.28±0.02 in NaCl of 0.1 M solution, respectively, while the values for AA and GA were detected

at 4.54±0.01 and 3.57±0.02, respectively. It can be found that the pKa ranges for HAHA, PYR, AA and GA within 0.1 to 3.0 M at 298.15K were observed from 9.32±0.02 to 9.12±0.01, from 9.38±0.02 to 9.38±0.02 to 9.21±0.04, from 4.73±0.05 to 4.41±0.02, and from 3.69±0.03 to 3.52±0.01 respectively. In most of cases, the highest and lowest pKa values were presented at 3.0 M and 1.0 M regardless of the increase of temperature among these four ligands. However, the peak value for HAHA at 298.15K was found at 0.1 M, and the bottom value for AA at 298.15K was found at 0.5M. Additionally, the effect of temperature on pKa values was negative in HAHA and PYR but obscure in AA and GA. For instance, there were significant decreases of pKa values for HAHA and PYR from 9.29±0.03 to 9.11±0.02 and from 9.38±0.02 to 8.94±0.001 as temperature increased from 298.15K to 335.15K at 3.0 M respectively, while pKa values for AA and GA presented no significant difference under the same conditions. Nevertheless, it was presumed that the effect of temperature on pKa values for AA and GA was enhanced at low ion strength (from 0.1 to 0.5 M). As temperature increased from 298.15K to 315.15K, the protonation of AA and GA was increased from pH of 4.54±0.01 to 4.58±0.01 and from 3.57±0.02 to 3.61±0.008 at 0.1 M similar to the variation at 0.5 M.

Table 14 The summary of pKa values measured from potentiometric titration for acetohydroxamic acid, pyrocatechol, acetic acid and glycolic acid according to potentiometric titration in NaCl solution of 0.1, 0.5, 1, 2 and 3 M at 298.15K, 315.15K and 335.15K

I, M	T	0.1	0.5	1	2	3
HAHA	298.15K	9.32±0.02	9.28±0.01	9.12±0.01	9.21±0.01	9.29±0.03
	315.15K	9.11±0.007	9.07±0.008	8.95±0.015	9.01±0.007	9.17±0.011
	335.15K			8.92±0.004	8.99±0.002	9.11±0.02
PYR	298.15K	9.28±0.02	9.23±0.03	9.21±0.04	9.28±0.04	9.38±0.02
	315.15K	9.11±0.008	9.02±0.02	8.89±0.04	9.05±0.03	9.11±0.02
	335.15K			8.77±0.04	8.89±0.04	8.94±0.001
AA	298.15K	4.54±0.01	4.41±0.02	4.51±0.02	4.62±0.01	4.73±0.05
	315.15K	4.58±0.01	4.56±0.006	4.53±0.003	4.70±0.005	4.73±0.001
	335.15K			4.53±0.02	4.59±0.02	4.76±0.01
GA	298.15K	3.57±0.02	3.53±0.01	3.52±0.01	3.62±0.02	3.69±0.03
	315.15K	3.61±0.008	3.60±0.007	3.60±0.007	3.64±0.015	3.68±0.01
	335.15K			3.57±0.02	3.61±0.002	3.68±0.02

In order to ensure the satisfactory data, the dissociation constants determined via acid-base titration were referred to former work in terms of their proximity under similar conditions. The study of (Evers, Hancock et al. 1989) indicated pKa values of HAHA at 0.1 M and 298.15K in potassium chloride (KCl) was 9.36 approaching pKa values of 9.32±0.02 determined in NaCl solution. The detected dissociation constant in catechol was 9.195 measured at 298.15K and in 0.1M KNO_3 solution nearby acquired pKa values of 9.28 in NaCl solution (Jameson and Wilson 1972). In the study of (Pedersen 2002), the dissociation constants of glycolic (4.46) and acetic acids (3.52) was determined by means of the quinhydrone electrode at 18°C. in solutions of sodium chloride up to 0.5 M. In this work, pKa values for AA and GA showed a slight difference with respect to 4.41±0.02 and 3.53±0.01 at 298.15K in 0.5 M NaCl solution. Considering the distinctions of temperature and electrolyte and low deviations among obtained pKa value, the results measured via PT experiments were regarded as within valid intervals.

In comparison of pKa values shown in literatures, there were differences found in chlorides or perchloride solution at same ion strength and temperature. In this work, the dissociation constant of HAHA was decreased from 9.36 in 0.1 M KCl solution to 9.32±0.02 in 0.1 M NaCl solution. The obtained pKa values of glycolic acid was 3.52±0.01 in 1.0 M NaCl solution which is lower than the value of 3.61 in 1.0 M NaClO₄. The situation of AA was similar to the ones of GA since pKa value measured in 1.0 M NaCl was 4.51±0.02 which is lower than pKa value of 4.59 found in 1.05 M NaClO₄ solution. However, pKa for pyrocatechol measured in NaCl denoted a converse trend which was larger than the values found in KCl solution. It can be found that the dissociation constant in the first protonation was 9.28[a]±0.02 and 9.21[a]±0.04 in 0.1 and 1.0 M NaCl solution, while the values were only 9.17 and 9.14 in 0.1 and 1.0 M KCl solution.

Table 15 The difference of dissociation constants of acetohydroxamic acid, glycolic acid, acetic acid and pyrocatechol observed at different ion strength between in previous work and in this work at 298.15K

Ligands	Ion strength (M)	pKa values	Medium	Ref.
HAHA	0.1	9.33	KNO₃	(Buglyó and Pótári 2005, Aksoy 2010)
	0.1	9.36	KCl	(Evers, Hancock et al. 1989)
	0.1	9.32±0.02	NaCl	this work
Glycolic acid	1.0	3.61	NaClO₄	(Kirishima, Onishi et al. 2007)
	0.0	3.83	NaCl	(Stokes and Robinson 1959)
	1.0	3.52±0.01	NaCl	This work
	0.1	3.57±0.02	NaCl	This work
Acetic acid	1.05	4.59	NaClO₄	(Jiang, Rao et al. 2002)
	1.0	4.51±0.02	NaCl	This work
Pyrocatechol	0.1	9.17[a]	KCl	(Nurchi, Pivetta et al. 2009)
	1.0	9.14[a]	KCl	(Nurchi, Pivetta et al. 2009)
	0.1	9.28[a]±0.02	NaCl	This work
	1.0	9.21[a]±0.04	NaCl	This work

[a] dissociation constants measured from the first protonation occurred in pyrocatechol.

The trend of pKa values found in these 4 ligands was descended as ion strength ranging from 0.1 to 1.0 M at 298.15K, and was similar to the situation at higher temperature. However, as the elevation of ion strength (>1.0M), a converse trend that indicated an increase of pKa values was found in these 4 ligands in spite of the upward temperature (shown in Figure 17). The relationship between the dissociation constants and ion strength ranging from 0.1 to 1.0 M was regarded as a negative relationship, while the constants went up as the subsequent increase of ion strength from 1.0 to 3.0 M among all of ligands in experiments. pKa values of acetohydroxamic acid and pyrocatechol from ion strength of 0.1 M to 1.0 M showed a significant decrease from 9.32±0.02 to 9.12±0.02 and from 9.28±0.02 to 9.21±0.04 at 298.15K, respectively. the situation was similar to acetic acid and glycolic acid with decreases from 4.54±0.01 to 4.51±0.02 and from 3.57±0.02 to 3.52±0.01 at 298.15K, respectively. However, there were converse trends observed in HAHA and PYR as the ion strength increased from 1.0 to 3.0 M. pKa values of HAHA and PYR released a significant increase from 9.12±0.01 to 9.29±0.03 and from 9.21±0.04 to 9.38±0.02, respectively. Meanwhile, the increase of ion strength ranging from 1 to 3M also enhanced the lift of dissociation constants found in AA and GA in terms of 0.22 and 0.17 log units compared with the constants at 1.0M NaCl solution. The variation of pKa values at 315.15K and 335.15K was similar to the one found at 298.15K. The values of HAHA and PYR at 315.15K were decreased by 0.16 and 0.22 log units as the ion strength up to 1.0 M, while the values of the two ligands were increased by 0.22 and 0.22 log units was found at ion strength from 1.0 to 3.0 M respectively. The

decreasing trend of pKa values from 0.1 to 1.0 M at 315.15 K was also found in AA from 4.58±0.01 to 4.53±0.03, while GA denoted an insignificant change of pKa values as ion strength up to 1.0 M. The increasing trend observed for pKa values of AA and GA from 4.53±0.003 to 4.73±0.001 and from 3.60±0.007 and 3.68±0.01 as ion strength up to 3.0M at 315.15K, respectively. According to values listed in Table 15, increasing pKa values among these 4 ligands were also observed from 1.0 to 3.0 M ion strength at 335.15K.
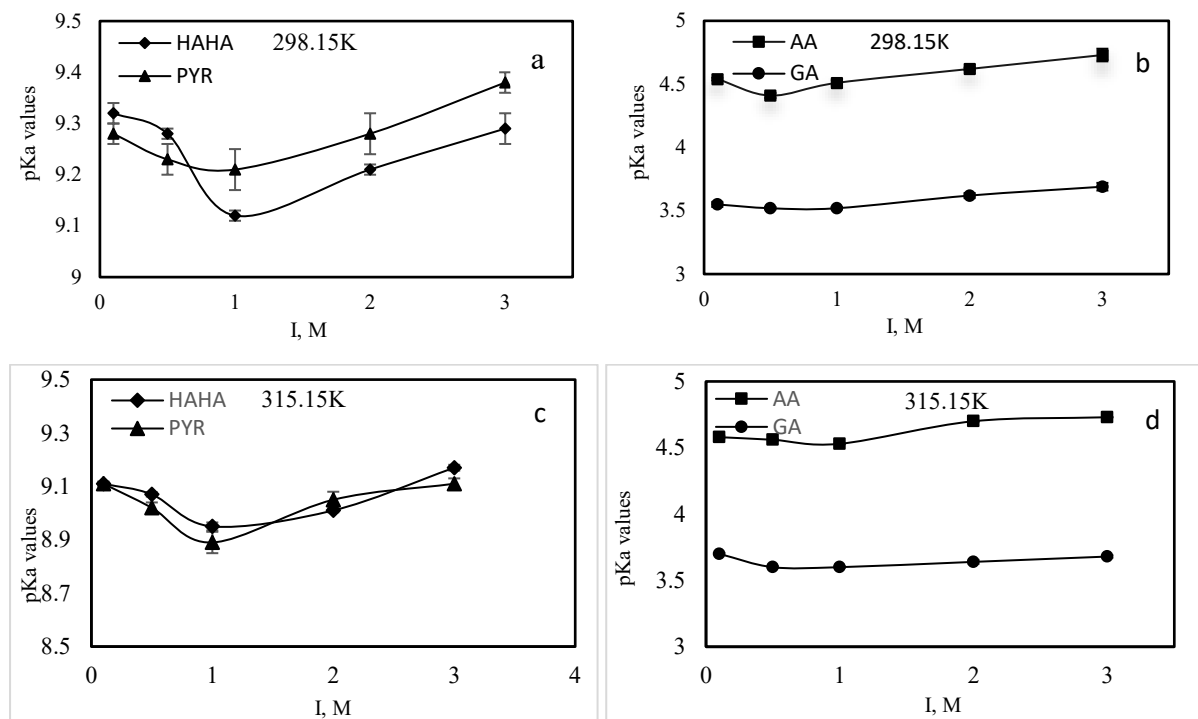

Figure 15 Dependence of ion strength on pKa values of HAHA, PYR, AA and GA at 298.15K and 315.15K. The NaCl solution was adapting to 0.1, 0.5, 1.0, 2.0 and 3.0 M ion strength (a) Dependence of I on pKa values of HAHA and PYR at 298.15K; (b) Dependence of I on pKa values of AA and GA at 298.15K; (c) Dependence of I on pKa values of HAHA and PYR at 315.15K; (d) the effect of I on pKa values of AA and GA at 315.15K. From 0.1 to 1.0 M, a decreasing trendline of pKa values was observed in targeted ligands. From 1.0 to 3.0 M an increasing trendline of pKa values was observed in targeted ligands.

There was generally a certain decrease of pKa values found in each ligand under the variable ion strength from 0.1 to 1.0, while a significant increase occurred in the following increase of ion strength from 1.0 to 3.0M. . Meanwhile, it can be found that the lifting temperature at 315.15K only influenced the varieties of pKa values at the same ion strength, but had a few impacts on trends of pKa values as the lifting ion strength. In the study of (Thakur, Mathur et al. 2007), it also indicated similar trends of IDA,NTA, and DTPA where their dissociation constants with increasing ion strength were an initial decrease to a minimum between I = 0.5 and 2.0 M followed by increases with further increases in ion strength as I increased from 0 0.3 to 6.0 M in $NaClO_4$ solution at 298.15K. The trendlines among these 4 ligands at low ion strength (from 0.1 to 1.0 M) can be explained in the previous study (Cohn, Heyroth et al. 1928). It can be found that the estimation of pKa values followed by Eq. 36 as the values indicated a negative relationship with $\sqrt{I}$. However, as I increased to 1.0 M or more, there is an extrapolation of pKa estimation favourable with the interaction coefficient of SIT. According to the results shown in Figure 15, the increase of ion strength enhance the function of ε (shown in Eq.21) where the effect of $\sqrt{I}$ on pKa values is smaller than the increase of ε. Thus, it was found that an increase of pKa among these 4 ligands was observed from 1.0 to 3.0 M.

4.2 The simulation of the complexation of uranyl and vanadyl ions with acetohydroxamic acid, glycolic acid, acetic acid and pyrocatechol in Hyss

To observe the effect of new pKa values on the M-L complexing speciation, Hyss models was employed to establish the corresponding curves consisting of the dissociation constants of ligands, the formation constants of complexes and the hydrolysis constant of metal ions under the setting conditions (I, T and the initial concentrations of reactants). To improve the accuracy of models for investigating the complexing progress carried out in NaCl solution, the hydrolysis constants of uranyl and vanadyl ions measured in NaCl (shown in Table 16) were using in the formative models.

Table 16 The hydrolysis constants of UO_2^{2+} and VO^{2+} in NaCl solution. The hydrolysing conditions for UO_2^{2+} was at I=0M, 298.15K and for VO^{2+} was at I=0.1M, 298.15K.

Species	Ion strength	logβ	Ref.
UO_2OH^+	0.0	-5.25±0.24	Altmaier, Yalçıntaş et al. 2017
$(UO_2)_2(OH)_2^0$	0.0	-5.62±0.04	
$(UO_2)_3(OH)_5^+$	0.0	-15.55±0.12	
$(VO)OH^+$	0.1	-5.65±0.15	Berto, Daniele et al. 2008
$(VO)_2(OH)_2^{2+}$	0.1	-7.02±0.03	

The stability constants (logβ) of the complexation of targeted metal ions (uranyl and vanadyl ions) with targeted ligands (AHA, PYR, AA and GA) were summarised in Table 17. The predication for the speciation of M-L complexes greatly depends on the application of specific logβ values with respect to their different forms of M:L. Normally, the use of their logβ values in the established models sourced from previous studies in prior to the potentiometric titration, and then the experimental curves will be fitted the established ones as a result of the iteration in HYPERQUAD under the practical conditions including (ion strength, temperature and concentrations of reactants). Due to the lack of logβ values in NaCl solution, the speciation models in this work basically were originated from the values in other media such as KCl, NaClO$_4$ and sea water at variable ion strength.

Table 17 The summary of logβ values for the complexation of uranyl, vanadyl ions with AHA, GA, AA and PYR at variable ion strength in basic media solution. T=298.15K.

Species	logβ	Medium	Ion strength/M	Ref.
$UO_2(AHA)^+$	8.22	NaClO$_4$	0.1	(Chung, Choi et al. 2011)
$UO_2(AHA)_2^0$	15.30	NaClO$_4$	0.1	
$VO(AHA)^+$	8.69	KCl	0.2	(Buglyó and Pótári 2005)
$VO(OH)(AHA)^0$	3.69	KCl	0.2	
$VO(AHA)_2^0$	15.90	KCl	0.2	
UO_2GA^+	2.35	NaClO$_4$	1.0	(Di Bernardo, Bismondo et al. 1976)
$UO_2(GA)_2^0$	3.97	NaClO$_4$	1.0	
$UO_2(GA)_3^-$	5.12	NaClO$_4$	1.0	
$VOGA^+$	2.56	NaClO$_4$	1.0	(Di Bernardo, Bismondo et al. 1976)
$VO(GA)_2^0$	4.22	NaClO$_4$	1.0	
$VO(GA)_3^-$	5.19	NaClO$_4$	1.0	
$UO_2(AA)^-$	2.37	NaClO$_4$	1.0	(Jiang, Rao et al. 2002)
$UO_2(AA)_2^0$	4.37	NaClO$_4$	1.0	

$UO_2(AA)_3^-$	6.86	$NaClO_4$	1.0	
$VO(AA)^-$	1.97	$NaClO_4$	1.0	(Di Bernardo, Tomat et al. 1988)
$VO(AA)_2^0$	3.46	$NaClO_4$	1.0	
UO_2PYR^0	6.2	Sea water	0.7	(Van Den Berg and Huang 1984)
UO_2HPYR^+	4.9	Sea water	0.7	
$UO_2H_2(PYR)_3^{2-}$	3.7	Sea water	0.7	
$VOPYR^0$	16.75	KCl	0.2	(Gergely and Kiss 1976, Jezowska-Bojczuk, Kozłowski et al. 1990)
$VO(PYR)_2^{2-}$	31.58	KCl	0.2	
$VOHPYR^-$	10.21	KCl	0.2	
$(VO)_2H_2(PYR)_2^{2-}$	22.92	KCl	0.2	

4.2.1   The speciation model of U(VI)-AHA and V(IV)-AHA complexes

The speciation curves of U(IV)-AHA and V(IV)-AHA showed two main species in the format of ML^+ and ML_2^0. The stability constants of their complexes conducted by dissociation constant of acetohydroxamic acid and hydrolysis constants of metal ion which is related to their interactions position with respect to pH increase. According to their stability constants in studies of *(Wehrli and Stumm 1989, Chung, Choi et al. 2011)*, models corresponding to U(IV)-AHA were established considering pKa values of AHA and hydrolysis constants of uranyl and vanadyl ions in Hyss (Figure 18). It was observed that $UO_2AHA_2^0$ likely tends to be more stable compared to UO_2AHA^- in terms of higher formation (%) contents. As pKa of HAHA was 9.36, It denoted formation (%) of two species that UO_2AHA^- and $UO_2AHA_2^0$ accounted for 50% and 73% at pH ranging from 3.5 to 8 and from 4 to 10.5 respectively. As the pKa value was 9.32, the largest percentages of UO_2AHA^- and $UO_2AHA_2^0$ was 50.7% and 75.1% respectively. it can be found that the speciation curves related to the experimental data showed the higher contents of $UO_2AHA_2^0$ in spite of a very slight increase (only 2%). However, the contents of uranyl hydrolytic species denoted an decrease as pKa value of HAHA increased from 9.32 to 9.36. it can be found that the peak portions of UO_2OH^+, $(UO_2)_2(OH)_2^{2+}$ and $(UO_2)_3(OH)_5^+$ got increased from 2.42%, 5.46% and 14.1% to 2.52%, 5.93% and 15.2%. thus, the complexing progress between UO_2^{2+} and AHA in NaCl solution likely presented higher level of the complexes formation and prevent uranyl ions from the hydrolysis progress according to results shown in Figure 18.
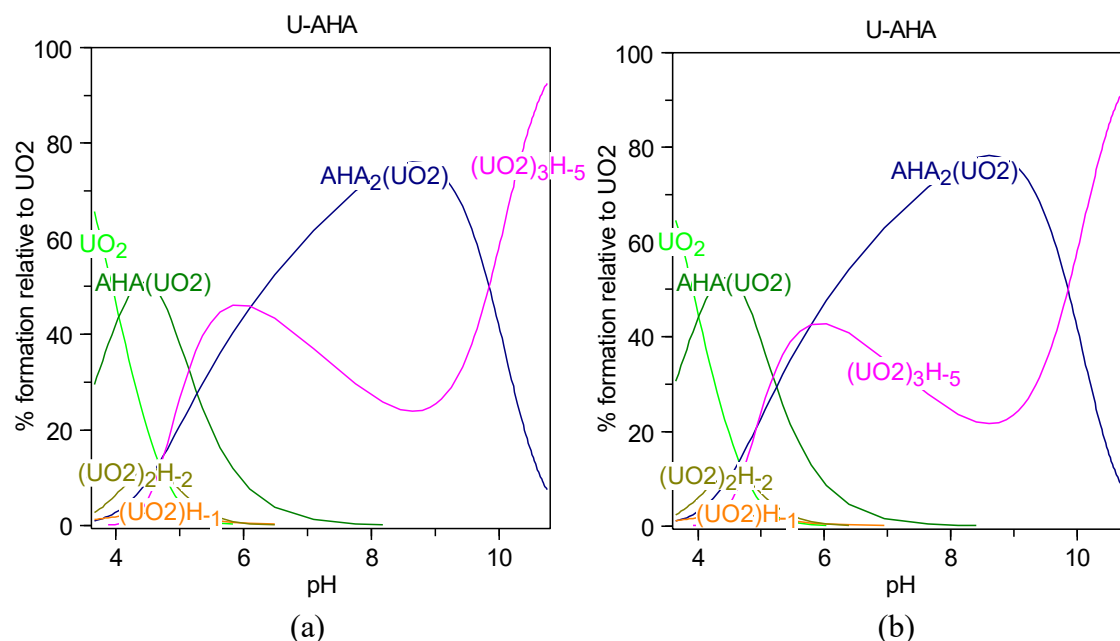
Figure 16 the speciation models for U(VI)-AHA were established in Hyss. In the model of U(VI)-AHA (a) pKa value of HAHA was 9.36 (Evers, Hancock et al. 1989). The complexing reaction occurred in 0.1M NaCl solution without CO2 at 25˚C. In the model of U(VI)-AHA (b) pKa of HAHA was 9.32 obtained from this work 0.1 M NaCl without CO2 at 25˚C. The total concentrations of uranyl ions was 0.62 mol·dm^{-3}, and the ones of HAHA was 1.54 mol·dm^{-3}. The pKw value used in this model was -13.78 as I = 0.1 M in NaCl solution.
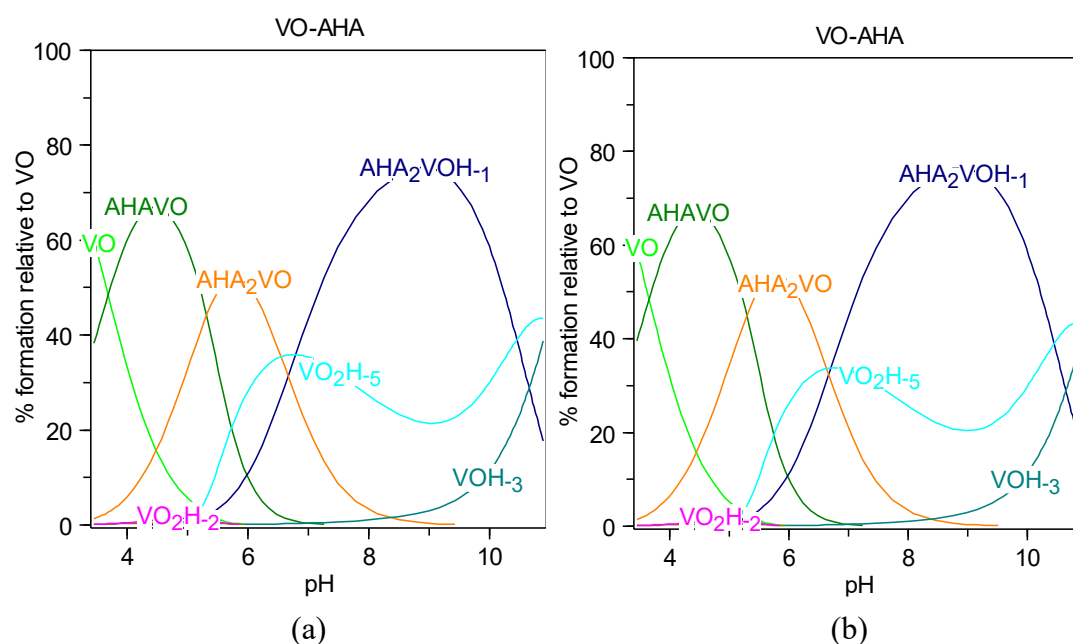

Figure 17 The speciation models for V(IV)-AHA were established in Hyss. In the model of V(IV)-AHA (a) pKa value of HAHA was 9.36 (Evers, Hancock et al. 1989). The complexing reaction occurred in 0.1M NaCl solution without CO2 at 25˚C. In the model of U(VI)-AHA (b) pKa of HAHA was 9.32 obtained from this work 0.1 M NaCl without CO2 at 25˚C. the total concentrations of vanadyl ions was 0.83 mmol·dm^{-3}, and the ones of HAHA was 1.67 mmol·dm^{-3}. The pKw value used in this model was -13.78 as I = 0.1 M in NaCl solution.

In the model of Vanadium (IV)-AHA shown in Figure 19, the formation contents of VOAHA$^-$ at pH ranging from 3.5 to 9 were similar to VOAHA$_2$ as pH increased to 8.5. it can be found that only ML$^+$ and ML$_2^0$ were predominating formats of products in their complexing reactions. The highest percentages of VOAHA$^+$, VO(AHA)$_2^0$ and VOOH(AHA)$_2^-$ was found at pH 4.48, 5.77 and 9.01. Compared with the literature pKa value, the peak percentages of VOAHA$^+$, VO(AHA)$_2^0$ and

VOOH(AHA)$_2^-$ increased by 0.2%, 1.6% and 1.1% respectively as the pKa value was 9.32. However, there was no significant difference of hydrolytic species between the experimental data and the literature one.

4.2.2 The speciation model of U(IV)-GA and Vanadium (IV)-GA complexes

According to their stability constants in studies of (Di Bernardo, Tomat et al. 1988), the models corresponding to U(IV)-GA and Vanadium (IV)-GA were established considering pKa values of AHA and hydrolysis constants of uranyl and vanadyl ions in Hyss (Figure 20 and 21). Although there were 3 species of UVI-GA complexes shown in Figure 20, the speciation curves of U(IV)-GA showed major species in the format of ML$^+$. According to formation curves shown in Figure 20, UO$_2$GA$^+$ accounting for 37.4% at pH 3.83 as pKa value was 3.61, while the contents of UO$_2$GA$^+$ accounted for 38.4% under the experimental conditions. The second species of UO$_2$GA$_2^0$ presented a remarkably low level in the model. It can be found the highest percentages was up to 5.51% at pH 4.13 even if an increase by 0.32% was found as the pKa value of GA was 3.52. the difference of hydrolysis species between the literature curves and the experimental ones was not clear with only 0.02% variation. The formation results were also supported via the study of (Szabó and Grenthe 2000) which denoted ML in U(IV)-GA complexing system was the major species and other species were hard to be observed during the potentiometric titration test.

Figure 18 The speciation models for U(IV)-GA were established in Hyss. In the model of U(IV)-GA (a) pKa value of HAHA was 3.61(Kirishima, Onishi et al. 2007). The complexing reaction occurred in 1.0 M NaCl solution without CO2 at 25˚C. In the model of U(VI)-AHA (b) pKa of GA was 3.52 obtained from this work 0.1 M NaCl without CO2 at 25˚C. the total concentrations of uranyl ions was 1.67 mmol·dm^{-3}, and the ones of GA was 6.67 mmol·dm^{-3}. The pKw value used in this model was -13.72 as I = 1.0 M in NaCl solution.

The situations of Vanadium (IV)-AHA was similar to the performance of the U(VI)-GA coordination since the species of VOGA$^-$ dominate the all forms of products. The highest contents of VOGA$^-$ presented 36.8% at pH 4.16 compared with 3.54% found in VOGA$_2^0$ at pH 4.46. The formation curves

with the new pKa value indicated a slight increase of the complexes that the largest contents of $VOGA^-$ and $VOGA_2^0$ were 37.5% and 3.65% respectively. However, the hydrolysis of VO was not sensitive to the variation of pKa values since there were only 0.1% content difference of $(VO)_2(OH)_2^{2+}$ and $(VO)_2(OH)_5^-$ between the literature model and the titration one.
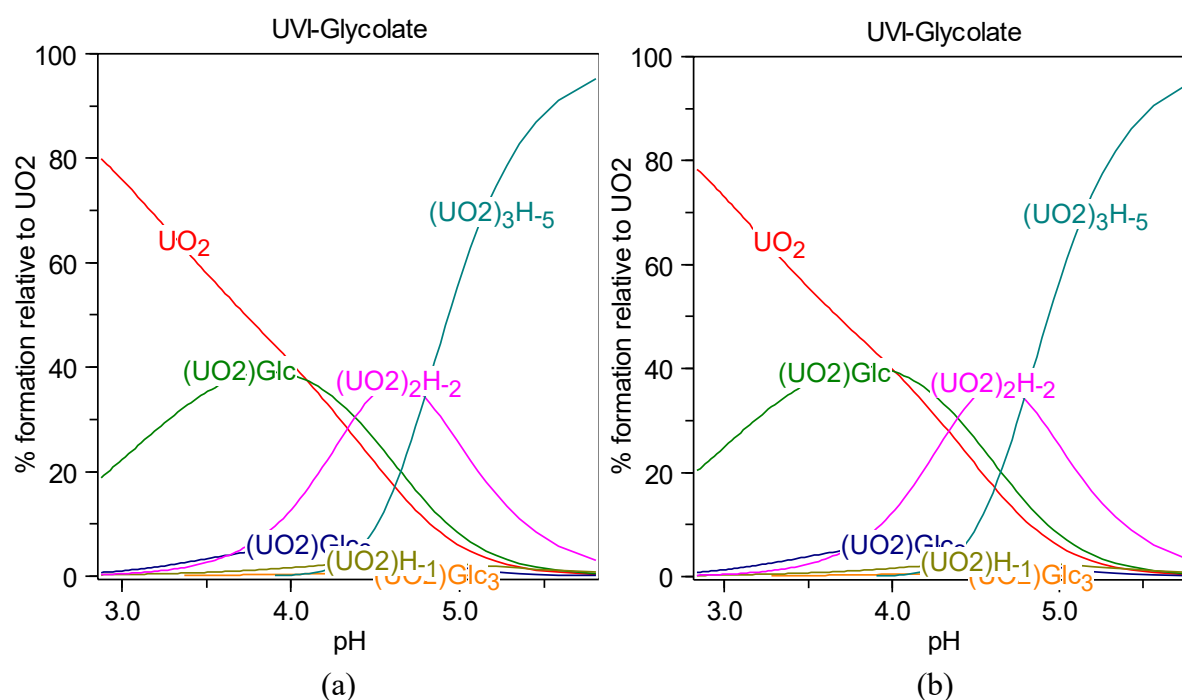

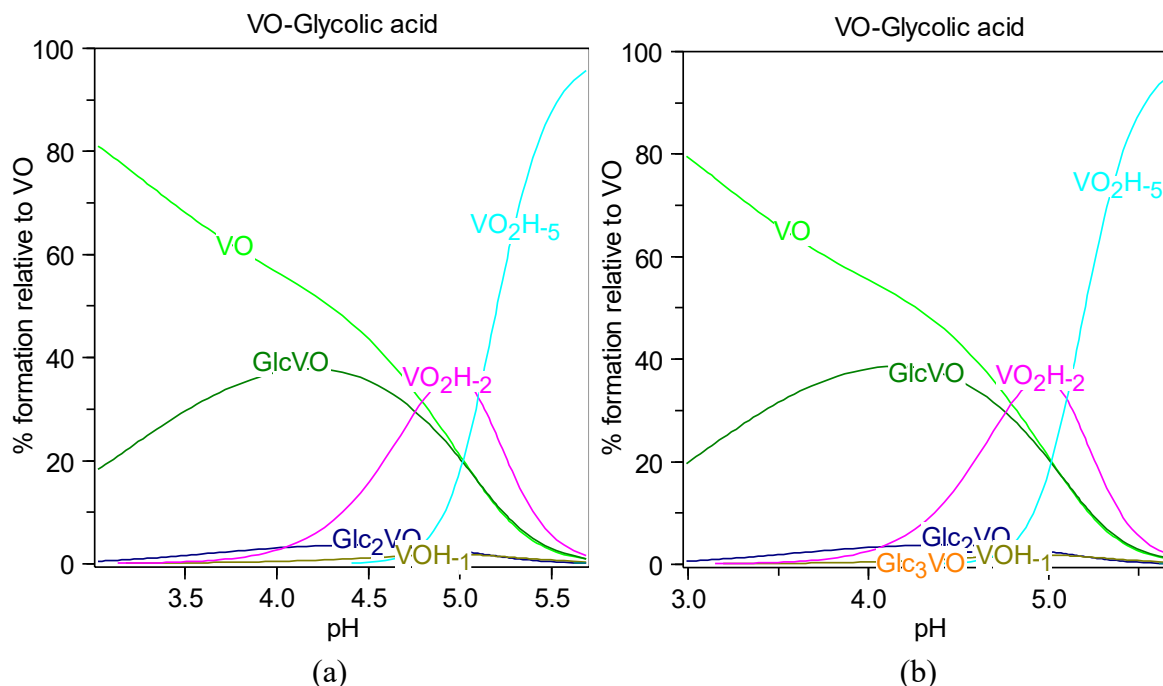Figure 19 The speciation models for V(IV)-GA were established in Hyss. In the model of V(IV)-GA (a) pKa value of HAHA was 3.61(Kirishima, Onishi et al. 2007). The complexing reaction occurred in 1.0 M NaCl solution without CO2 at 25°C. In the model of V(VI)-AHA (b) pKa of GA was 3.52 obtained from this work 0.1 M NaCl without CO2 at 25°C. the total concentrations of vanadyl ions was 1.67 mmol·dm⁻³, and the ones of GA was 3.33 mmol·dm⁻³. The pKw value used in this model was -13.72 as I = 1.0 M in NaCl solution.

4.2.3 The speciation model of U(IV)-AA and Vanadium (IV)-AA complexes

Two species in the format of ML^+ and ML_2^0 found in the complexing progress of U(IV)-AA and Vanadium (IV)-AA. In the model of U(IV)-AA shown in Figure 22, it is found the formation curves were similar to the ones found in the U(VI)-GA model that UO_2GA^+ became the major species of their complexing products. The species of UO_2AA^- predominates all of U(VI)-AA complexes with 13.1% formation at pH 4.07, while the highest contents of $UO_2(AA)_2^0$ accounted for only 0.78% at pH 4.42. However, an increase by 1.4% found in UO_2AA^- and the values of $UO_2(AA)_2^0$ was only 0.94% with the new pKa value (4.51). It can be found that the formation of $(UO_2)_2(OH)_2^{2+}$ arrived at the highest level of 16.2% at pH 4.31, while a decrease by 0.5% at same pH value was found the model with the new pKa.

Figure 20 The speciation models for U(VI)-AA were established in Hyss. In the model of U(VI)-GA (a) pKa value of HAHA was 4.59 (Jiang, Rao et al. 2002). The complexing reaction occurred in 1.0 M NaCl solution without CO2 at 25˚C. In the model of V(VI)-AHA (b) pKa of AA was 4.51 obtained from this work 0.1 M NaCl without CO2 at 25˚C. the total concentrations of uranyl ions was 1.67 mmol·dm^{-3}, and the ones of AA was 3.33 mmol·dm^{-3}. The pKw value used in this model was -13.72 as I = 1.0 M in NaCl solution.
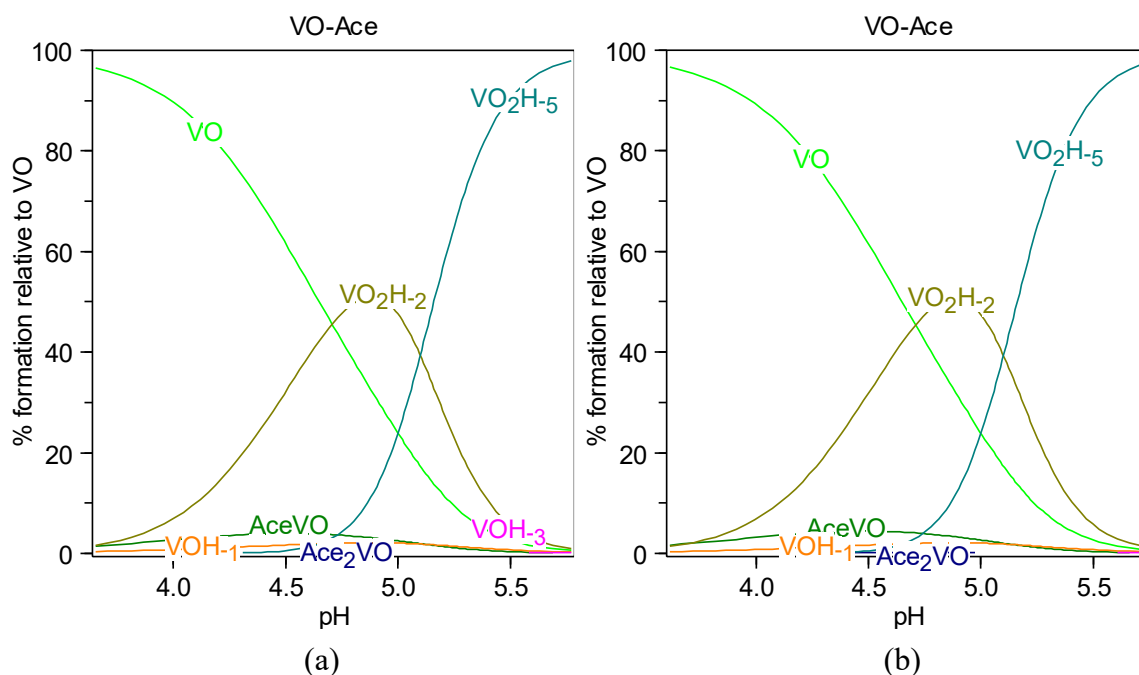
Figure 21 The speciation models for V(IV)-AA were established in Hyss. In the model of V(IV)-GA (a) pKa value of HAHA was 4.59 (Jiang, Rao et al. 2002). The complexing reaction occurred in 1.0 M NaCl solution without CO2 at 25˚C. In the model of V(VI)-AHA (b) pKa of AA was 4.51 obtained from this work 0.1 M NaCl without CO2 at 25˚C. the total concentrations of uranyl ions was 1.67 mmol·dm^{-3}, and the ones of AA was 1.67 mmol·dm^{-3}. The pKw value used in this model was -13.72 as I = 1.0 M in NaCl solution.

The curves in the VIV-AA model were similar to the ones in the UVI-AA model. However, the portions of VOAA$^+$ was greatly lower than UO$_2$AA$^+$ which only arrived at 4.0% at pH 4.46, and the formation of VO(AA)$_2^0$ was too low to be observed with only 0.1% at pH 4.73. the model with the new pKa value

compared with the literature one only presented an increase by 0.38%. it, thus, likely assumed that the ability of the contaminated metal uptake via carboxylate was not the mainstream for the M-L coordination. However, the hydrolysis of vanadyls during the complexing progress was more significant attributed to nearly 24.9 % of the $(VO)_2(OH)_2^{2+}$ in spite of the decrease by 0.2% as introducing the new pka value shown in Figure 23b.

4.2.4   The speciation model of U(IV)-PYR and Vanadium (IV)-PYR complexes

According to available stability constants in studies of (Van Den Berg and Huang 1984) and (Jezowska-Bojczuk, Kozłowski et al. 1990), pH changes lead to the distribution of complexed ions with catechol and reflect a function of pH in aqueous enrvionment related to the speciation contents in basic media. Their models corresponding to U(IV)-PYR and Vanadium (IV)-PYR were established considering pKa values of pyrocatechol and hydrolysis constants of uranyl and vanadyl ions in Hyss (Figure 24). In U(IV)-PYR complexing model, $UO_2(PYR)^0$ predominated the largest portion of products with 37.5% formation of total UO_2^+ concentrations at pH 9.05, while the model with the new pKa value (9.28) revealed that $UO_2(PYR)^0$ was only decreased to 37.1% .

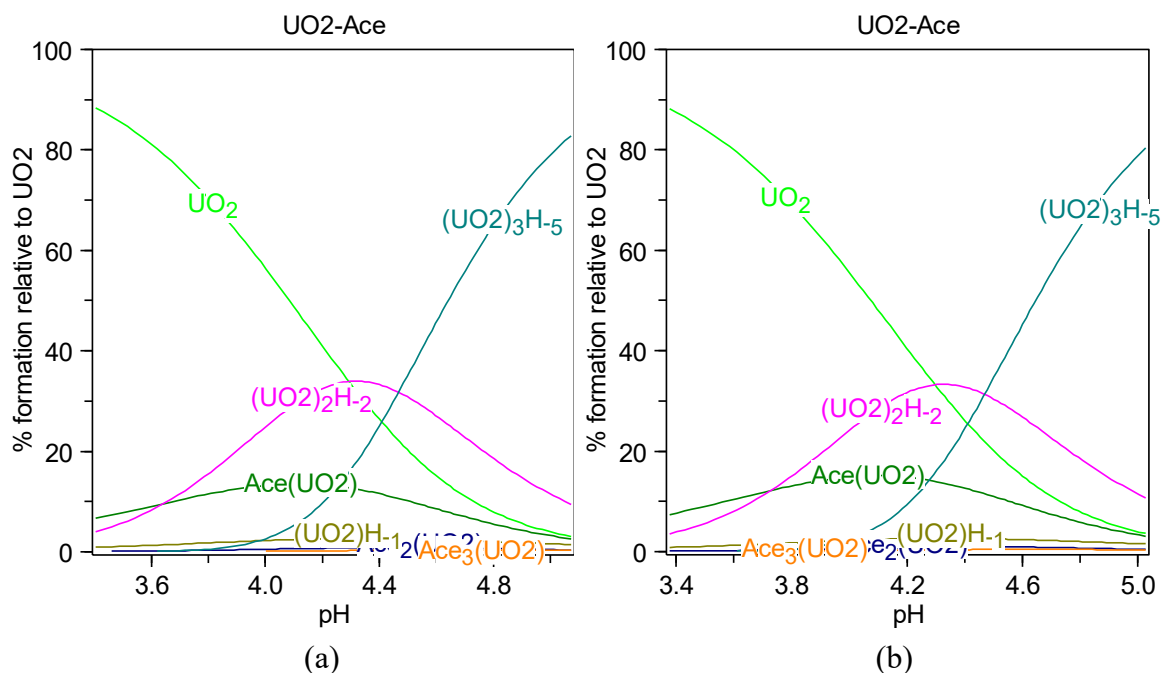Figure 22 The speciation models for U(VI)-PYR were established in Hyss. In the model of U(VI)-PYR (a) pKa value of HAHA was 9.17 (Nurchi, Pivetta et al. 2009). The complexing reaction occurred in 1.0 M NaCl solution without CO2 at 25˚C. In the model of V(VI)-AHA (b) pKa of PYR was 9.28 obtained from this work 0.1 M NaCl without CO2 at 25˚C. the total concentrations of uranyl ions was 1.67 mmol·dm⁻³, and the ones of AA was 3.33 mmol·dm⁻³. The pKw value used in this model was -13.78 as I = 0.1 M in NaCl solution.

$VO(PYR)^0$ and $VO(PYR)_2^{2-}$ were two main species (>80%) ranging from pH 3.5 to 5.2 and pH 5.2 to 10.5 respectively. The model with the new pKa denoted the highest percentages of $VO(PYR)^0$ and $VO(PYR)_2^{2-}$ were 73.7% at pH 5.0 and 81.4% at pH 6.5 respectively. However, although pKa of PYR got increased from 9.17 to 9.28, only a deviation of 0.4% found in their products. The complexes of vanadyl-catecholate was following complexing formats [VOA] and $[VOA_2]^{2-}$ because of two major O⁻

(Jezowska-Bojczuk, Kozłowski et al. 1990), while only $UO_2(PYR)^0$ can be observed in Hyss model simulation in spite of 4 species advised in the study of Martell and Smith (1977). It likely denoted that the species of $UO_2(PYR)^0$ with $\log\beta$ of 15.7 was greatly higher than others and thus readily was converted to $UO_2(PYR)^0$ as the second deprotonated progress occurred in catecholate.
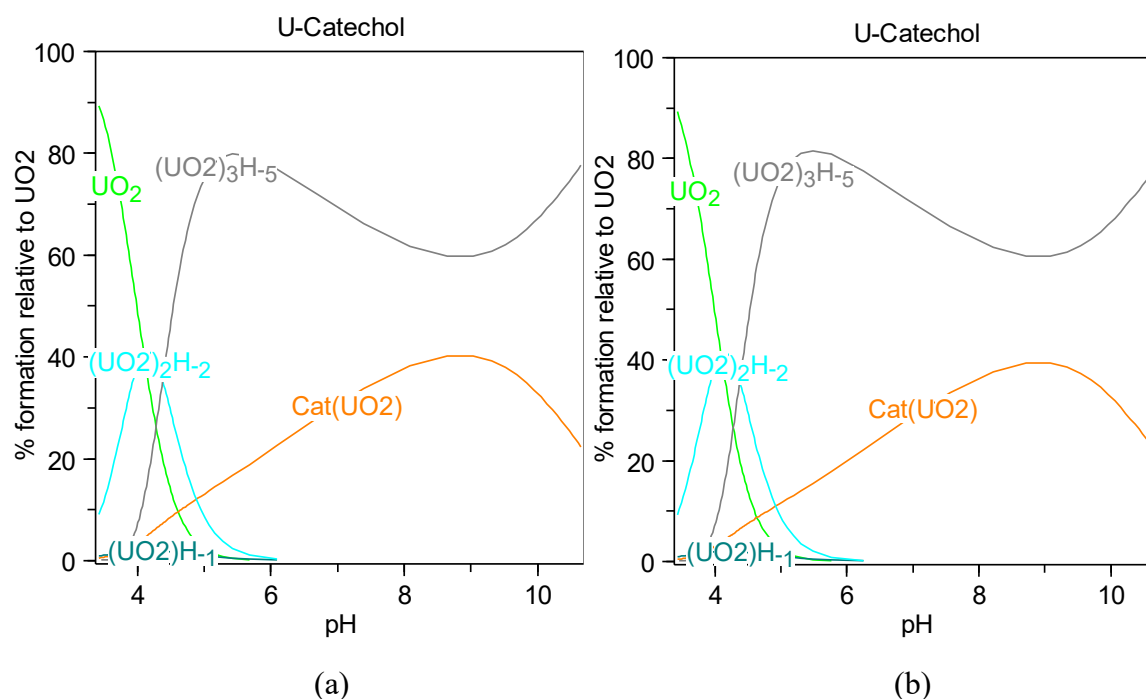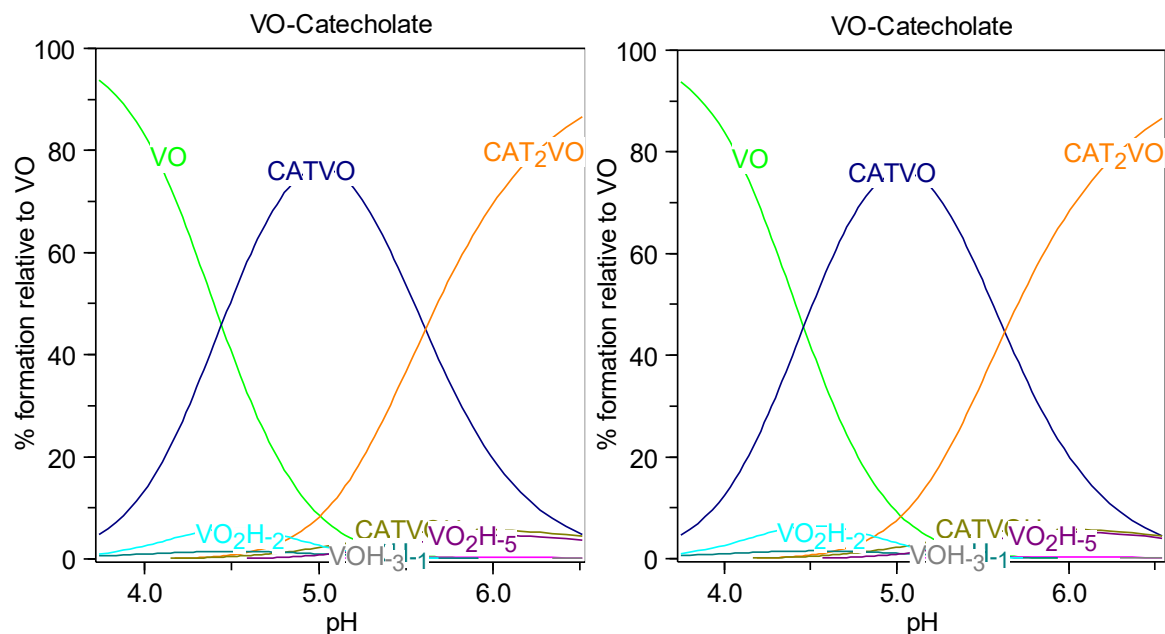

Figure 23 The speciation models for V(IV)-PYR were established in Hyss. In the model of V(IV)-PYR (a) pKa value of HAHA was 9.17. The complexing reaction occurred in 1.0 M NaCl solution without CO2 at 25˚C. In the model of V(VI)-AHA (b) pKa of PYR was 9.28 obtained from this work 0.1 M NaCl without CO2 at 25˚C. the total concentrations of uranyl ions was 1.67 mmol·dm^{-3}, and the ones of AA was 3.33 mmol·dm^{-3}. The pKw value used in this model was -13.78 as I = 0.1 M in NaCl solution.

The formation curves among the complexation of targeted metal ions with these 4 ligands denoted an order related to the affinity of ligands to metal ions in terms of their formative percentages in the models above. In the speciation curves of U-L complexing , the affinity of ligands to uranyl ions presented the order followed by U-AHA>U-PYR>U-GA>U-AA according to practical formative percentages of their complexing species. Furthermore, in V(IV)-L models, the affinity of pyrocatechol to vanadyl ions revealed a large lift in the formative percentage which was increased to approximately 81% from VOPYR in 1:1 M-L species in Figure 17. Therefore, the new order of the ligand affinity in V-L complexing models was followed by V-PYR>V-AHA>V-GA>V-AA.

In this work , two ligands, acetohydroxamic acid and pyrocatechol, played an important role in the complexing function of uranyl and vanadyl ions compared with the lower affinity found in acetic acid and glycolic acid. Moreover, it was also found that coordinated forms via α-hydroxycarboxylate was much stronger than the ones found in carboxylate in terms of models related to formative percentages with respect to metal-GA and metal-AA. It was reported that the stability of U(VI)-L complexed in the order followed by : α-hydroxycarboxylate>catecholate>hydroxamate>carboxylate in terms of their DFT calculating results (Guo, Xiong et al. 2016, Kirby, Simperler et al. 2018). Based on their binding modes, UVI-GA and UVI-AHA were attributed to monodentate structure on the axis and bidentate structure (via O atoms) on the equatorial plane in terms of their stability constants which resulted in a

difference for formative percentages. Moreover, the variation of pKa values among these 4 complexing models had few impacts on the hydrolysis or the distribution of hydrolytic species as pH increase.

4.3 Determination of conditional and intrinsic pKa values at variable temperature and calculate thermodynamic variables (ΔG, ΔH, ΔS).

4.3.1 The effect of temperature on the experimental pKa values in NaCl solution of 1.0, 2.0 and 3.0 M

pKa values among these 4 ligands indicated a different sensitivity to temperature in Fig. 24. In results of HAHA and PYR, there were obvious decreasing trends of pKa values from 298.15K to 335.15K regardless of ion strength increased from 1 to 3M. It can be found that pKa values in HAHA and PYR at 1.0M showed a significant drop from 9.12±0.01 to 8.92±0.004 and from 9.21±0.04 to 8.77±0.04, respectively. The situations at 2.0 and 3.0 M were similar to the one at 1.0 M and also showed significant decreases of pKa values as the increase of temperature.

Nevertheless, The effect of temperature on AA and GA was likely to be weaker than the ones in HAHA and PYR. Although their pKa values presented significant lifts as ion strength increased from 1.0 to 3.0M, the relationship between their values and temperature was obscure in terms of their performance in Fig 24. pKa values of AA were 4.51±0.02 to 4.53±0.02 at 298.15 K and 335.15K at 1.0 M respectively. The variation of GA was similar to the one of AA which denoted a slight change from 3.52±0.01 to 3.57±0.02 as temperature up to 335.15K, while there were insignificant varieties with respect to the pKa values from 298.15 to 335.15K were 3.62±0.02 and 3.61±0.002 at 2.0 M, and 3.69±0.03 and 3.68±0.02 at 3.0M. It was reported that the effect of temperature on pKa values of GA showed an increase from 273.15 to 310.65K and presented a decrease up to 323.15K (Nims 1936). In study of (Harned and Ehlers 1932), there was a rapid climb of pKa values of AA from 273.15K to 288.15K, while the values tended to be more stable as T up to 303.15K and presented a slight drop at T equals to 308.15K. It was reported that the carboxylic acid attached to α-carbon and the pK of the carboxylic acid on the sided chain of glutamic acid were almost independent of temperature (Nagai, Kuwabara et al. 2008). Therefore, it was explained that the weak temperature sensitivity of AA and GA shown in Figure 26c and 26d were attributed to their carboxylate structures. Furthermore, In this work, there were significant increases of pKa values occurred in AA and GA at 1.0 M and 2.0 M in NaCl solution, while there was no significant variation found in other ion strength. it was likely assumed that AA and GA had arrived at a temperature range threshold that presented a slow diversion compared with the performance at low temperature.
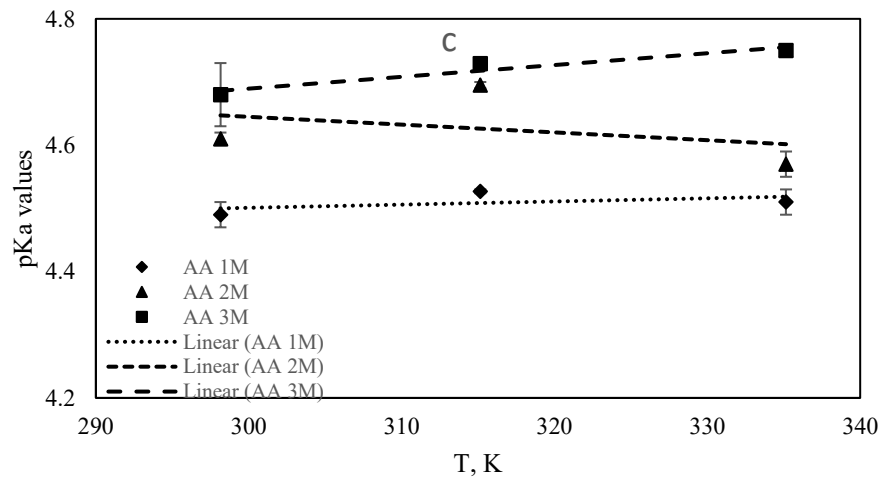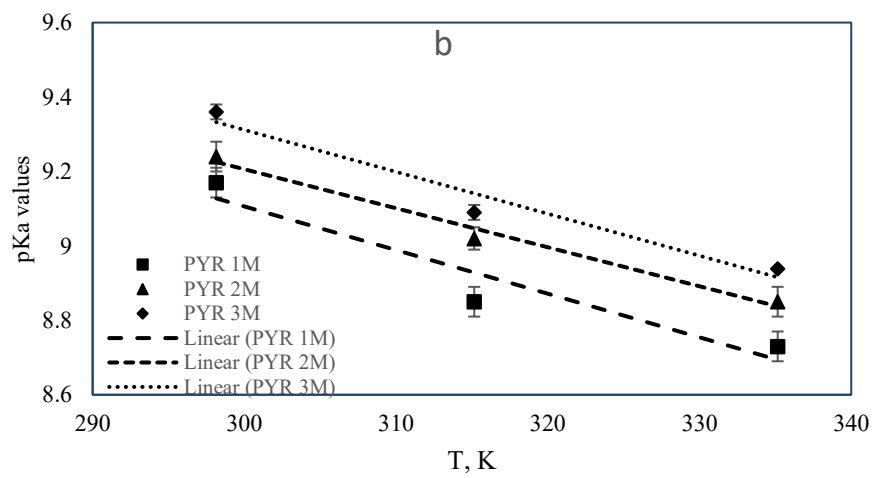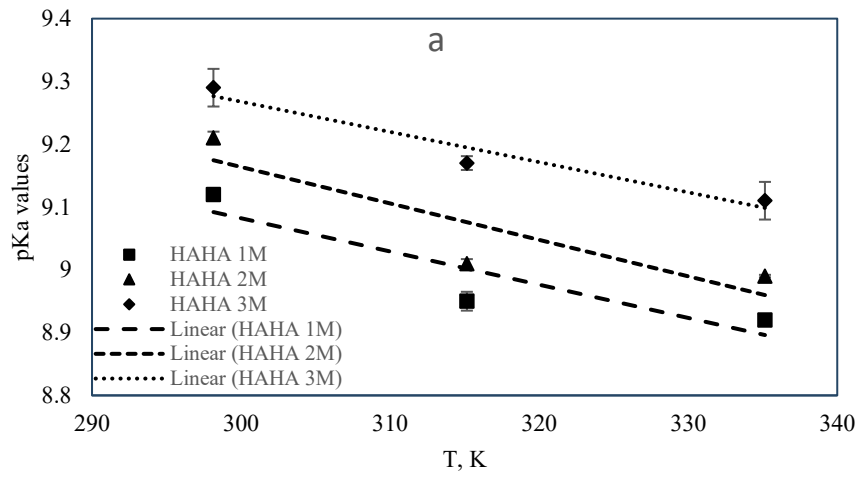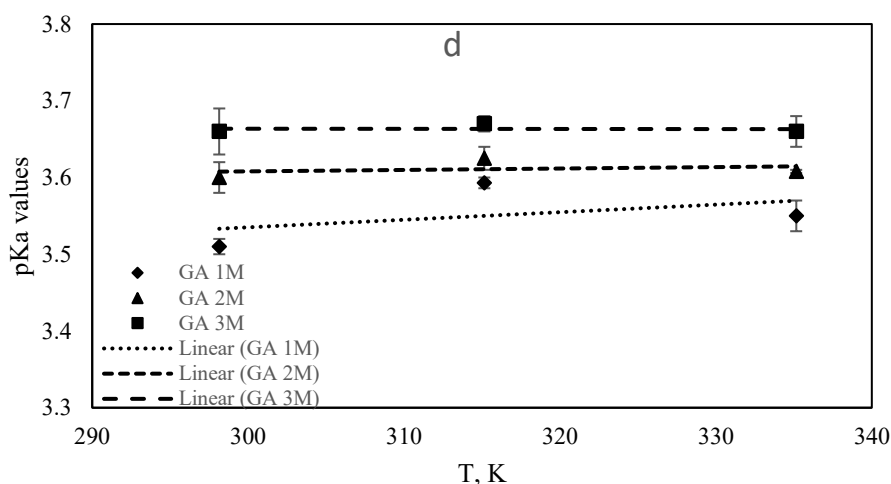
Figure 26 The effect of temperature on pKa values among acetohydroxamic acid (a), pyrocatechol (b), acetic acid (c) and glycolic acid (d) at ion strength of 1.0, 2.0 and 3.0 M in NaCl solution. The dash line represented linear trendlines plotting pKa values vs temperature . In linear relationship of HAHA and PYR, their R^2 value were 0.94 and 0.99 which indicated a high reliability of temperature to their pKa values, while the R^2 values for AA and GA were only 0.25 and 0.19 respectively which showed a low relativity of temperature.

4.3.2 The calculation of thermodynamic parameters via Van't Hoff equation

To have a better understanding of the thermodynamics of the deprotonation in ligands, thermodynamic parameters were determined based on Van't Hoff equation via establishing relationships between pKa values and their corresponding temperature. It was reported that the application of Van't Hoff equation was applied at three different temperature gradients (298.15K, 315.15K and 335.15K) and was divided into 2 steps: (i) the determination of standard enthalpy values (ΔH) and entropy values (ΔS) was carried out via Eq. 29 and (ii) the determination of standard Gibbs free energy (ΔG) resulting from results from step (i) implemented in Eq. 27 (Alam, Varshney et al. 2018, Zakaria, El Kurdi et al. 2022). Thereby, plotting Gibbs energy vs T produced the intercept and the slope derived from ΔH and ΔS respectively.

Table 18 Thermodynamic parameters for the dissociation progress of acetohydroxamic acid, pyrocatechol, acetic acid and glycolic acid in NaCl solution of 1.0, 2.0 and 3.0 M at 298.15, 315.15 and 335.15K

L	Temperature	Ion strength / M	ΔH (kJ·mol⁻¹)	ΔG (kJ·mol⁻¹)	ΔS (J·mol⁻¹ ·K⁻¹)
HAHA	298.15K	1	-4.34±0.151	-22.61±0.025	61.04±0.399
	315.15K			-23.45±0.039	
	335.15K			-24.86±0.011	
	298.15K	2	-4.75±0.182	-22.83±0.025	60.36±0.523
	315.15K			-23.61±0.018	
	335.15K			-25.05±0.006	
	298.15K	3	-3.98±0.050	-23.03±0.074	63.79±0.341
	315.15K			-24.04±0.017	
	335.15K			-25.38±0.084	
PYR	298.15K	1	-9.66±0.000	-22.83±0.099	43.84±0.332
	315.15K			-23.29±0.105	

	335.15K			-24.44±0.111	
	298.15K	2	-8.67±0.021	-23.00±0.099	47.93±0.371
	315.15K			-23.71±0.079	
	335.15K			-24.77±0.111	
	298.15K	3	-9.77±0.446	-23.25±0.050	45.06±1.300
	315.15K			-23.87±0.052	
	335.15K			-24.91±0.003	
AA	298.15K	1	0.43±0.035	-11.18±0.050	38.96±0.231
	315.15K			-11.87±0.008	
	335.15K			-12.62±0.056	
	298.15K	2	-0.87±0.245	-11.45±0.025	35.79±0.874
	315.15K			-12.31±0.013	
	335.15K			-12.79±0.056	
	298.15K	3	0.70±0.837	-11.72±0.124	38.80±0.460
	315.15K			-12.39±0.003	
	335.15K			-13.26±0.028	
GA	298.15K	1	1.01±0.241	-8.73±0.025	31.82±0.866
	315.15K			-9.43±0.018	
	335.15K			-9.95±0.056	
	298.15K	2	-0.28±0.412	-8.97±0.050	29.25±1.205
	315.15K			-9.54±0.039	
	335.15K			-10.06±0.006	
	298.15K	3	-0.21±0.193	-9.15±0.074	29.95±0.446
	315.15K			-9.64±0.026	
	335.15K			-10.25±0.056	

The effect of temperature and ion strength on ΔG for these 4 ligands was positive in Table 20. It can be found that a significant variation of ΔG values found in HAHA tended to increase from -22.61±0.025 to -24.86±0.011 as the temperature climbed from 298.15K to 330.15K in 1.0 M NaCl solution. Subsequently, The ΔG values went up to -25.38±0.084 as the solution condition reaching ion strength of 3.0 M and 335.15K. The situations of PYR, AA and GA were similar to the ones of HAHA in spite of differences in thermodynamic parameters. The ΔG values for PYR were nearing the values for HAHA and kept increaseing from -22.83±0.099 to -24.91±0.003 with respect to the solution altering from 1.0 M at 298.15K to 3.0 M at 335.15K. ΔG values for AA were closing the ones for GA and also denoted a significant increase as the lifting temperature and ion strength. It can be found that ΔG values for both of ligands eventually arrived at -13.26±0.028 and -10.25±0.056 at 335.15K in 3.0 M NaCl solution. Furthermore, according to negative values of ΔG values for these 4 ligands regardless of the change of reacting conditions (T and I), the deprotonation of these ligands was based on spontaneous progress.

The calculated enthalpy values (ΔH) and entropy values (ΔS) based on the method above are shown in Table 20. Although some of the significant variation occurred in these values, the effect of temperature

and ion strength on ΔH and ΔS values was not clear or presented non-linear relationship in Table. For instance, in comparison of ΔH values for PYR at 1.0, 2.0 and 3.0 M, there was no significant deviation found between at 1.0 and 3.0 M in spite of a significant decrease found at 2.0 M compared with the others. The performance of ΔS values in HAHA was similar to the ones of ΔH values in PYR, it was difficult to exploit the relationship between the temperature or ion strength and ΔS values since the values had no particular trend for increase or decrease. Therefore, the factors to influence ΔH and ΔS values were independent on the temperature and ion strength in their dissociation progress (Zhao and Gao 2006). According to significant variations of ΔG values in HAHA and PYR, it was clear that ΔH and ΔS in the progresses were compensating since the presence of ΔG variations came up as the variations in both of ΔH and ΔS values in spite of their different direction (Brink and Crumbliss 1982). However, based on TΔS calculation, it can be found that ΔH in AA and GA was quite low with the small deviation (only from -1.11 to 1.21 KJ·mol^{-1}), it can be found that ΔS values control the dissociation exclusively in these two ligands (Brink and Crumbliss 1982). However, it was difficult to determine the effect of ΔH and ΔS values on pKa values among these 4 ligands due to non-linear entropic or enthalpic contribution to ΔG values (Thakur, Mathur et al. 2007).

4.4   Determination of intrinsic pKa values via Davies equation and SIT

The selection for the calculation of intrinsic pKa values among these 4 ligands depended on employed ion strength ranging from 0.1 to 3.0 M. In the study of (Samson, Lemaire et al. 1999), established models for intrinsic pKa values prediction presented different degrees of deviation with experimental linear models as the climbing ion strength. It can be found that the smallest deviation was found between experimental ones and Davies-equation model from 0.1 to 0.5 M (Figure 10). However, the shortage of the established model was expressed after ion strength exceeding 0.5M ion strength because of a larger deviation found in successively increasing ion strength. The selection of SIT was normally performed to fit activity coefficient ($ɤ$) at high ion strength (1 to 3 M). Previous studies have figured out an appropriate interval of ion strength (2-3M) and showed two low accuracy interval (bad performance with the deviation) (<0.5M) and (>3.0M)(Bretti, Foti et al. 2004, Thakur, Mathur et al. 2007). Activity correction is related to the effect of ion strength on pKa values since measurements of these values at zero ion strength are likely difficult to be fulfilled under laboratory conditions such as a dramatic drop of conductivity of working electrode occurred in 0 M solution. In this work, ion strength ranging from 0.1 to 3.0 M were provided with regarding pKa values among these 4 ligands shown in Figure 19. Considering their pKa values acquired in wide ranges of ion strength, the calculation of their intrinsic pKa values were divided into the application of the Davies equation and of SIT with respect to the low ion (<0.5M) and high (<3.0M)ion strength in this work.

4.4.1   The activity correction from 0.1 to 0.5 M ion strength using Davies equation

The intrinsic pKa values for HAHA, PYR, AA and GA calculated via Davies equation were tended to be fitting with model produced from experimental data less than 0.5M in this work. The equation aimed to acquire activity coefficients via logarithm of reactants and products at equilibria deprotonation or named as Davies values ($-A \times z_i^2(\sqrt{I}/(1+\sqrt{I})-0.3I)$)) for calibrating pKa values at ion strength equals to

zero. In this work, pKa values carried out ranging from 0.1 to 0.5M ion strength were investigated at 298.15K and 315.15K (shown in Figure 17) respectively.

Table 19 Intrinsic pKa values caculated via Davies equation in 0.1M and 0.5M NaCl solution at 298.15K, 315.15K. Reference data was measured at 298.15K in particular solution and approaching to acquired data in this work.

Ligands	298.15K	315.15K	Ref. at 298.15K	Ref.
HAHA	9.54±0.016	9.34±0.011	9.52 (KCl)	(Farkas, Enyedy et al. 1999)
PYR*	9.38±0.026	9.19±0.036	9.27 (KCl)	(Nurchi, Pivetta et al. 2009)
AA	4.73±0.035	4.82±0.021	4.75 (NaCl)	(Kilpatrick and Eanes 1953)
GA	3.79±0.016	3.85±0.026	3.83 (NaCl)	(Kilpatrick and Eanes 1953)

* the pKa value of PYR in the first deprotonation.

Intrinsic pKa values measured via Davies equation showed a declined trend of pKa values within ion strength from 0.0 to 0.5 M. The intrinsic values arrived at the highest values in the valid ranges for the use of Davies equation. Compared with other values calculated from previous papers, a low deviation (approximately 0.91% in PYR) denoted the species of electrolytes has few impacts on the calculation of Davies equation up to 0.5M since the calculation of SIT is required to consider the types of solution reflected by their interaction coefficients under higher ion strength conditions.

However, the effect of temperature likely influence activity calibration greatly, especially in HAHA and PYR. There were significant varies occurred in these 4 ligands as temperature increased by 17˚C in Table 19. A sharp increase was found in HAHA and PYR with respect to 0.20 and 0.19 log units respectively, while a significant decline was observed in AA and GA with respect to 0.09 and 0.06 log units respectively. Compared with differences between intrinsic values acquired in this work and in references, differences between the values found at 298.15K and at 315.15K demonstrated larger numbers. The largest variety was found in HAHA from 0.02 log units increased to 0.2 log units, and the smallest one was found in GA from 0.04 log units increased to 0.06 log units. Therefore, it was likely assumed that the effect of temperature on ligands with catecholate and hydroxamate was more sensitive to on ligands with carboxylate or α-hydroxycarboxylate in this work.

Intrinsic pKa values among the 4 ligands lacked consistency compared with the intrinsic ones calculated from SIT as ion strength increased to 2.0 M. The large deviation of pKa values was illustrated between ion strength from 0.1 to 1.0 M and from 2.0 to 3.0 M within 4 ligands via Davies equation calibration shown in Figrue 27. Compared with the values at 0.1 M, there were remarkable decreases at ion strength of 2.0 M according to 0.37 log units in HAHA, 0.16 log units in PYR, 0.18 log units in AA and 0.19 log units in GA. The largest deviation at ion strength up to 0.5 M was only 0.08 found in PYR. Subsequently, the deviation observed at higher ion strength (3M) was continuously expanded led to the low-accuracy performance of Davies equation at high ion strength. It can be found a larger fluctuation that the intrinsic values found in HAHA, GA, AA and PYR at 3.0 M was decreased by 0.54, 0.35,0.27 and 0.15 log units compared with their mean values from 0.1M to 0.5 M.
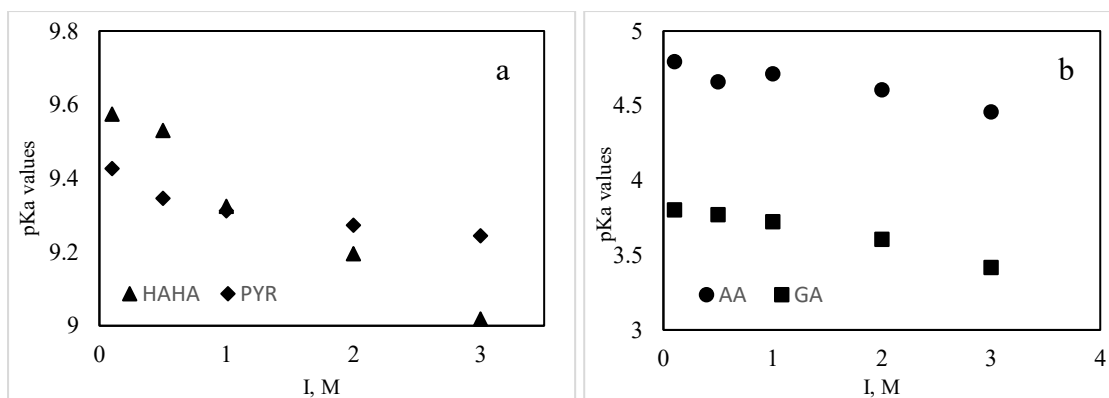
Figure 27 Intrinsic values acquired via the calculation of Davies equation within 4 ligands at ion strength from 0.1 to 3.0 M at 298.15 K. Figure 27a represents intrinsic values of HAHA and PYR obtained from ion strength ranging from 0.1 to 3.0 M via the DE calculation Figure 27b represents intrinsic values of AA and GA obtained from ion strength ranging from 0.1 to 3.0 M via the DE calculation. A larger decrease of pKa values was observed at ion strength at 2.0 M based on the values at 0.1 M and the variety continually was expanded as ion strength kept increasing.

4.4.2 The activity correction from 1.0 to 3.0 M ion strength via SIT

The use of SIT was to replace the reasonable method for activity correction with Davies equation in higher ion strength solution (1.0 M<I<3.0 M) and was implemented readily in terms of a direct calculating progress. Required parameters involving the method are similar to the other methods including Davies and Extended-Debye Huckle equation excluding interaction coefficient (ε_i) which is able to reflect the effect of ion strength on species i as result of short range non-electrostatic influence (Thakur, Mathur et al. 2007).

The determination of ε_i for measuring intrinsic pKa values was reported as a slope attributed to plotting $pKa_i + AZ^2\sqrt{I}/(1+1.5\sqrt{I})$ versus I, and the intrinsic values as the intercept of the plot (Thakur, Mathur et al. 2007). The summary of interaction coefficients and intrinsic values via the method of SIT from 1.0 to 3.0 M ion strength was shown in Table 20. Meanwhile, intrinsic values originated from DE and literatures were also shown in Table 20 for observing the difference between the method of SIT and DE. It can be found that intrinsic pKa values acquired from high ion strength were approaching the values from papers and Davies equation in terms of small differences up to only 0.04 log units (in PYR) at 298.15K. However, the values found in HAHA denoted a large difference up to 0.11 log units compared with Ref. values and a large difference up to 0.13 log units compared with Davies values as well. Meanwhile, the intrinsic values (9.31±0.05) for PYR measured via SIT was also lower than the ones (9.38±0.026) found in Davies equation but higher than the value (9.27) in paper in spite of a lower deviation (only 0.04 log units) presented in Table 20. It thus likely indicated that pKa values measured at high ion strength influenced short range non-electrostatic force remarkably which led to lower intrinsic values found in hydroxamate and catecholate ligands.

Table 20 Comparison of intrinsic values among four ligands: acetohydroxamic acid, pyrocatechol, acetic acid and glycolic acid between via SIT and via Davies equation, and interaction coefficient ε_i at 298.15K.

Species	pKa0 (SIT)	pKa0 (Davies)	Ref. at 298.15K	ε_i
HAHA	9.41±0.003	9.54±0.016	9.52 (KCl)	0.13±0.01
PYR	9.31±0.05	9.38±0.026	9.27 (KCl)	0.10±0.006
AA	4.77±0.003	4.73±0.035	4.75 (NaCl)	0.16±0.009
GA	3.80±0.01	3.79±0.016	3.83 (NaCl)	0.12±0.01

The effect of temperature on intrinsic values was similar to results from Davies equation calculation. In HAHA and PYR, intrinsic values calibrated via SIT at higher temperature were smaller than the values at lower one. It can be found that the values for HAHA and PYR of 9.41±0.003 and 9.31±0.05 at 298.15K declined to 9.22±0.02 and 8.99±0.05 at 315.15K respectively. However, there were extremely slight varieties within intrinsic values in HAHA and PYR in the following temperature increase. The representative of carboxylate and α-hydroxycarboxylate indicated a converse trendline as the increase of temperature. As the temperature increased from 298.15K to 315.15K, intrinsic values of AA and GA showed insignificant lifts from 4.77±0.02 and 3.79±0.007 to 4.82±0.005 and 3.85±0.008 respectively. However, it was observed that a slight decrease (0.05 to 0.01 log units) was found in AA, and an insignificant change was found in GA. Thereby, the measuring results inferred that intrinsic pKa values found in these 4 ligands altering by high temperature conditions (from 315.15K to 330.15K) probably presented a low sensitivity.
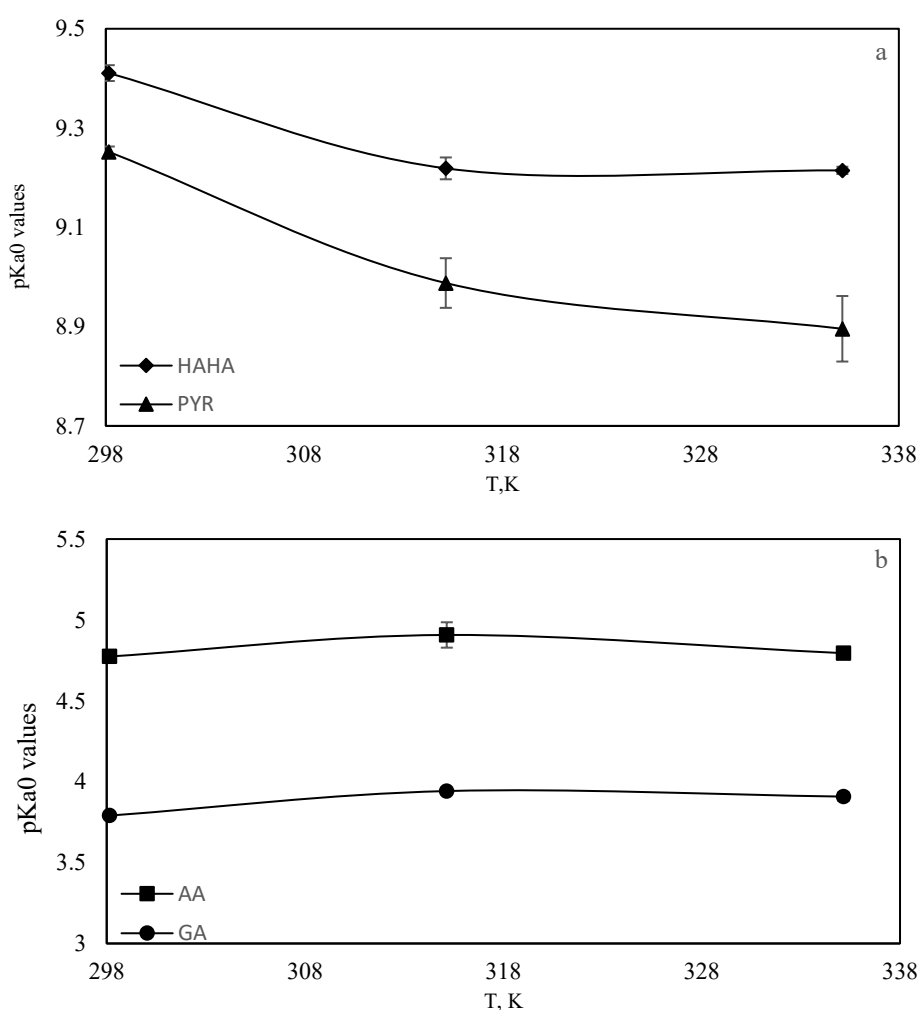
Figure 28 a relationship between temperature and intrinsic pKa values of ligands in Figure (a): acetohydroxamic acid and pyrocatechol; and Figure (b): acetic acid and glycolic acid. The values were determined at 298.15, 315.15 and 335.15K in NaCl solution. There were 3 points representing from ion strength of 1.0 to 3.0 M calculated via SIT for measuring their average values and standard deviation in figures.

In the progress of activity correction, The validity of Davies equation and SIT depending on ion strength ranges has been discussed. In this work, since the calculation via Davies equation demonstrated a high deviation found in intrinsic values from ion strength of 1.0 to 3.0 M, the available ion strength ranges were determined from 0.1 to 0.5 M whereby stable results. However, the calibrating results via SIT

indicated similar values from 0.1 to 0.5 M in some of cases (HAHA and PYR) especially in situations at 0.5 M. However, the performance of SIT in AA and GA indicated a large fluctuation from 0.1 to 0.5 M. it thus inferred that the reasonable ranges in the most of cases were still followed by the high ion strength one (from 1.0 to 3.0 M) attributed to a stable yield of intrinsic values.

4.5 Present representative U and V speciation diagrams using intrinsic pKa values and the effect of the values on the species formation

The models established via the literature data have been displayed in this work (in chapter 4.2). It was proved that the practical quantifying work greatly depended on the conditions of ion strength, background electrolyte and temperature etc.. pKa values measured at the setting experimental conditions as an essential factor for the determination of complexing stability constants to influence the work greatly. However, the experimental pKa values only were suitable for the single environmental conditions and charge contribution from specific ligands. Thus, the understanding of a M-L complexing system was obligatory to focus on intrinsic pKa values with fundamental properties of the interactions (Tsui, Ojcius et al. 1986).

In this work, the complexation of uranyl and vanadyl ions with ligands was discussed to indicate the contribution of the intrinsic values via the different methods for activity correction to quantifying the complexing systems. Although the application of SIT and Davies equation produced intrinsic pKa values (in chapter 4.4) for each ligand in NaCl solution at three different temperatures (298.15K, 315.15K and 335.15K), the influence of medium like NaCl also made huge contribution to the species formation in the models. Since the background electrolyte in the models was NaCl, the specific hydrolysis constants of uranyl and vanadyl ions were necessary to be considered improving the accuracy of the formation curves compared with the other models. The hydrolysis constants of UO_2^{2+} and VO^{2+} were reported in the study of (Berto, Daniele et al. 2008, Altmaier, Yalçıntaş et al. 2017) shown in Table 16.

Based on the data measured via potentiometric titration in this work, the new models were established derived from introduced intrinsic pKa values and the hydrolysis constants of uranyl and vanadyl ions in NaCl soltion. Meanwhile, the intrinsic values calculated via DE and SIT represented the intrinsic values based on the protonation occurred in the solution at ion strength from 0.1 to 0.5 M and from 1.0 to 3.0 M respectively. However, due to the lack of data for indicating the effect of ion strength on the stability constants of M-L complexes, the intrinsic constants for the complexing species was difficult to be determined. Thus, the constants applied in the speciation model were originated from literatures discussed in Chapter 2.1.The established models were followed by the practical conditions for the application of titration experiments involving the appropriate concentrations of ligands and metal ions and the valid ranges of pH regarding the detecting limitation.

4.5.1 The effect of intrinsic pKa values on UVI-AHA and VIV-AHA formation models

It was reported that two species as products of the complexation of uranyl with HAHA can be detected (Chung, Choi et al. 2011). Compared with other actinides like plutonium, uranyl ions was not be

reduced in presence of HAHA in spite of the speciation of hydroxylamine converted from HAHA (Govindan, Sukumar et al. 2008). Thus, the quantifying work for the complexing reactions only considered the initial concentrations of uranyl ions.

To understand the effect of way how we calculated intrinsic pKa values on the UO2-AHA complexing formation, the values calculated from DE and SIT were used to produce the speciation curves for observing the variation of complexes contents derived from the experimental ones (in Figure 25). The experimental pKa values of HAHA equals to 9.32 calculated at 298.15K in 0.1 M 298.15K, while intrinsic values calculated from SIT and DE were respective to 9.41 and 9.54 at 298.15K. The ratio of participated concentrations of M:L was 1:4 as the excessive ligand complexing metal ions. According to the stability constants of the species shown in Table 7, The M-L complexes arrive at the largest portions at specific pH values in terms of their stability constants. In Figure 29, the species of UO_2AHA^+ and $UO_2(AHA)_2^0$ at pH 4.64 and 8.7 denoted the peak values with respect to 50.7% and 75.1%, while the hydrolytic species of UO_2OH^+,$(UO_2)_2(OH)_2^0$ and $(UO_2)_3(OH)_5^+$ were only up to 2.52%, 5.91% and 27.6% at pH 4.56, 4.50 and 10.5respectively in spite of the subsequent increase for $(UO_2)_3(OH)_5^+$as pH increase continuously. The values for pKa of ligands were demonstrated in terms of the formation percentages to total uranyl ions. There were 2 intersections found at pH 5.37 and pH 10.27 which means the main species of $UO_2(AHA)^+$ was replaced with $UO_2(AHA)_2^0$, and then the species of $(UO_2)_3(OH)_5^+$ gradually dominated the species in the hyperalkaline environment. In the proportions of the first species $UO_2(AHA)^+$, the order of formative concentrations derived from the pKa values was followed by 9.32(experiment)>9.41(SIT)>9.54(Davies) corresponding to 50.7%>48.6%>42.6% at pH 4.45. Afterward, the concentrations of the second species $UO_2(AHA)_2^0$ were increased substantially and were also followed by the same order with respect to the proportional order followed by: 75.1%> 72.2%>64.2%. The differences between the method of SIT and Davies equation were related to the high ion strength which resulted in the enhancement of the non-electrostatic forces between the ion strength and other species in the solution, while it was reported no significant deviation was found as the use of SIT and Davies in reasonable I ranges(Dong and Brooks 2008).
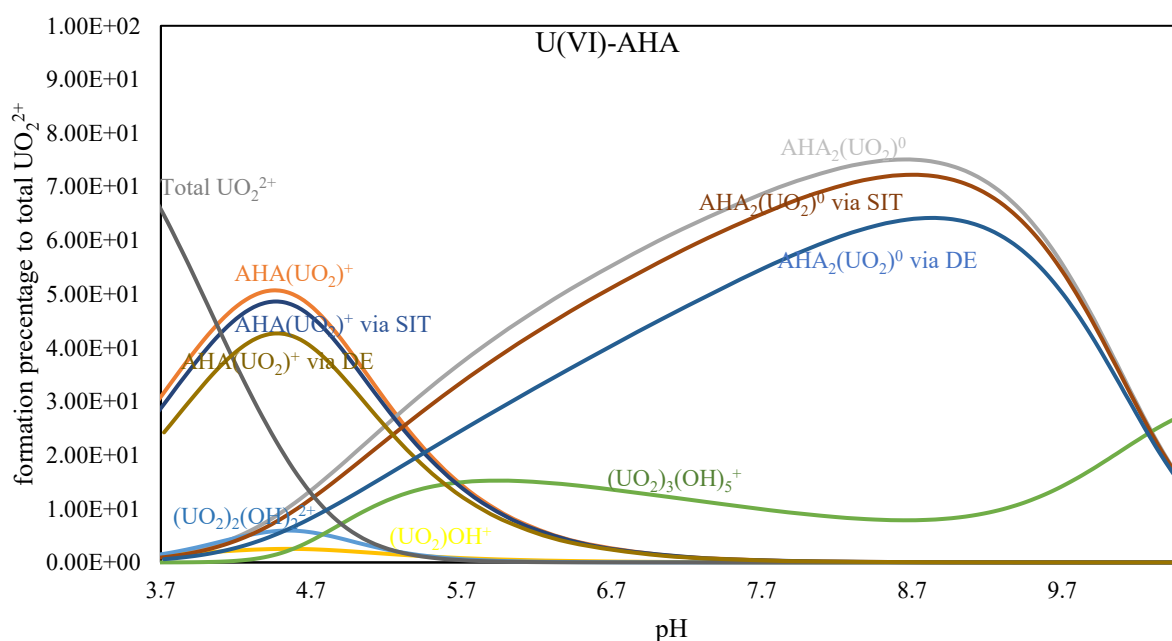
Figure 29 The formation curves of the complexation of uranyl ions with acetohydroxamic acid (HAHA) without dioxide carbon (CO_2) produced from Hyss. The $\log\beta$ values for U(VI)-AHA were shown in Table 17. The total volume of sample solution was 32.5 ml at the beginning. 1.1 ml of 0.1 M NaOH solution was added into the solution for pH conditioning. The initial concentrations of uranyl ions and HAHA were 0.62 mM and 1.54 mM respectively. The experimental pKa values was 9.32 at 0.1 M at 298.15 K. The endpoint for the simulation was up to pH 10.5.

There are three major species of the VO-AHA complexes consisting of $VO(AHA)^+$, $VO(AHA)_2^0$ and $VO(OH)(AHA)_2^-$ shown in Figure 29. The pKa values and the conditions used in the speciation model were same as the ones in the UVI-AHA complexing model. The stability constants of V(VI)-AHA complexes were provided by the values shown in Table 8. The ratio of participated concentrations of M:L was 1:2 as the excessive ligand complexing metal ions. In spite of the known hydrolytic constant of $(VO)OH^+$ and $(VO)_2(OH)_2^{2+}$ in the VO-AHA speciation model, the application of Davies equation and SIT required the complexing system considering more hydrolysing species of vanadyl ions to improve the accuracy in the model (Buglyó and Pótári 2005). The effect of the new intrinsic values calculated via SIT or Davies equation on the formation curves reflected by the deviation with the experimental values at the peak concentrations. The comparative consequence was similar to the situations found in the complexation of uranyl ions with HAHA. The order of the largest formative concentrations within the three dissociation constants was followed by: experiments>SIT>Davies. For $VO(AHA)^+$, the formative percentages of experiments, SIT and Davies were 66.5%, 66.3% and 65.6% at pH 4.48 respectively. Afterward, $VO(AHA)_2^0$ decreases (from pH 5.74 to pH 10.5), while $(VO)_2(OH)_5^-$ starts to form and subsequently increases with pH. As the pH values in the solution up to 5.77, the concentrations of the second species climbed to the largest portions which were 51.4%, 49.3% and 43.5% corresponding to the experimental data, SIT and Davies equation respectively. The peak concentrations of V(IV)-AHA complexes were observed in the species of $VO(OH)(AHA)_2^-$ at pH 8.79. It can be found that the largest contents in the sample solution of experimental data, SIT and Davies equation accounted for 73.4%, 72% and 67.8%, respectively. the difference of peak values for $VO(OH)(AHA)_2^-$ between the SIT curves and the experimental ones was only 1.4% in comparison of a decrease of 5.6% found in the DE curves. Afterward, the continuous lift of the concentrations of $(VO)_2(OH)_5^-$ and $VO(OH)_3^-$ eventually led to a drop of $VO(OH)(AHA)_2^-$ from pH from 8.79 to the endpoint of the model.
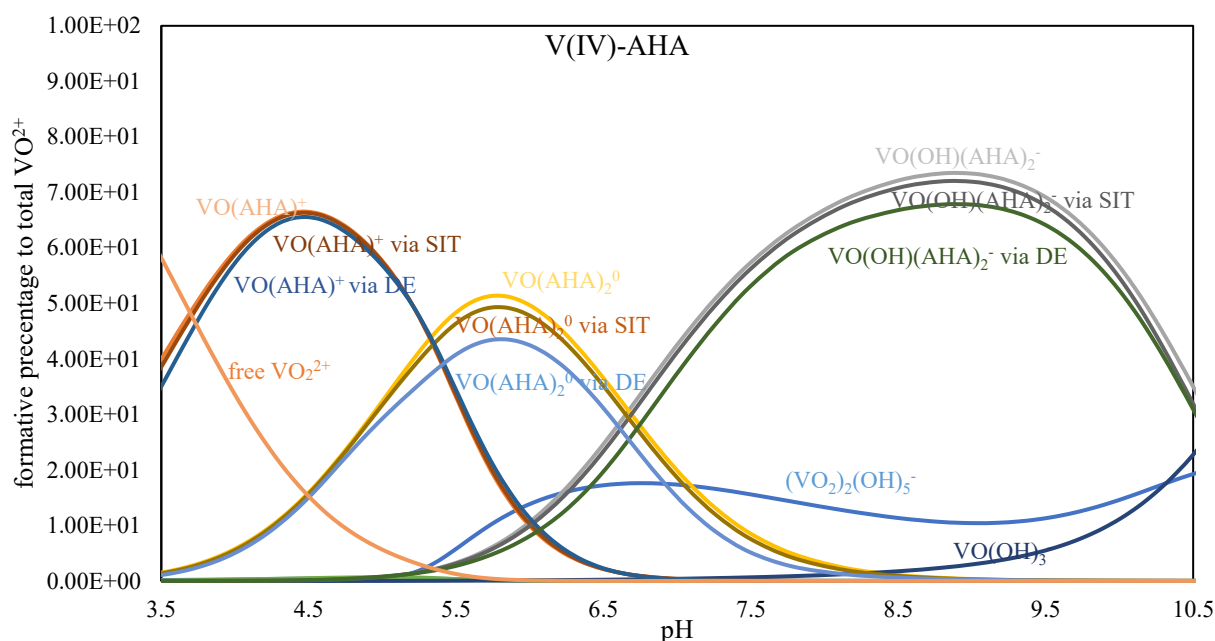
Figure 30 The speciation curves of the complexs between vanadyl ions and acetohydroxamic acid (AHA) without CO_2 produced from Hyss. The logβ values for V(IV)-AHA were shown in Table 17. The initial volume of sample was 30 mL at 298.15K in 0.1 M NaOH of 1.5 mL was used to increase pH values up to 10.89. The total concentrations of vanadyl ions and HAHA were 0.83 M and 1.67 M respectively. The experimental pKa values that came from the study of Evers, Hancock et al. (1989) was 9.36 at 0.1 M.

In the formation models of U(VI)-AHA and V(IV)-AHA complexes, the pKa values produced from SIT is mostly approaching the experimental ones, while the values calculated via Davies equation presented a larger deviation with the experimental curves since the obtained intrinsic values via SIT were lower than the ones via DE. It was obvious that the application of SIT resulting in the concentrations of U(VI)-AHA and V(IV)-AHA complexes were higher than the ones applied in Davies equation. However, the evidence in Table 19 indicated a similar value to the DE one with a low deviation (only 0.01 log unit) in 0 M solution from the study of (Farkas, Enyedy et al. 1999). Therefore, the application of SIT for measuring the intrinsic values of HAHA at ion strength from 1.0 to 3.0 M showed a lower relativity to the variation of ion strength which is in agreement with the results of chapter 4.4.2. Moreover, the major contents of U(VI)-AHA and V(IV)-AHA was maintained up to pH 8.7 and 8.79 respectively, and then their contents were replaced with the species of hydrolytic species of uranyl ions $((UO_2)_3(OH)_5^+)$ and vanadyl ions $((VO)_2(OH)_5^-$ and $VO(OH)_3^-)$ within higher pH ranges.

4.5.2   The effect of intrinsic pKa values on the U(VI)-GA and V(IV)-GA formation models

Compared with the speciation model of U(VI)-AHA species, the glycolate uranyl indicated only 2 species consisting of $UO_2(GA)^+$ and $UO_2(GA)_2^0$ up to pH 5.88 shown in the model (Figure 27). According to the conditions of established model, the simulation was occurred in 0.1 M NaCl solution at 298.15 K. pKa values used for the experiment, SIT and DE were 3.57, 3.79 and 3.81 respectively. The stability constants of U(VI)-GA applied in the model were shown in Table 10. The ratio of M:L

applied in this model was 1:4 to make GA complex with UO_2^{2+} completely. The pKa_0 values calculated from the method of SIT and DE for glycolic acids presented few deviation with no significant difference.

The complexation of glycolate with U(VI) was observed at low pH ranges since the protonation occurred in carboxylate, while the aliphatic hydroxy group begins to dissociate a proton at pH above 3.5 (Szabó and Grenthe 2000). In this work, There were 2 species of the U(VI)-GA complexes formed together from pH 3.0 to 5.5, while the species of $UO_2(GA)^+$ dominated the major complexes in excess of the largest contents of $UO_2(GA)_2^0$ in the model. However, the species $UO_2(GA)^+$ only kept the high level of products in the system up to pH 4.71, and then the concentrations of $(UO_2)(OH)_2^0$ exceeded it. Afterward, at pH 4.82, the contents of $(UO_2)_3(OH)_5^+$ firstly surpassed the ones of $UO_2(GA)^+$ and then became the main species for taking over $(UO_2)(OH)_2^0$ at pH 4.89. The formative curves for intrinsic values calculated via SIT and Davies equation presented the very small deviation but with the experimental data. It can be found that the largest percentages of $UO_2(GA)^+$ calculated from the experiment, SIT one and DE curves were respective to 37.4%, 34.3% and 34.6% at pH 3.76, while the species of $UO_2(GA)_2^0$ derived from these 3 methods were only 5.51%, 4.7% and 4.78% respectively. Therefore, it can be found that the variation based on the peak concentrations of $UO_2(GA)^+$ experimental curves compared with the SIT and DE were only 3.1% and 2.5%. Compared with the performance of the SIT for U(VI)-AHA, the difference compared with the DE for the largest concentrations of major species decreased from 8% to 0.3%. As a result, the intrinsic pKa values for GA calculated via the SIT and DE exhibited the high homogeneity in not only low ion strength ranges (from 0.1 to 0.5 M) but also high ion strength ranges (from 1.0 to 3.0 M).

Figure 31 The formation curves of the complexation of uranyl ions with glycolic acid (GA) without CO2 produced from Hyss. The logβ values for U(VI)-GA were shown in Table 17. The total background volume was 30 ml at the beginning for the simulation, and 2.8 ml of 0.1 M NaOH solution was added into the sample solution for pH adapting up to pH 5.5. The concentrations of uranyl ions and GA were 1.67 mM and 6.67 mM respectively. The experimental pKa values that came from this work was 3.57 at 0.1 M and 298.15 K.

The speciation of VO^{2+}-GA complexes was similar to the ones of UO_2^{2+}-GA in terms of the distribution of their two species and the hydrolytic behaviours of vanadyl ions as pH increase in the model. The parameters of pKa values and $\log\beta$ values for the speciation model was same as in the U(VI)-GA model. The hydrolytic constants were shown in Table 16. In this work, the progress of VO^{2+}-GA coordination was carried out at 0.1 M and 298.15 K. The observed products consisted of $VO(GA)^+$, $VO(GA)_2^0$ and $VO(GA)_3^-$. However, the species of formed $VO(GA)_3^-$ hardly influenced the distribution of free VO^{2+} in the speciation model since the contents were greatly lower than others and difficultly observed from pH 3.40 to pH 5.37 (only up to 0.075%) in the model. The concentrations of $(VO)_2(OH)_2^0$ firstly exceeded the ones of $VO(GA)^+$ and $VO(GA)_2^0$ at pH 5.07 and 4.25 respectively, while the contents of $(VO)_2(OH)_5^-$ displaced the ones of $VO(GA)^+$ and $VO(GA)_2^0$ at pH 5.10 and 4.83 respectively. The species of $(VO)_2(OH)_5^-$ then kept climbing to be the predominating species as the increasing level of $VO(OH)_3^-$ in the model. The curves established via SIT and Davies equation pKa_0 values tended to be analogous based on no significant difference found within their values. In the analysis of formative levels of $VO(GA)^+$, the experimental data was at the highest position whereby 36.8% compared with 35% and 35.2% respective to the peak values of curves for SIT and Davies equation. The presence of $VO(GA)_2^0$ was much lower than the species of $VO(GA)^+$ with respect to only 3.53% found in the experimental curves, while the curves as result of the intrinsic pKa values only arrived at 3.24% for SIT and 3.27% for Davies equation. Therefore, it was observed that the presence of $VO(GA)^+$ likely indicated the high affinity of GA to vanadyl ions in the form of 1:1 M-L complexes in acidic environment. Meanwhile, the stability of their complexes tended to be weak as the increasing of numbers of glycolate binding to vanadyl.
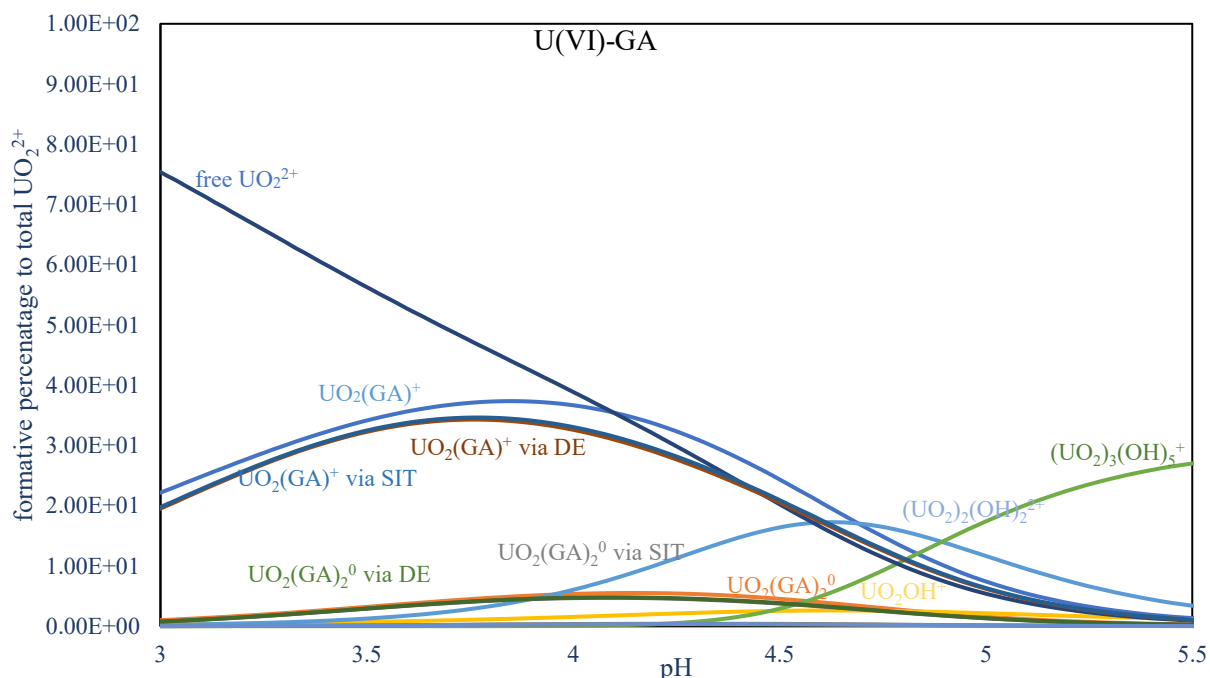

Figure 32 The formation curves of the complexation of vanadyl ions with glycolic acid (GA) without CO2 produced from Hyss. The $\log\beta$ values for V(IV)-GA were shown in Table 17. The total volume was 30 ml at the beginning of the titration, and 2.2 ml of 0.1 M NaOH solution was added into the solution for pH adapting. The concentrations of vanadyl and GA were 1.67 mM and 3.33 mM respectively. The experimental pKa values that came from the study of Kirishima, Onishi et al. 2007 was 3.61 at 1.0 M. The endpoint for the titration was up to pH 5.5.

In the formation of U(VI)-GA and V(IV)-GA complexes, the curves of SIT and Davies equation were infinitely approaching with each other but presented a large deviation with the experimental curves. Based on the largest formative percentages of the species, despite the speciation of either U(VI)-GA or V(VI)-GA complexes occurred in pH from 3.0 to 5.0, the complexing ability of glycolic acid was feebler than the ones of HAHA in terms of their difference of 13.3 % and 29.7 for 1:1 U(VI)-L and V(IV)-L species, and the formation of the secondary species like $UO_2(GA)_2^0$ and $VO(GA)_2^0$ was remarkably rare shown in Figure 31 and 32. Furthermore, as the increase of pH, the hydrolytic behaviours of metal ions gradually displaced the complexing progress. It was assumed the function of glycolate to uranyl and vanadyl ions was available only in acidic environment from pH 3.1 to 5.5 in the model. However, in this work, there was no detection of the large portions of UO_2GA^0 complexes where the second protonation occurred in the ligand even if the DFT calculation for the U(VI)-α-hydroxycarboxylate coordination indicated the highest stability constant (17.08) (Kirby, Simperler et al. 2018). Therefore, it was assumed that the binding structure between uranyl and glycolate in this work was probably at axis plane rather than at equatorial plane in terms of the smaller stability constant (Kirby, Simperler et al. 2018).

4.5.3 The effect of intrinsic pKa values on the U(VI)-PYR and V(IV)-PYR formation models

According to the speciation model shown in Figure 33, the species of U(VI)-PYR was displayed mainly in the form of 1:1 M-L in spite of the other three species reported in the paper in the model (Van Den Berg and Huang 1984). The concentrations of UO_2PYR^0 firstly exceeded the ones of $(UO_2)_2(OH)_2^{2+}$ and $(UO_2)_3(OH)_5^+$ at pH 4.63 and 7.35 respectively. It can be found that the largest contents to total UO_2^+ of UO_2PYR^0 corresponding to the experimental data, SIT and Davies equation were 37.3%, 35.9% and 34.8% at pH 8.88 respectively, while the species of UO_2HPYR^+, $UO_2HPYR_2^-$ and $UO_2H_2PYR_3^{2-}$ accounts for few proportions relative to total UO_2^{2+}. Afterward, the concentrations of UO_2PYR^0 eventually were replaced with the ones of $(UO_2)_3(OH)_5^+$ up to pH 10.50. It likely assumed that the stabilities of the species of UO_2HPYR^+, $UO_2HPYR_2^-$ and $UO_2H_2PYR_3^{2-}$ was much lower than the ones of UO_2PYR^0 in the concentrations of 3.33mM/1.67mM of M:L. Thus, In the study of the complexing uranyl ions in alkaline environment, the role of catecholate in the transport of uranyl ions was not likely negligible in terms of the formation of the high stability complexes at high pH values.

In the simulation of U(VI)-PYR, the hydrolysis species shown in Figure 33 consisted of UO_2OH^-, $(UO_2)_2(OH)_2^{2+}$ and $(UO_2)_3(OH)_5^+$. Nevertheless, considering the concentrations of U(VI)-PYR complexes in the model, the total concentrations of UO_2^{2+} were less than the initial ones at the beginning. Therefore, during the pH from 5.5 to 10.5 in the model, there was likely precipitation of uranyl ions since the concentrations of UO_2^{2+} were 3.33 mM (more than 0.5 mM) which probably led to precipitation as pH increase (Roßberg, Baraniak et al. 2000). However, in the application of PT techniques, the low level of UO_2^{2+} contents likely results in the absence of corresponding complexes with PYR due to the detecting limitations.
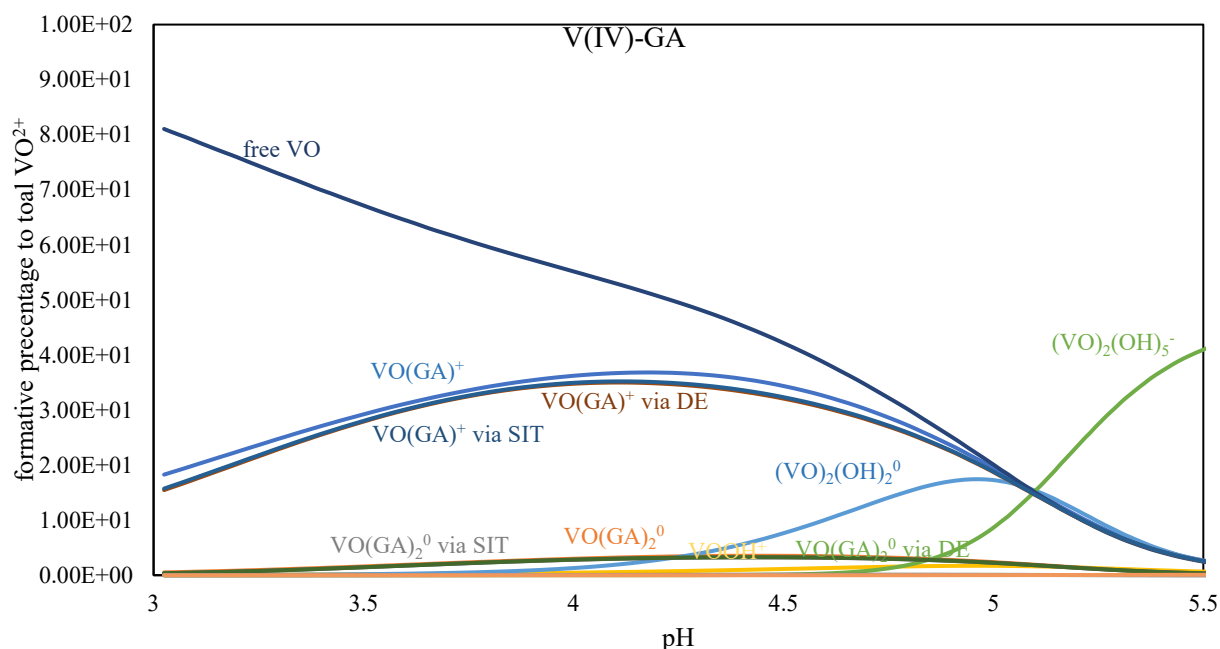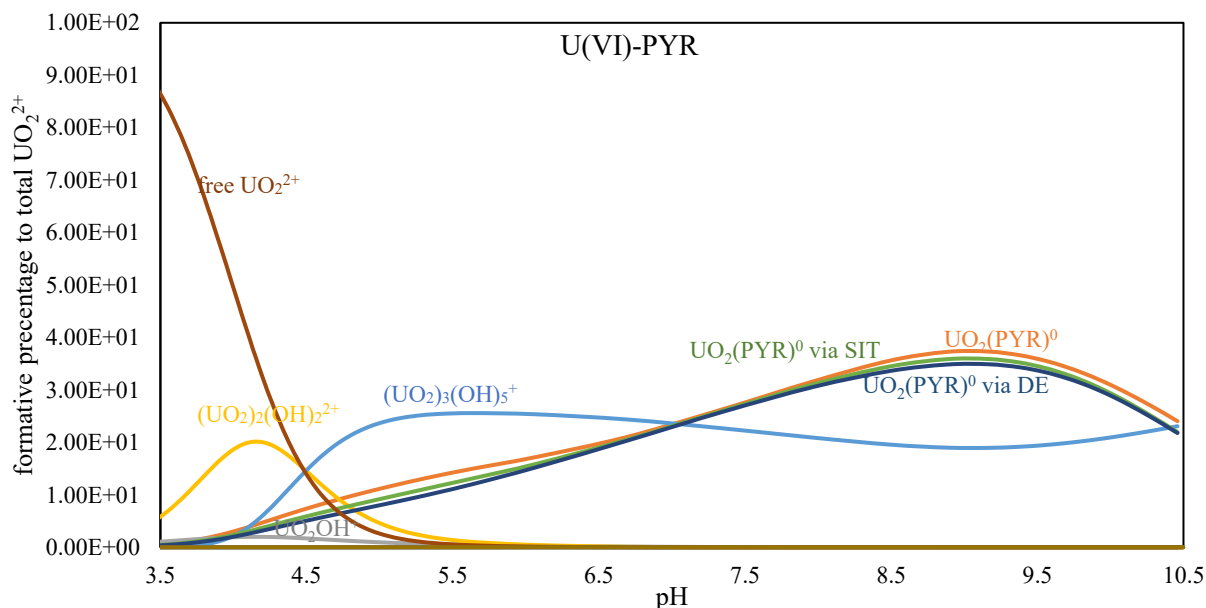
Figure 33 The formation curves of the complexation of uranyl ions with pyrocatechol (PYR) without CO2 produced from Hyss. The logβ values for U(VI)-PYR were shown in Table 17. The setting volume was 30 ml at the beginning of the simulation, and 2.2 ml of 0.1 M NaOH solution was added into the solution for pH conditioning. The concentrations of uranyl and PYR were 3.33 mM and 1.67 mM respectively. The experimental pKa values was 9.28 at 0.1 M calculated in this work. The endpoint for the model was up to pH 10.50.

The high formative percentages of V(IV)-PYR complexes were observed in the species of $VOPYR^0$ and $VO(PYR)_2^{2-}$, while the formation of $VOOHPYR^-$ was at a low level occurred in the replacement of $VOPYR^0$ with $VO(PYR)_2^{2-}$. Although the considerations of VO^{2+} hydrolytic behaviours was introduced in the model, the speciation of its hydrolysis species was difficult to be observed in the complete complexing progress. However, it was reflected that the most of VO^{2+} ions were coordinated via catecholate in the forms of 1:1 and 1:2 M-L complexes. From pH 3.51 to 5.20, the species of $VOPYR^0$ accounted for the largest percentages within the complexing products. The peak percentages of the species resulted from the experimental data, SIT and Davies equation were respective to 78%, 77.7% and 77.5%. Thus, the performance of catecholate to chelate VO^{2+} is much stronger than to chelate UO_2^{2+} because of a formative difference of 40.7% between $VOPYR^0$ and UO_2PYR. Afterward, the species of $VOPYR^0$ was displaced by $VO(PYR)_2^{2-}$ which was continuously formed up to pH 9.65 and then kept stable till to the endpoint of the model. In the study of (Jezowska-Bojczuk, Kozłowski et al. 1990), it was reflected that the species of $VO(PYR)_2^{2-}$ was formed in excess of ligands and was stable to hydrolysis even at pH >12. Thus, the formative curves shown in Figure 34 indicated that $VO(PYR)_2^{2-}$ was the major formats of V(IV)-PYR complexes under high-pH conditions in terms of the experimental data (up to 93.5%), while the largest percentages of $VO(PYR)_2^{2-}$ calculated via SIT and Davies equation were increased to 93.5% and 93.4% respectively. It thus was observed that the speciation curves for SIT and Davies equation presented an extremely small deviation with the experimental ones. Furthermore, there were slight contents of $VO(OH)PYR^-$ found only up to 3.23% calculate via Davies equation. In the study of (Jezowska-Bojczuk, Kozłowski et al. 1990), it reported that catecholate and its derivatives presents an extremely strong ability to bind oxovanadium ions in the form of tridentate or ambidentate complexes in basic media over the intermediate pH ranges. Compared with logβ values related to AHA, GA and AA, the complexation occurred in PYR also shows a remarkably high stability

in terms of their logβ values. Therefore, although there were differences between the experimental pKa values and the intrinsic ones, the deviation within their species were difficult to be observed. Meanwhile, it was likely assumed that the coordination progress was readily ongoing and led to the attenuation of vanadyl hydrolysis.
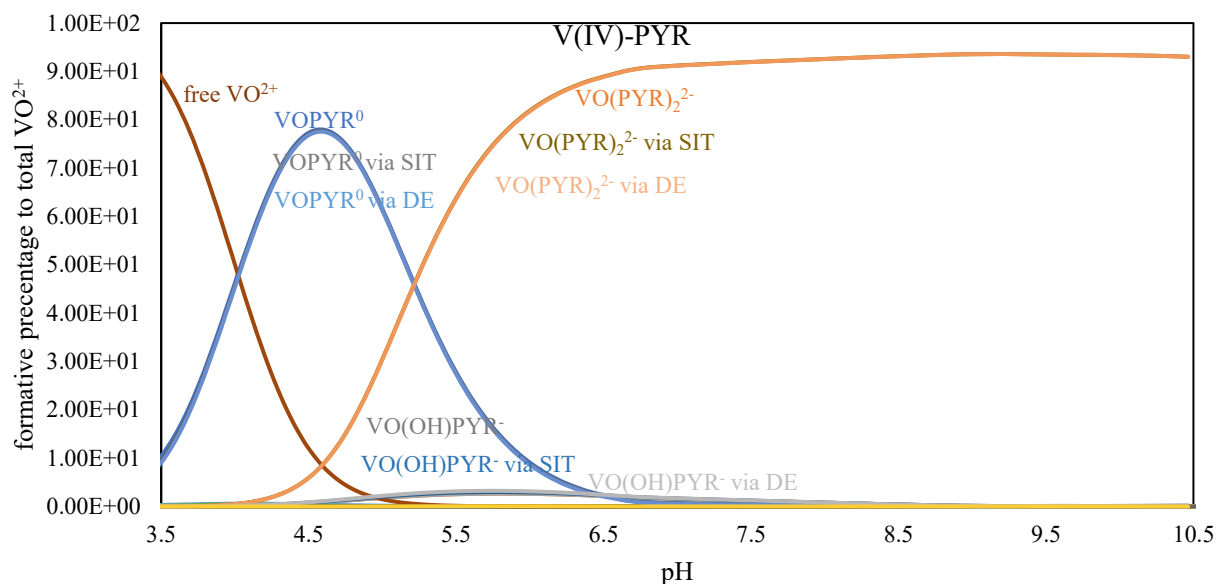

Figure 34 The formation curves of the complexation of vanadyl ions with pyrocatechol (PYR) without CO2 produced from HYPERQUAD. The logβ values for V(IV)-PYR were shown in Table 17. The total volume was 30 ml at the beginning of the titration, and 2.2 ml of 0.1 M NaOH solution was added into the solution for pH adapting. The concentrations of vanadyl and PYR were 1.67 mM and 3.33 mM respectively. The experimental pKa values that came from the study of Jezowska-Bojczuk, Kozłowski et al. (1990) was 9.19 at 0.7 M. The endpoint for the titration was up to pH 10.53.

Based on the models of U(VI)-PYR and V(IV)-PYR formation, the suitable pH ranges for the ongoing progress was extended to the alkaline condition. The performance of the two models indicated the importance of catecholate similar to hydroxamate for the transport of contaminated metal ions in the vicinity of GDF. It was noticeable the increase of pH values enhanced the formation of UOPYR^0 and VO(PYR)$_2$$^{2-}$ in terms of the less speciation of their hydrolysing species compared with the situations of the Metal-GA coordination. In this work, the largest stability constant for U(VI)-PYR was only arrived at 15.8 which was approaching to the value of 16.8 reported in the study of Kirby, Simperler et al. (2018). Therefore, the binding format for U(VI)-PYR tended to be at equatorial lane with the high stability structure (Kirby, Simperler et al. 2018).

4.5.4 The effect of intrinsic pKa values on the U(VI)-AA and V(IV)-AA formation model

The affinity of acetic acid (AA) to uranyl ions as a representative of the carboxylate coordination was similar to the performance of glycolic acids (GA) in the acidic solution because of the binding sites occurred in carboxylate. However, the ability for the complexing metal ions was greatly less than the ones performed in GA since the stabilities of complexes with glycolate is much high than the ones with acetate reported in (Di Bernardo, Tomat et al. 1988). In this work, it, therefore, can be found that the largest formation contents of U(VI)-AA or V(IV)-AA was much less than the ones of U(VI)-GA and V(IV)-GA. The complexation of uranyl ions with AA preferred to be carried out in acidic environment shown in Figure 35. The complete complexing progress was replaced with the hydrolytic performance of uranyl ions at pH 4.05 where the contents of $(UO_2)_2(OH)_2$$^{2+}$ commenced to exceed the ones of

UO_2AA^+. Subsequently, the species of $(UO_2)_3(OH)_5^+$ became the predominating one of all products at pH 4.57 during the progress. The species of UO_2AA^+ dominated among other products in the model with respect to the highest formative percentages in Figure 35. The peak percentages derived from the experimental data, SIT and Davies equation were 13.7%, 10% and 11% respectively. Although there were the subsequent speciation of complexes concluding $UO_2(AA)_2^0$ and $UO_2(AA)_3^-$ in this work, the model denoted the extremely low level of their contents only up to 0.50% and 0.2% respectively. It likley was explained that the total concentrations of acidc acid and uranyl ions maintained a low level which was less than 53mM/26mM (Jiang, Rao et al. 2002). Compared with the larger differences between the experimental curves and SIT curves, the ones produced from Davies equation tended to be more adjacent to the ones of SIT regarding the small ones within their intrinsic pKa values.
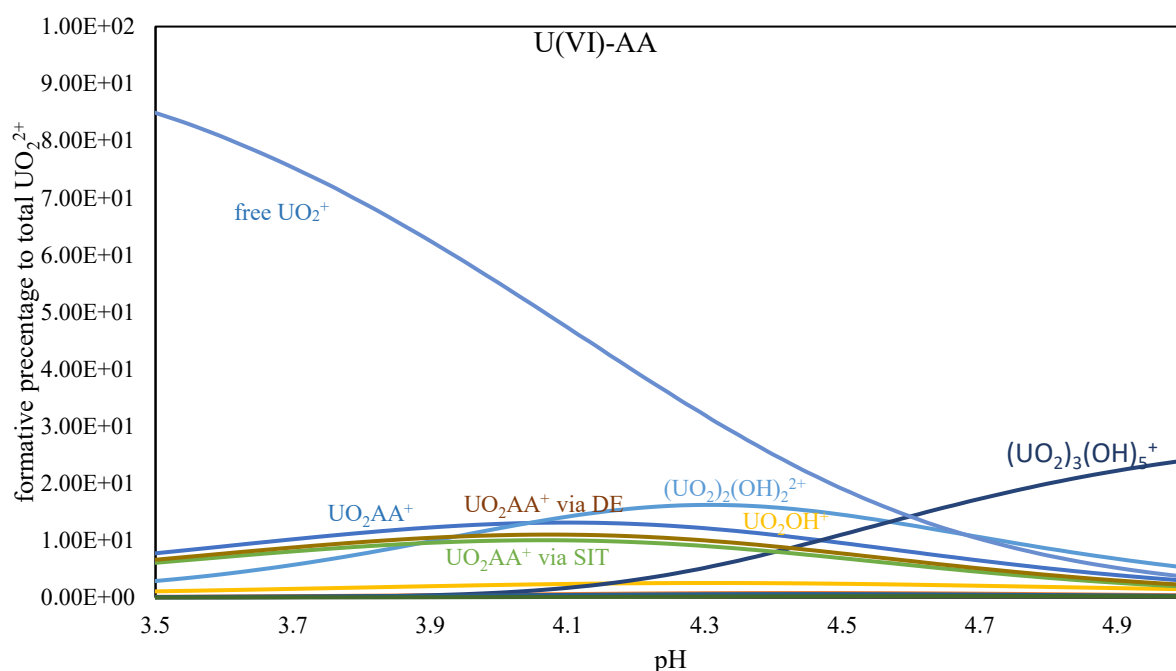

Figure 24 The formation curves of the complexation of uranyl ions with acetic acid (AA) without CO2 produced from Hyss. The logβ values for U(VI)-AA were shown in Table 17. The total sample volume was 30 ml at the beginning of the simulation, and 3.0 ml of 0.1 M NaOH solution was added into the system for establish a function of pH. The concentrations of vanadyl and AA were 1.67 mM and 3.33 mM respectively. The experimental pKa values was 4.54 at 0.1 M. 298.15K. pH in this model was only up to 3.0 since it will lead to approximately 10% error in the simulation as the added volume of NaOH was more than 3.0 ml.

The speciation of VO^{2+}-AA curves shown in Figure 36 indicated the large percentages of $(VO)_2(OH)_2^{2+}$ and $(VO)_2(OH)_5^-$ compared with the formed complexes. $(VO)_2(OH)_2^{2+}$ in excess of all of complexing species accounted for the critical level among the total species ranging from pH 3.95 to 5.10 then was replaced with the species of $(VO)_2(OH)_5^-$ as the subsequent increasing of pH values. Meanwhile, AA was not sensitive to VO^{2+} ions attributed to the largest converting rate to total VO^{2+} with respect to only 4.05% at pH 4.48. Meanwhile, the largest rates corresponding to the methods of SIT and Davies equation were 3.20% and 3.45% respectively.
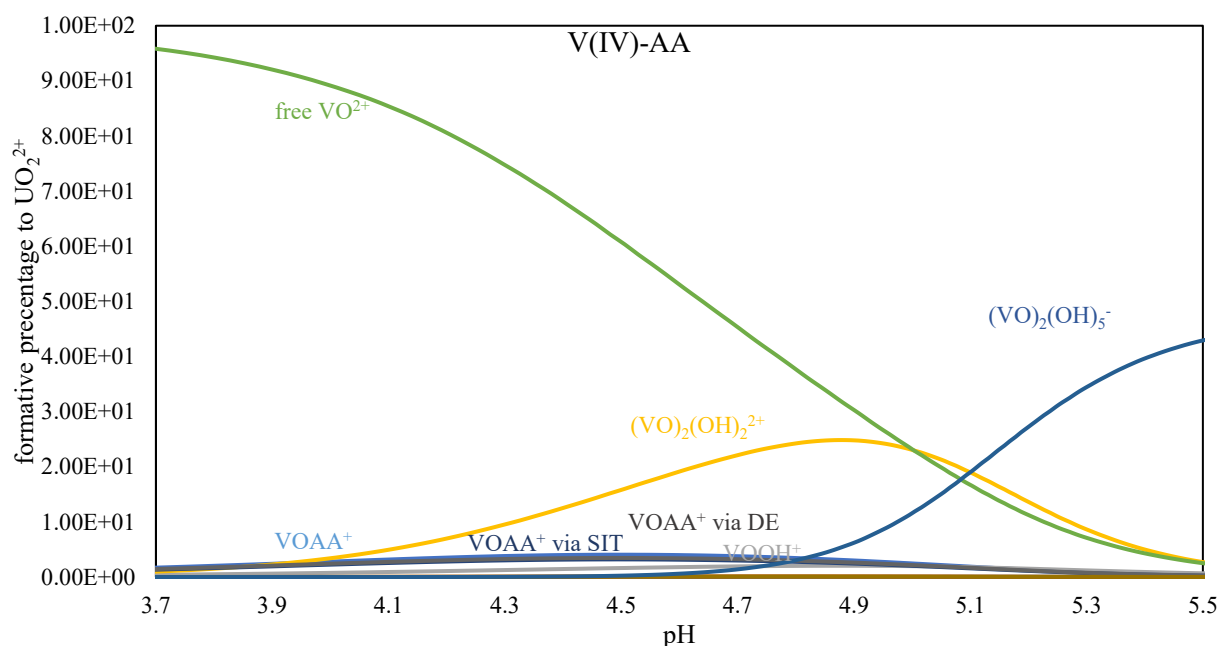
Figure 36 The formation curves of the complexation of vanadyl ions with acetic acid (AA) without CO2 produced from Hyss. The logβ values for V(IV)-AHA were shown in Table 17. The setting volume was 30 ml at the beginning of the simulation, and 1.7 ml of 0.1 M NaOH solution was added into the solution to establish the function of pH in the model. The concentrations of vanadyl and AA were 1.67 mM and 1.67 mM respectively. The experimental pKa values was 4.54 at 0.1 M, 298.15K.

The affinity of AA to uranyl and vanadyl ions in this work was estimated according to the converting rates to total metal ions in the system. Compared with the performance of the other ligands, the direct binding mode via carboxylate likely had a slight impact on the transport of these metal ions. In the study of Kirby, Simperler et al. (2018) and (Guo, Xiong et al. 2016), the DFT calculation was applied in the uranyl-carboxylate interactions and led to a relatively low affinity to metal ions attributed to their low stability constants of 7.51and the formation of a monodentate host-architeture.

5   Conclusion and Further Work

5.1   Conclusion

In this work, the effect of ion strength (from 0.1 to 3.0 M) and temperature (from 298.15 K to 335.15 K) on the dissociation constants for HAHA, AA, GA and PYR were investigated based on the techniques of potentiometric titration. The determined pKa values referred to literatures were available in terms of their closer proximity. In NaCl solution, the pKa values for acetohydroxamic acid and pyrocatechol indicated a significant decrease from 0.1 M to 1.0 M and placed a converse trendline as ion strength up to 3.0 M. Meanwhile, as the increase of temperature, their pKa values presented a remarkable decrease with a good linear relativity ($R^2 > 0.99$). However, although the effect of ion strength on pKa values of AA and GA was similar to the ones of HAHA and PYR, the effect of temperature on the variation of their pKa values was not sensitive as same as the performance in HAHA and PYR because of a low sensitivity ($R^2 < 0.1$).

According to the SIT calculation results in high ion strength solutions, the intrinsic values of PYR, GA and AA tended to be more approaching to the values from previous studies and also approaching to the values calculated (from 0.1 to 0.5 M) via Davies equation. However, compared with the difference between the values from Davies equation and literatures, the ones for acetohydroxamic acid (HAHA) produced from the method of SIT was not good to be used in other ion strength because of a large deviation with the values not only from Davies equation, but also from literatures. However, the situations found in PYR were conversed since the SIT values presented a lower deviation comparted with the DE ones. The enthalpies of protonation found in HAHA and PYR were exothermic from 1M to 3M, while it was found that the protonation of GA and AA at 1.0M were endothermic reactions because of their positive enthalpies. It was also noticeable that the thermodynamic properties in GA and AA were greatly depended on their entropies.

Based on the known stability constants and pKa values, the speciation models to simulate all of complexing progresses among these 4 ligands were established and considered the addition of the new pKa$_0$ values in HYPERQUAD. Despite the complexing progress occurred in all ligands, the coordinating ability in high pH environment basically focused on HAHA and PYR, while the function of GA and AA to the targeted metal ions was only observed in acidic environment. Notably, the coordination related to uranyl ions showed stronger than the corresponding vanadyl ions in terms of the higher formative contents of their species. Therefore, it was likely supported the electrostatic forces prevalently govern the coordination progress between metal ions and ligands in this work. The numbers of effective charges on uranyl ions (+4) was much higher than on vanadyl ions (+2.4) (Di Bernardo, Tomat et al. 1988). However, the situations of GA and PYR were opposite. It was likely assumed that vanadyl ions presented a higher inner sphere nature than the ones of uranyl ions, where a water molecule participates in their coordination progress (Di Bernardo, Bismondo et al. 1976). Although previous studies suggested the hydroxycarboxylate (HC) with the high affinity to uranyl ions, the complexing ability of glycolate for the metal uptake was not fitted the results. It thus presumed that the binding mode for GA was on axis lane not on equatorial lane occurred in the other ligands in presence of HC. Moreover, due to the detecting limitation of potentiometric titration, the second protonation (pKa of 17 to 20) occurred in GA was difficult to be observed. Therefore, the role of GA in uranyl or vanadyl uptake in hyper alkaline environments was suggested to be investigated via the alternative method which owns high-tolerance ability in hyper alkaline environments. Meanwhile, the extremely high pH conditions was not suitable for the HYPERQUAD models because of the shortage of potentiometric titration experiments.

The role of ligands HAHA, PYR, AA and GA in the quantification of uranium and vanadium migration released from the GDF was replenished based on the new values obtained in this study. It was identified that the cement leachate originated from in the vicinity of GDF mainly consists of the cement (calcium, silicon, sulphate) and chloride solution (Bobirică, Long et al. 2018). As the existence of halite (NaCl) widely distributed in underground environment, the role of NaCl in the measurement of pKa values and thermodynamic parameters of our targeted ligands and was discussed in this study. Since there are many geological models (PHREEQC, MinteQ and Hyss etc.) producing M-L complexing speciation relied on known values and parameters of ligands and regarding stability constants. Therefore, the improvement of modelling predication for the speciation of U(VI)-L and V(IV)-L in NaCl can be fulfilled attributed to the acquired results. Meanwhile, the study exhibited the availability of technique of potentiometric

titration as an alternatives to measure pKa values of other ligands sourced from vegetation, bacteria and fungi in the specific electrolyte solution such as KCl, $NaClO_4$ and $NaNO_3$ in old cement leachate (pH<10.5).

5.2   Further work

In this work, although the understanding of the deprotonation of these 4 ligands and their coordination with uranyl and vanadyl ions has been increased via the application of activity correction and the measurement of their thermodynamic parameters, there are several areas need further work.

1.   The measurement of thermodynamic parameters with respect to these 4 ligands was carried out via a thermometer and a potentiometric titration for recording real-time data. However, the method was argued with a larger experimental error than the determination by the calorimetric method (Thakur, Mathur et al. 2007). The improvement of the thermodynamic parameters can be determined replaced with the calorimetric method.

2.   The limitation of the potentiometric titration was only up to the pH threshold of old cement leachate (OCL). Nevertheless, the investigation of complexing progress occurred in immediate cement leachate (ICL) and young cement leachate (YCL) lacks the appropriate method. The method of voltammetry measurement which was prevalently applied in most of natural solutions including in the hyperalkaline leachate since the electrode only detects the free metal ions rather than free hydrogen ions in the solution. Based on the transported uranyl or vanadyl ions coordinated via the uptake of targeted ligands, a chelate -scale established via Voltammetry is available to increase the understanding of the complexation of the metal ions with these 4 ligands in ICL and YCL.

3.   In our study, the complexing models were established in basis of the shortage of CO_2. However, the function of these 4 ligands even more natural ligands to the carbonate uranyl or vanadyl was lacked to be understanding even if some of DFT works investigated the reactions between carbonate UO_2^{2+} and carboxyl or amidoximate (Guo, Xiong et al. 2016). Therefore, the enhancement of the accuracy of the models applied in the surface environment needs considered the influence of CO_2.

4.   Although the established models denoted the affinity of these 4 ligands to uranyl and vanadyl ions, the understanding of their ability to mobilize these metal needs more works. The determination of the effect of the ligand contents on the precipitation of uranyl and vanadyl is also a critical evidence to infer the importance of the ligands in environmental safety. Meanwhile, the further studies need to consider the characterization of M-L complexes according to their binding methods and chemical structure which was commonly applied in the demonstration of the stability of their complexing species for geochemical models.

5.   During the discussion of the effect of intrinsic pKa values on M-L complexing models, the stability constants (logβ) of complexes were only obtained from previous studies under certain conditions (including the fixed ion strength, temperature and electrolyte). However, most of studies lack the calculation of intrinsic stability constants. Therefore, the study to investigate the effect of ion strength on the formation of U(VI)-L and V(IV)-L was obligatory to obtain their intrinsic logβ values for improving the precision of the speciation models.

6.   Previous studies via the method of DFT and EXAFs have determined the stability constants of U(VI)-L and V(VI)-L and their binding modes during the coordination progress. However, it was in shortage of that the determination of their thermodynamics in basic media for supporting their

sensitivity to temperature in different M-L formats. In the further work, the effect of temperature on the speciation of their complexes is also worth to be investigated to explain their stability in more complicated conditions for the quantifying simulation.

6 Reference

Ahmed, E. and S. J. Holmström (2014). "Siderophores in environmental research: roles and applications." Microbial biotechnology **7**(3): 196-208.

Aksoy, M. S. (2010). "Study of the interaction between chromium (III) and hydroxamic acids." Journal of Chemical & Engineering Data **55**(6): 2252-2256.

Alam, M. F., et al. (2018). "In vitro DNA binding studies of therapeutic and prophylactic drug citral." International journal of biological macromolecules **113**: 300-308.

Alexander, W. R., et al. (2008). "A new natural analogue study of the interaction of low-alkali cement leachates and the bentonite buffer of a radioactive waste repository." MRS Online Proceedings Library (OPL) **1107**.

Ali, K., et al. (2005). "Comparative Study of Thermodynamic Parameters of Vanadium (IV) and (V) Acetohydroxamate Complexes."

Altmaier, M., et al. (2017). "Solubility of U (VI) in chloride solutions. I. The stable oxides/hydroxides in NaCl systems, solubility products, hydrolysis constants and SIT coefficients." The Journal of Chemical Thermodynamics **114**: 2-13.

Berto, S., et al. (2008). "Interaction of oxovanadium (IV) with carboxylic ligands in aqueous solution: A thermodynamic and visible spectrophotometric study." Journal of Molecular Liquids **142**(1-3): 57-63.

Bobirică, C., et al. (2018). "Examination of the influence of dissolved halite (NaCl) on the leaching of lead (Pb) from cement-based solidified wastes." Journal of Material Cycles and Waste Management **20**: 59-70.

Bockris, J. O. M., et al. (1998). Modern electrochemistry 2B: electrodics in chemistry, engineering, biology and environmental science, Springer Science & Business Media.

Bretti, C., et al. (2004). "A new approach in the use of SIT in determining the dependence on ionic strength of activity coefficients. Application to some chloride salts of interest in the speciation of natural fluids." Chemical Speciation & Bioavailability **16**(3): 105-110.

Brink, C. P. and A. L. Crumbliss (1982). "Temperature-dependent acid dissociation constants (Ka,. DELTA. Ha,. DELTA. Sa) for a series of nitrogen-substituted hydroxamic acids in aqueous solution." The Journal of organic chemistry **47**(7): 1171-1176.

Brown, P. L. (2002). "The hydrolysis of uranium (VI)." Radiochimica Acta **90**(9-11): 589-593.

Buglyó, P. and N. Pótári (2005). "Study of the interaction between oxovanadium (IV) and hydroxamic acids." Polyhedron **24**(7): 837-845.

Cahill, A. E. and L. E. Burkhart (1990). "Continuous precipitation of uranium with hydrogen peroxide." Metallurgical Transactions B **21**(5): 819-826.

Cao, J., et al. (2004). "The effect of pH, ion strength and reactant content on the complexation of Cu2+ by various natural organic ligands from water and soil in Hong Kong." Chemosphere **54**(4): 507-514.

Cardiano, P., et al. (2011). "Methylmercury (II)-sulfur containing ligand interactions: a potentiometric, calorimetric and 1H-NMR study in aqueous solution." New Journal of Chemistry **35**(4): 800-806.

Charkoudian, L. K. and K. J. Franz (2006). "Fe (III)-coordination properties of neuromelanin components: 5, 6-dihydroxyindole and 5, 6-dihydroxyindole-2-carboxylic acid." Inorganic chemistry **45**(9): 3657-3664.

Chung, D.-Y., et al. (2011). "Complexation of U (VI), Ce (III) and Nd (III) with acetohydroxamic acid in perchlorate aqueous solution." Journal of Radioanalytical and Nuclear Chemistry **289**(2): 315-319.

Cohn, E. J., et al. (1928). "THE DISSOCIATION CONSTANT OF ACETIC ACID AND THE ACTIVITY COEFFICIENTS OF THE IONS IN CERTAIN ACETATE SOLUTIONS1." Journal of the American Chemical Society **50**(3): 696-714.

Comarmond, M. J. and P. L. Brown (2000). "The hydrolysis of uranium (VI) in sulfate media." Radiochimica Acta **88**(9-11): 573-578.

Daniele, P. G., et al. (1981). "The formation of proton and alkali-metal complexes with ligands of biological interest in aqueous solution. Thermodynamics of H+, Na+ and K+—oxalate complexes." Thermochimica Acta **46**(2): 103-116.

Daniele, P. G., et al. (1983). "Ionic strength dependence of formation constants—I: Protonation constants of organic and inorganic acids." Talanta **30**(2): 81-87.

Daughney, C. J. and J. B. Fein (1998). "The Effect of Ionic Strength on the Adsorption of H+, Cd2+, Pb2+, and Cu2+ byBacillus subtilisandBacillus licheniformis: A Surface Complexation Model." Journal of Colloid and Interface Science **198**(1): 53-77.

Davies, C. (1938). "J. chem. Soc.[London]."

De Stefano, C., et al. (2002). "Dependence on ionic strength of the hydrolysis constants for dioxouranium (VI) in NaCl (aq) and NaNO3 (aq), at pH< 6 and t= 25° C." Journal of Chemical & Engineering Data **47**(3): 533-538.

Di Bernardo, P., et al. (1976). "Thermodynamic properties of actinide complexes. Part. III. Uranyl (VI)-glycolate system." Inorganica Chimica Acta **18**: 47-50.

Di Bernardo, P., et al. (1988). "Thermodynamics of vanadyl (IV)—carboxylate complex formation in aqueous solution." Inorganica Chimica Acta **145**(2): 285-288.

do Nascimento, A., et al. (2017). "Thermal behavior of glycolic acid, sodium glycolate and its compounds with some bivalent transition metal ions in the solid state." Journal of Thermal Analysis and Calorimetry **130**(3): 1463-1472.

Dong, W. and S. C. Brooks (2008). "Formation of aqueous MgUO2 (CO3) 32− complex and uranium anion exchange mechanism onto an exchange resin." Environmental Science & Technology **42**(6): 1979-1983.

Edwards, C. and A. Oliver (2000). "Uranium processing: a review of current methods and technology." Jom **52**(9): 12-20.

Evers, A., et al. (1989). "Metal ion recognition in ligands with negatively charged oxygen donor groups. Complexation of iron (III), gallium (III), indium (III), aluminum (III), and other highly charged metal ions." Inorganic chemistry **28**(11): 2189-2195.

Farkas, E., et al. (1999). "A comparison between the chelating properties of some dihydroxamic acids, desferrioxamine B and acetohydroxamic acid." Polyhedron **18**(18): 2391-2398.

Fazary, A. E. (2005). "Thermodynamic studies on the protonation equilibria of some hydroxamic acids in NaNO3 solutions in water and in mixtures of water and dioxane." Journal of Chemical & Engineering Data **50**(3): 888-895.

Fazary, A. E., et al. (2020). "Protonation equilibria of N-acetylcysteine." ACS omega **5**(31): 19598-19605.

Gagliardi, L. G., et al. (2007). "Static Dielectric Constants of Acetonitrile/Water Mixtures at Different Temperatures and Debye– Hückel A and a 0 B Parameters for Activity Coefficients." Journal of Chemical & Engineering Data **52**(3): 1103-1107.

Gans, P., et al. (1996). "Investigation of equilibria in solution. Determination of equilibrium constants with the HYPERQUAD suite of programs." Talanta **43**(10): 1739-1753.

Gergely, A. and T. Kiss (1976). "Complexes of 3, 4-dihydroxyphenyl derivatives. I. Copper (II) complexes of DL-3, 4-dihydroxyphenylalanine." Inorganica Chimica Acta **16**: 51-59.

Goncalves, M. S. and A. Mota (1987). "Complexes of vanadyl and uranyl ions with the chelating groups of humic matter." Talanta **34**(10): 839-847.

Govindan, P., et al. (2008). "Partitioning of uranium and plutonium by acetohydroxamic acid." Desalination **232**(1-3): 166-171.

Guo, X., et al. (2016). "DFT investigations of uranium complexation with amidoxime-, carboxyl-and mixed amidoxime/carboxyl-based host architectures for sequestering uranium from seawater." Inorganica Chimica Acta **441**: 117-125.

Harned, H. and B. Owen (1958). "The physical chemistry of electrolytic solutions, Reinhold Pub." Corp., New York **354**.

Harned, H. S. and R. W. Ehlers (1932). "THE DISSOCIATION CONSTANT OF ACETIC ACID FROM 0 TO 35° CENTIGRADE1." Journal of the American Chemical Society **54**(4): 1350-1357.

Hausmann, J. N., et al. (2021). "The pH of aqueous NaOH/KOH solutions: a critical and non-trivial parameter for electrocatalysis." ACS Energy Letters **6**(10): 3567-3571.

Hicks, T., et al. (2008). "Concepts for the geological disposal of intermediate-level radioactive waste." Sign **736**(1).

Jameson, R. and M. Wilson (1972). "Thermodynamics of the interactions of catechol with transition metals. Part I. Free energy, enthalpy, and entropy changes for the ionisation of catechol at 25 C. Comparison of the temperature-coefficient method with direct calorimetry." Journal of the Chemical Society, Dalton Transactions(23): 2610-2614.

Jezowska-Bojczuk, M., et al. (1990). "Potentiometric and spectroscopic studies on oxovanadium (IV) complexes of salicylic acid and catechol and some derivatives." Journal of the Chemical Society, Dalton Transactions(9): 2903-2907.

Jiang, J., et al. (2002). "Complexation of uranium (VI) with acetate at variable temperatures." Journal of the Chemical Society, Dalton Transactions(8): 1832-1838.

Kielland, J. (1937). "Individual activity coefficients of ions in aqueous solutions." Journal of the American Chemical Society **59**(9): 1675-1678.

Kilpatrick, M. and R. D. Eanes (1953). "The dissociation constants of acids in salt solutions. II. Acetic acid." Journal of the American Chemical Society **75**(3): 586-587.

Kilpatrick, M. and R. D. Eanes (1953). "The dissociation constants of acids in salt solutions. III. Glycolic acid." Journal of the American Chemical Society **75**(3): 587-587.

Kirby, M., et al. (2020). "Prevention of UVI Precipitation in Alkaline Aqueous Solutions by the Siderophore Desferrioxamine B."

Kirby, M. E., et al. (2018). "Computational tools for calculating log β values of geochemically relevant uranium organometallic complexes." The Journal of Physical Chemistry A **122**(40): 8007-8019.

Kirishima, A., et al. (2007). "Determination of the thermodynamic quantities of uranium (VI)–carboxylate complexes by microcalorimetry." The Journal of Chemical Thermodynamics **39**(11): 1432-1438.

Koide, Y., et al. (1989). "Studies of collectors. X. Complexing ability of amino hydroxamic acid ligands with dioxouranium (VI) in aqueous solution." Bulletin of the Chemical Society of Japan **62**(11): 3714-3715.

Komura, A., et al. (1977). "Hydrolytic behavior of oxovanadium (IV) ions." Bulletin of the Chemical Society of Japan **50**(11): 2927-2931.

Kontogeorgis, G. M., et al. (2018). "The Debye-Hückel theory and its importance in modeling electrolyte solutions." Fluid Phase Equilibria **462**: 130-152.

Kuippers, G., et al. (2021). "Biomineralization of uranium-phosphates fueled by microbial degradation of isosaccharinic acid (ISA)." Environmental Science & Technology **55**(8): 4597-4606.

Li, L. and C. Page (1998). "Modelling of electrochemical chloride extraction from concrete: Influence of ionic activity coefficients." Computational Materials Science **9**(3-4): 303-308.

Liang, S.-Y., et al. (2021). "A review of geochemical modeling for the performance assessment of radioactive waste disposal in a subsurface system." Applied Sciences **11**(13): 5879.

Linder, P. W. and K. Murray (1982). "Correction of formation constants for ionic strength, from only one or two data points: An examination of the use of the extended Debye—Hückel equation." Talanta **29**(5): 377-382.

Lopes, A., et al. (2001). "Activity coefficients of sodium chloride in water–ethanol mixtures: a comparative study of Pitzer and Pitzer–Simonson models." Journal of solution chemistry **30**(9): 757-770.

Lucks, C., et al. (2012). "Aqueous uranium (VI) complexes with acetic and succinic acid: speciation and structure revisited." Inorganic chemistry **51**(22): 12288-12300.

Majlesi, K. and S. Rezaienejad (2009). "Application of the Parabolic Model, Specific Ion Interaction, and Debye– Hückel Theories for the Complexation of Dioxovanadium (V) with Ethylenediamine-N, N′-diacetic Acid." Journal of Chemical & Engineering Data **54**(5): 1483-1492.

Manov, G. G., et al. (1943). "Values of the constants in the Debye—Hückel equation for activity coefficients1." Journal of the American Chemical Society **65**(9): 1765-1767.

Martell, A. and R. Smith (1977). "Critical stability constants, vol 3 Plenum Press." New York, NY.[Google Scholar].

McKinley, I. G., et al. (2007). "Development of geological disposal concepts." Radioactivity in the Environment **9**: 41-76.

Meloun, M., et al. (2011). "The thermodynamic dissociation constant of naphazoline by the regression analysis of potentiometric data." Central European Journal of Chemistry **9**(1): 66-74.

Meloun, M., et al. (2004). "The thermodynamic dissociation constants of ambroxol, antazoline, naphazoline, oxymetazoline and ranitidine by the regression analysis of spectrophotometric data." Talanta **62**(3): 511-522.

Miller, H., et al. (1954). "Survey of Radioactive-Waste Disposal Practices." Nucleonics (US) Ceased publication **12**.

Moll, H., et al. (2003). "Uranyl (VI) complexes with alpha-substituted carboxylic acids in aqueous solution." Radiochimica Acta **91**(1): 11-20.

Morris, K. (2016). "Summary of the BIGRAD project and its implications for a geological disposal facility."

Mullen, L., et al. (2007). "Complexation of uranium (VI) with the siderophore desferrioxamine B." Journal of Radioanalytical and Nuclear Chemistry **273**(3): 683-688.

Munoz-Caro, C., et al. (2000). "Modeling of protonation processes in acetohydroxamic acid." The Journal of organic chemistry **65**(2): 405-410.

Nagai, H., et al. (2008). "Temperature dependence of the dissociation constants of several amino acids." Journal of Chemical & Engineering Data **53**(3): 619-627.

Nims, L. F. (1936). "The ionization constant of glycolic acid from 0 to 50°." Journal of the American Chemical Society **58**(6): 987-989.

Northover, G. H., et al. (2021). "Effect of salinity on the zinc (II) binding efficiency of siderophore functional groups and implications for salinity tolerance mechanisms in barley." Scientific Reports **11**(1): 1-12.

NRC (1999). <u>Disposition of high-level radioactive waste through geological isolation: development, current status, and technical and policy challenges</u>, National Academies Press.

Nurchi, V. M., et al. (2009). "Effect of substituents on complex stability aimed at designing new iron (III) and aluminum (III) chelators." <u>Journal of inorganic biochemistry</u> **103**(2): 227-236.

Pankow, J. F. (2018). <u>Aquatic chemistry concepts</u>, CRC Press.

Partanen, J. I., et al. (2001). "Determination of stoichiometric dissociation constants of glycolic acid in dilute aqueous sodium or potassium chloride solutions at 298.15 K."

Pedersen, K. J. (2002). "The Dissociation Constants of Acetoacetic, Glycolic, and Acetic Acids in Solutions of Sodium Chloride." <u>The Journal of Physical Chemistry</u> **38**(8): 993-998.

Perron, N. R. and J. L. Brumaghim (2009). "A review of the antioxidant mechanisms of polyphenol compounds related to iron binding." <u>Cell biochemistry and biophysics</u> **53**(2): 75-100.

Pitzer, K. S. and C. Press (1991). <u>Activity coefficients in electrolyte solutions</u>, CRC press Boca Raton, FL.

Po, H. N. and N. Senozan (2001). "The Henderson-Hasselbalch equation: its history and limitations." <u>Journal of chemical education</u> **78**(11): 1499.

Reijenga, J., et al. (2013). "Development of methods for the determination of pKa values." <u>Analytical chemistry insights</u> **8**: ACI. S12304.

Romero, R., et al. (2018). "An experimental validated computational method for pKa determination of substituted 1, 2-dihydroxybenzenes." <u>Frontiers in chemistry</u> **6**: 208.

Roßberg, A., et al. (2000). "EXAFS structural analysis of aqueous uranium (VI) complexes with lignin degradation products." <u>Radiochimica Acta</u> **88**(9-11): 593-598.

Rossotti, F. and H. Rossotti (1965). "Potentiometric titrations using Gran plots: A textbook omission." <u>Journal of chemical education</u> **42**(7): 375.

Runde, W. (2000). "The chemical interactions of actinides in the environment." <u>Los Alamos Science</u> **26**: 392-411.

Salusjärvi, L., et al. (2019). "Biotechnological production of glycolic acid and ethylene glycol: current state and perspectives." <u>Applied microbiology and biotechnology</u> **103**(6): 2525-2535.

Samson, E., et al. (1999). "Modeling chemical activity effects in strong ionic solutions." <u>Computational Materials Science</u> **15**(3): 285-294.

Scatchard, G. (2013). Equilibrium in solutions and Surface and Colloid Chemistry. <u>Equilibrium in Solutions and Surface and Colloid Chemistry</u>, Harvard University Press.

Shedlovsky, T. (1943). Introduction to Electrochemistry (Glasstone, Samuel), ACS Publications.

Sherene, T. (2010). "Mobility and transport of heavy metals in polluted soil environment." <u>an international journal</u> **2**: 112-121.

Stokes, R. H. and R. A. Robinson (1959). Electrolyte Solutions: The Measuremwnt and Interpretation of Conductance, Chemical Potential and Diffusion in Solutions of Si, Butterworth Scientific, London.

Sun, M. S., et al. (1980). "Activity corrections for ionic equilibria in aqueous solutions." Canadian Journal of Chemistry **58**(12): 1253-1257.

Sylva, R. and M. Davidson (1979). J. Chem. Soc. Dalton Trans.

Sylva, R. N. and M. R. Davidson (1979). "The hydrolysis of metal ions. Part 2. Dioxouranium (VI)." Journal of the Chemical Society, Dalton Transactions(3): 465-471.

Szabo, Z. and I. Grenthe (2000). "Potentiometric and Multinuclear NMR Study of the Binary and Ternary Uranium (VI)– L– Fluoride Systems, Where L Is α-Hydroxycarboxylate or Glycine." Inorganic chemistry **39**(22): 5036-5043.

Szabó, Z. and I. Grenthe (2000). "Potentiometric and Multinuclear NMR Study of the Binary and Ternary Uranium (VI)– L– Fluoride Systems, Where L Is α-Hydroxycarboxylate or Glycine." Inorganic chemistry **39**(22): 5036-5043.

Thakur, P., et al. (2007). "Thermodynamics and dissociation constants of carboxylic acids at high ionic strength and temperature." Inorganica Chimica Acta **360**(12): 3671-3680.

Tsui, F. C., et al. (1986). "The intrinsic pKa values for phosphatidylserine and phosphatidylethanolamine in phosphatidylcholine host bilayers." Biophysical journal **49**(2): 459-468.

Urbaniak, B. and Z. J. Kokot (2009). "Analysis of the factors that significantly influence the stability of fluoroquinolone–metal complexes." Analytica chimica acta **647**(1): 54-59.

Van Den Berg, C. M. and Z. Q. Huang (1984). "Determination of uranium (VI) in sea water by cathodic stripping voltammetry of complexes with catechol." Analytica chimica acta **164**: 209-222.

Wagner, F. S. and U. b. Staff (2000). "Acetic acid." Kirk‐Othmer Encyclopedia of Chemical Technology: 1-21.

Wehrli, B. and W. Stumm (1989). "Vanadyl in natural waters: Adsorption and hydrolysis promote oxygenation." Geochimica et Cosmochimica Acta **53**(1): 69-77.

Yale, H. L. (1943). "The Hydroxamic Acids." Chemical Reviews **33**(3): 209-256.

Yamaki, R. T., et al. (1997). "Interaction of N-hydroxyacetamide with vanadate in aqueous solution." Journal of the Chemical Society, Dalton Transactions(24): 4817-4822.

Yamaki, R. T., et al. (1999). "Interaction of 2-amino-N-hydroxypropanamide with vanadium (V) in aqueous solution." Journal of the Chemical Society, Dalton Transactions(24): 4407-4412.

Zakaria, H., et al. (2022). "Interaction of Curcumin with Poly Lactic-Co-Glycolic Acid and Poly Diallyldimethylammonium Chloride By Fluorescence Spectroscopy." Journal of Fluorescence: 1-9.

Zhao, L. and P. Gao (2006). "Evaluation of zeotropic refrigerants based on nonlinear relationship between temperature and enthalpy." Science in China Series E **49**(3): 322-331.